GEOTECHNICAL
ENGINEERING

GEOTECHNICAL ENGINEERING

VOLUME 18   NUMBER 2   DECEMBER 1987

A CASE HISTORY OF SLOPE DESIGN IN COMPLEX WEATHERED LOW GRADE METAMORPHIC ROCK

D.R. GREENWAY*, G.E. POWELL*, and T.Y. IRFAN*,

SYNOPSIS

A large tank-type water reservoir has been constructed on top of a remote hill in Hong Kong to provide water for a new town development. Formation of an access road and the reservoir required slopes to be constructed in weathered low grade metamorphic rocks, mainly metasandstones and phyllites.

The site investigations showed that both the geological structure and the weathering profile at the site were complex and variable. Although the rocks had weathered to soil-like materials for considerable depths, a strongly developed foliation variable in dip and direction, persisted almost to the ground surface.

The laboratory testing programme was oriented towards determination of shear strength of relict foliation planes, since the strength of the relict discontinuities rather than the strength of the intact material would be the dominant factor in controlling slope stability. These foliations together with environmental factors, were critical in deciding the road alignment, orientation and slope angles of the reservoir slopes.

A number of steep temporary cuts failed during construction, both on steeply dipping foliation planes and fault zones containing clayey infill. The permanent road and reservoir cuttings, which were up to 24 m high and were cut at relatively gentle angles varying from 28° to 34° depending on orientation, performed satisfactorily.

INTRODUCTION

Rapid development in Hong Kong has reached into the hinterland, with construction of several "new towns" underway in close proximity to the Hong Kong-China border. These developments are typically situated in broad valleys and flat low-lying plains, in contrast to the more mountainous setting of the main urban centre surrounding Victoria Harbour. One such new town, Fanling, will reach a design population of 220,000 by the early 1990s, after a decade of phenomenal growth from the 1981 population of 50,000. Fanling's rapid development has presented a full range of engineering challenges, including the need for adequate water supplies.

The Fanling water supply scheme, designed by the Water Supply Department of Hong Kong Government, includes the construction of a holding reservoir at the summit of the prominent Table Hill, adjacent to the town

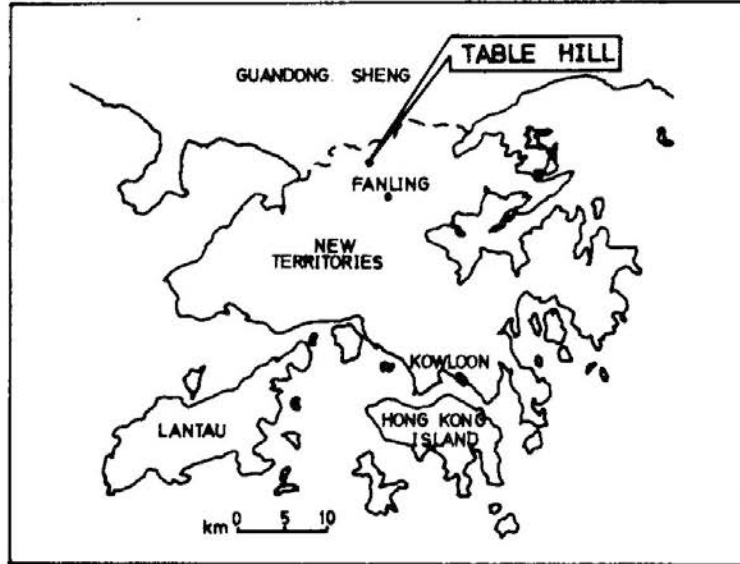* Geotechnical Control Office, Hong Kong

Fig. 1. Locality plan.

(Figure 1). The concrete reservoir, with a capacity of 28,000 m³, occupies a 70 m by 70 m plan area at an elevation approximately 100 m above the town. Road access to the site was constructed along a northeasterly trending ridge for a distance of 0.8 km at relatively steep gradients. The site is within 2 km of the China border and is prominently visible from the surrounding area (Plate 1).

This paper describes the design and construction of cut slopes in weathered low grade metamorphic rocks, mainly metasandstones and phyllites, encountered at Table Hill. The height of the main cutslope at the reservoir was 25 m, and cuttings along the access road ranged up to 16 m high. The nature of the complex metamorphic rocks at the site had a profound influence on all aspects of the slope design.

<div align="center">PRELIMINARY INVESTIGATIONS</div>

Desk Study

Desk studies were undertaken utilising topographic maps, a geological map, and aerial photographs. The available geological map was at 1 : 50,000 scale (ALLEN & STEPHENS, 1971), and indicated that the site consisted of a low grade metamorphosed sedimentary sequence of silty shales, siltstones and sandstones of Jurassic age, known as Lok Ma Chau forma-
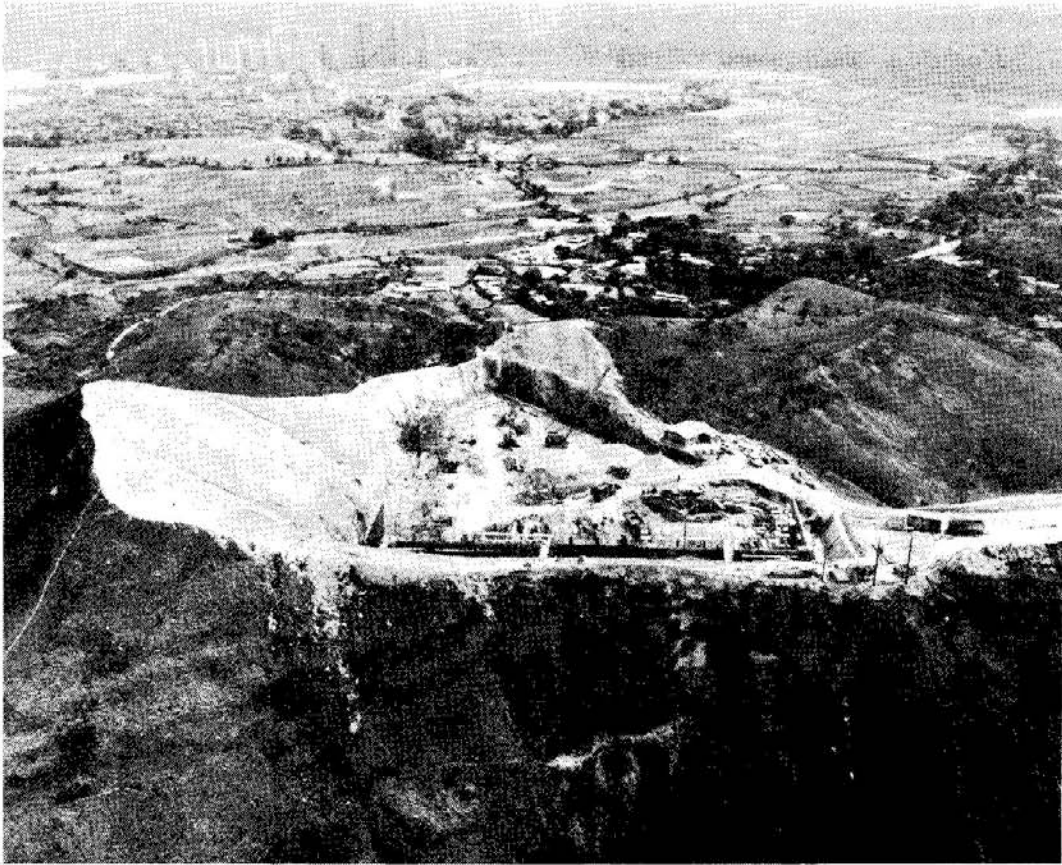
146

Plate 1 Overview of Site.

tion. The map also indicated that this formation had a prominent foliation which generally dipped to the northwest at 30° to 35°. Volcanic rocks, also of Jurassic age, dominantly rhyolitic tuffs and lavas, were shown immediately to the south of the project area. Neither the geological map nor a study of aerial photographs revealed any major faults or photolineaments at Table Hill. The aerial photographs did however reveal a number of ancient landslip scars on the flanks of the hill, and along the ridge line to be traversed by the access road. These bowl-shaped and elongated depressions were typically 100 m across and from 100 to 200 m long. They had been completely revegetated, supporting a cover of grass, shrubs and small pine trees indistinguishable from the adjacent hillside.

Field Reconnaissance

A field reconnaissance revealed that along the ridge line the sideslopes were noticeably steeper on the south side as compared to the north, with

147

south facing slopes being typically 35° and north facing slopes 25°. This is apparently a geomorphological expression of the overall foliation dip to the northwest within the Lok Ma Chau formation.

A number of shallow trenches were discovered on Table Hill, believed to have been constructed for military purposes. An examination of these
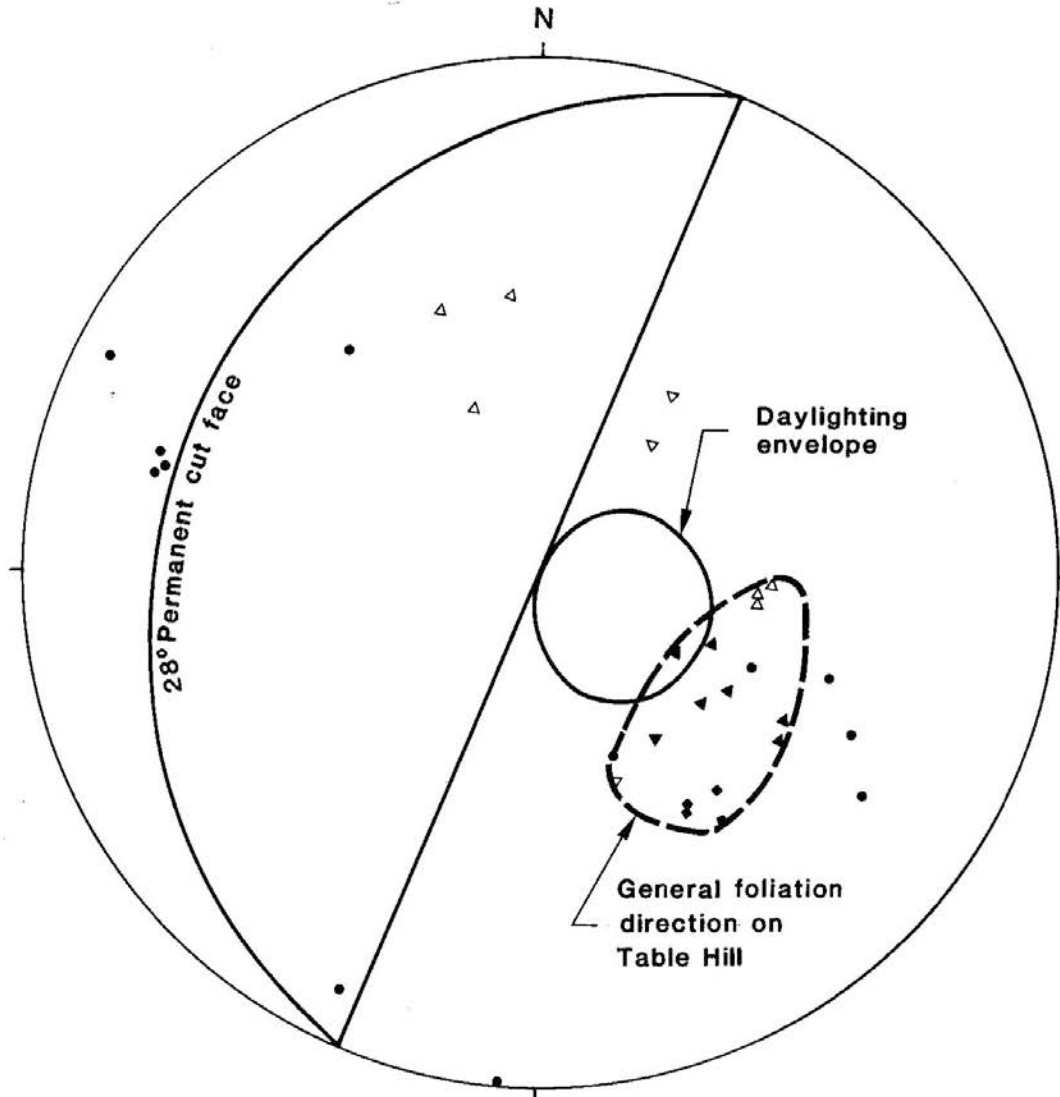
Fig. 2. Geological structural data from field reconnaissance.

revealed a dense soil mantle showing pronounced relict structure. Weathering effects were pervasive, with no hard rock outcrops to be found at the site. In sideslope locations, a thin layer of colluvium was also frequently observed.

In general the weathered Lok Ma Chau was observed to contain in addition to joints, three sets of discontinuities all having nearly the same dip and strike: a strong cleavage or schistosity, a second weaker cleavage and sedimentary bedding. Field mapping confirmed that the general dip of stronger foliations was 25° to 40° to the northwest, as shown in ALLEN & STEPHENS (1971). However, a wide scatter in the measurements was observed, possibly indicating that intense folding had taken place (Figure 2).

Geological structural data obtained during the field reconnaissance is shown on the equal area stereonet in Figure 2. Measurements were taken outside the immediate project area to gain a wider appreciation of the geology, structure and slope stability. The field observations made were not extensive however, being hampered by dense vegetation and colluvial cover in many locations. The observations were supplemented as time went along and more field exposures were available, for example the small cuttings required to form drilling platforms on the sideslopes.

Existing Cut Slopes in the Vicinity

A visual and geological survey of existing cutslopes within about 1 km of the project site was undertaken to obtain an indication of likely performance of cutslopes within the Lok Ma Chau formation. This survey showed that steep (over 60°) stable slopes of moderate height (20 m) could be achieved when massive or thickly bedded sandstones were encountered and when the pronounced foliation dipped into the slope. Where a succession of interbedded phyllite and metasandstone occurred, the stable slope gradients were shallower, even when the foliation dipped into the slope. In slopes composed dominantly of phyllite and oriented in general alignment with the foliation, the slope gradient was much gentler, being close to the foliation dip angle. It was discovered that one slope had a history of repeated failure until it was redesigned with a face batter equal to the angle of the foliation (HOWAT, 1985).

DESIGN

Interaction with the Civil Design

Initial design proposals included a rectangular reservoir with an associ-

149

ORIGINAL PROPOSAL

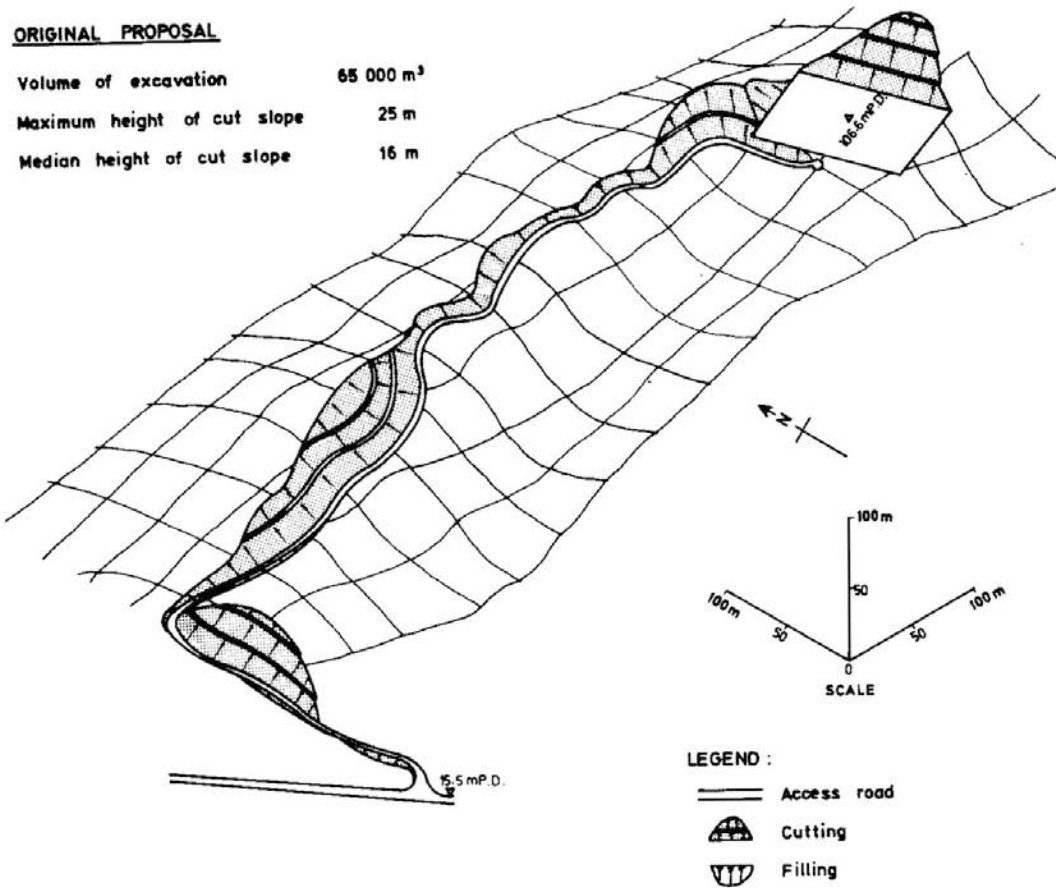|	
Volume of excavation	65 000 m³
Maximum height of cut slope	25 m
Median height of cut slope	16 m

Fig. 3. Original earthworks proposal.

ated west facing cut slope, with an access road and 800 mm diameter pipeline traversing the ridge along the south face in a midslope position. The road was to be single lane with intervisible passing bays, and to be concrete paved. Road grades up to 18 or 20% could be tolerated for short distances.

It was apparent that slope construction would be problematical at this site, and considerable effort was therefore made to minimise the extent of associated cut slopes. This effort primarily centred on the access road, but at the reservoir site it eventually led to the adoption of a five sided reservoir configuration to minimise the extent of the main cutting. For the proposed south flank location of the access road, it was envisioned that stable cuts would essentially parallel the existing sideslope, requiring

150

FINAL SCHEME

Volume of excavation	25 000 m³
Maximum height of cut slope	22 m
Median height of cut slope	9 m

LEGEND :

═══ Access road
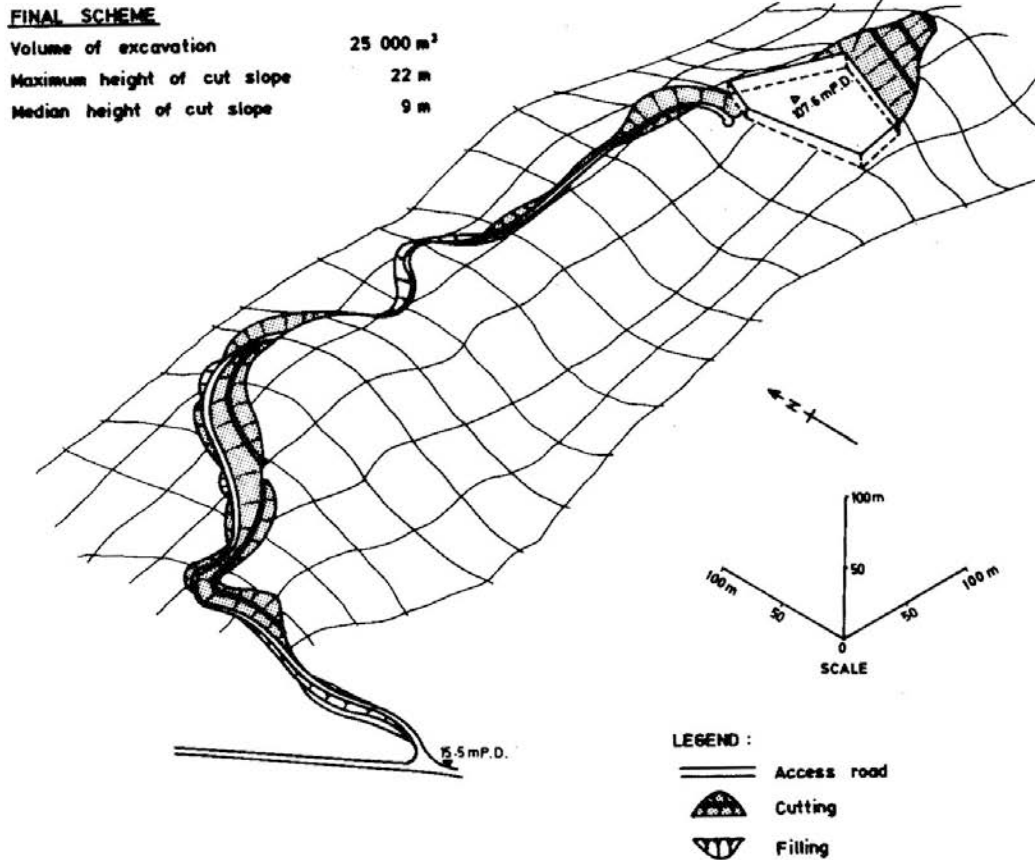
🛡 Cutting

⛰ Filling

SCALE

Fig. 4. Adopted earthworks (following geotechnical investigation).

major cut slopes reaching to the ridge line along the entire route. It was found that this condition could be significantly improved if road grades near the maximum were used at the beginning of the road, resulting in the road being located on the ridge top for the latter half of the access road. This approach required the use of a retaining wall and minor fills to support the road in several places, as well as an alignment on the north face of the ridge in the lower portion of the road. While it was fully appreciated that a north side location was generally unfavourable with regard to the foliation dip, the gentler sideslopes on the north were a mitigating factor. The originally proposed works and those finally adopted are shown in Figures 3 and 4. The orientation of the main reservoir cutting face was to the northwest, the worst possible orientation with respect to slope stability, but this orientation had been chosen in order to minimise visual impact of the works when viewed from the new towns to the southwest.

151

Detailed Site Investigation

A total of 14 drillholes were sunk at the reservoir site and along the access road location. These were used to assess bulk excavation characteristics and reservoir foundation conditions as well as to obtain data for slope design. The drillholes were advanced by rotary coring using water as the flushing medium. A triple tube Mazier core barrel with a spring loaded cutting shoe was utilised during most of the coring, which minimised disturbance and produced relatively high core recovery even in the relatively soft and weathered rock. Standard penetration tests were generally performed at 2 m depth intervals, and open hydraulic piezometers were installed in each drillhole upon completion of drilling.

A detailed description of strata exposed on site is given later.

Laboratory Testing

Direct shear testing of foliations from within the weathered metamorphic rock were undertaken to obtain slope design parameters. Ten representative foliations were selected from the drill cores and tested in a Golder-type shear box using a multistage technique. The tests were conducted wet (submerged) and with an increasing sequence of normal pressure, except for one specimen that was tested dry and one specimen that was tested in a decreasing normal stress sequence. Normal stresses ranging from 100 to 1000 kPa were used, with specimen preparation and test data reduction following the procedures outlined by HENCHER (1987). In the Golder apparatus, the test itself involves the application of a fixed normal load by lever arm and weights, and the application of a shear force by a hand operated hydraulic pump. Both horizontal and vertical displacements are measured during the test, with the rate of increase in shear force regulated to maintain a reasonable pace for manual recording of data.

A typical direct shear result is shown in Figure 5. The specimen was tested in either four or five stages, with the shear load completely removed between stages. Increased vertical compression occurred under increased normal stress in each stage. Reduction of the test data included corrections for effective area, dilation during shear, and misalignment of the discontinuity within the shear box.

The shear test results are summarised in Figure 6. The specimen that was tested dry yielded a relatively high shear strength, and has been excluded from this plot. The results were generally linear over the stress range tested, indicating that accumulating strain during the multistage testing had a small
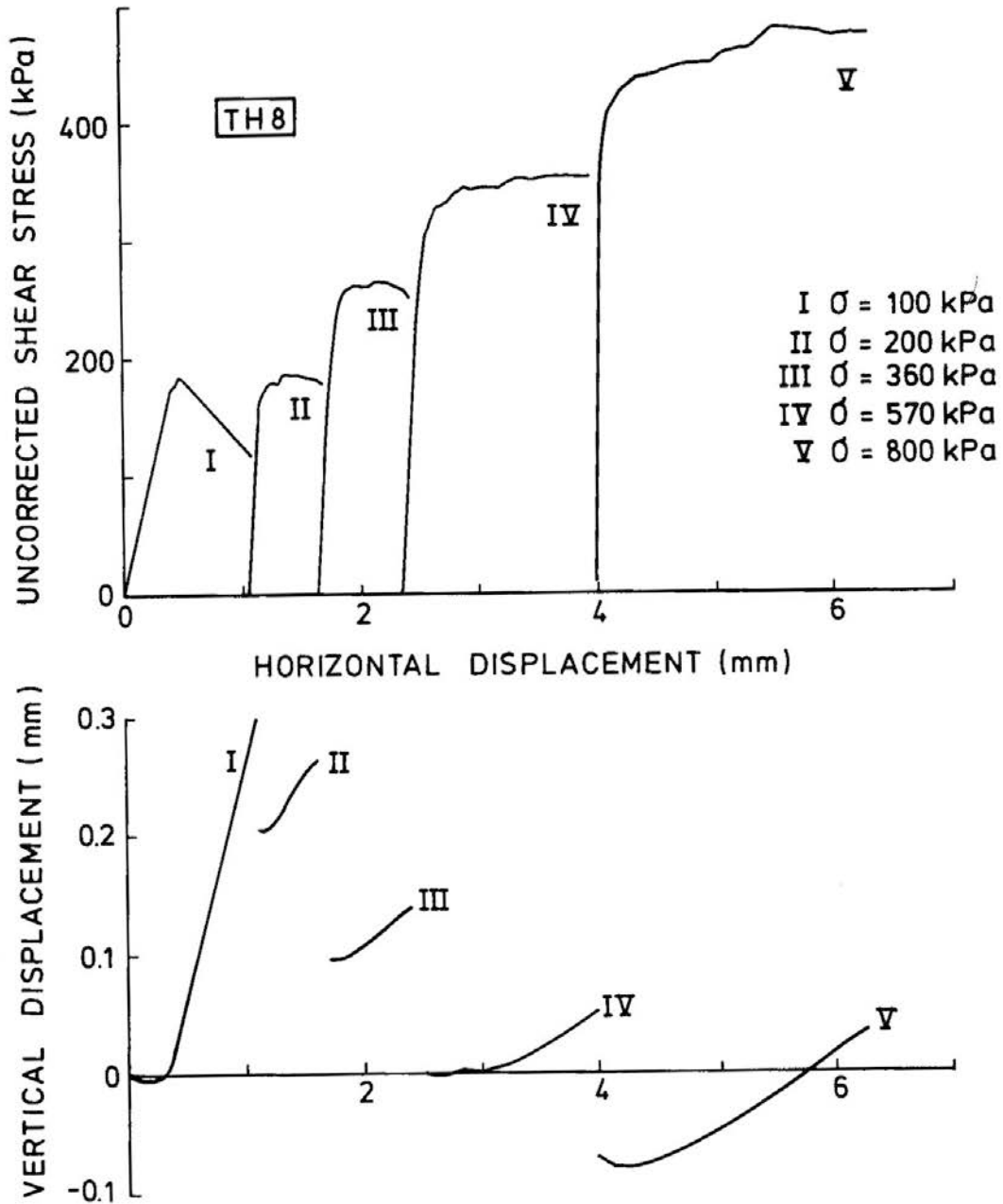
152

Fig. 5. Typical shear test result.

or negligible effect. In about half of the specimens higher strengths were measured during the first test stage when small asperities were sheared through. These could be regarded as an effective cohesion, but in the final

153
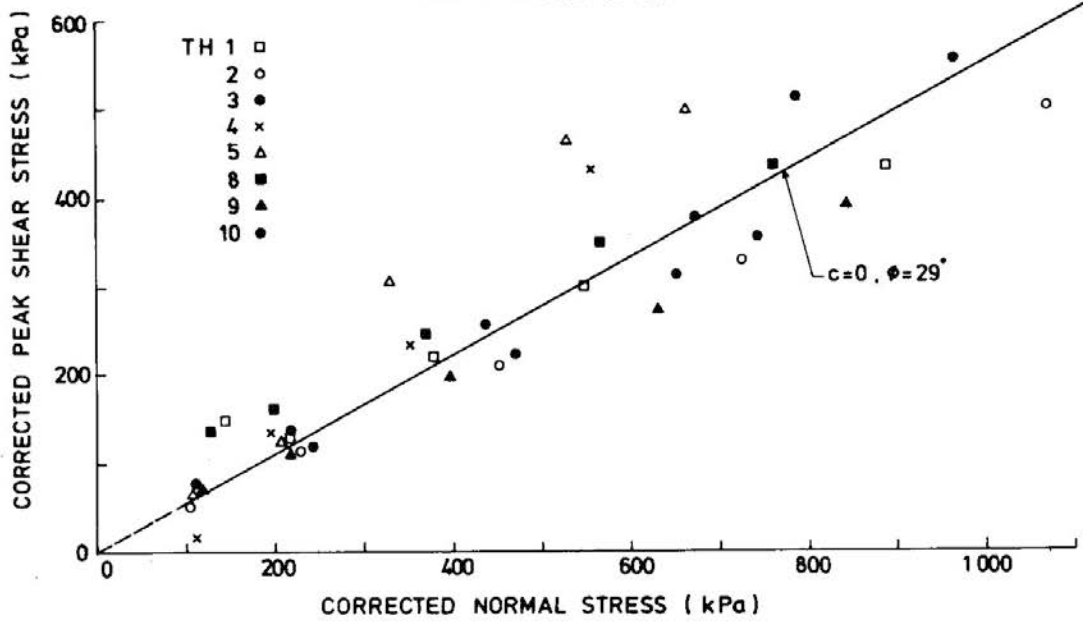
Fig. 6. Summary of direct shear test results.
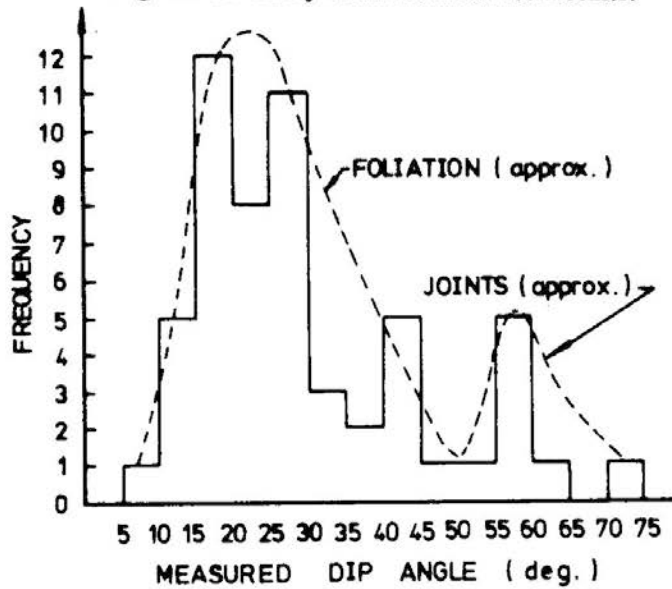
Fig. 7. Histogram of dip angle of foliation and joints measured from drill cores.

interpretation of the results, this was neglected and the basic frictional resistance of foliations was taken as 29°.

Observations of the foliations in cores showed a wide variation in dip angles (Figure 7). Nearly all the foliations were remarkably smooth at this scale. In limited field exposures such as trial pits no macro waviness was observed, apart from some attributed to hillside creep. Although faulting

154
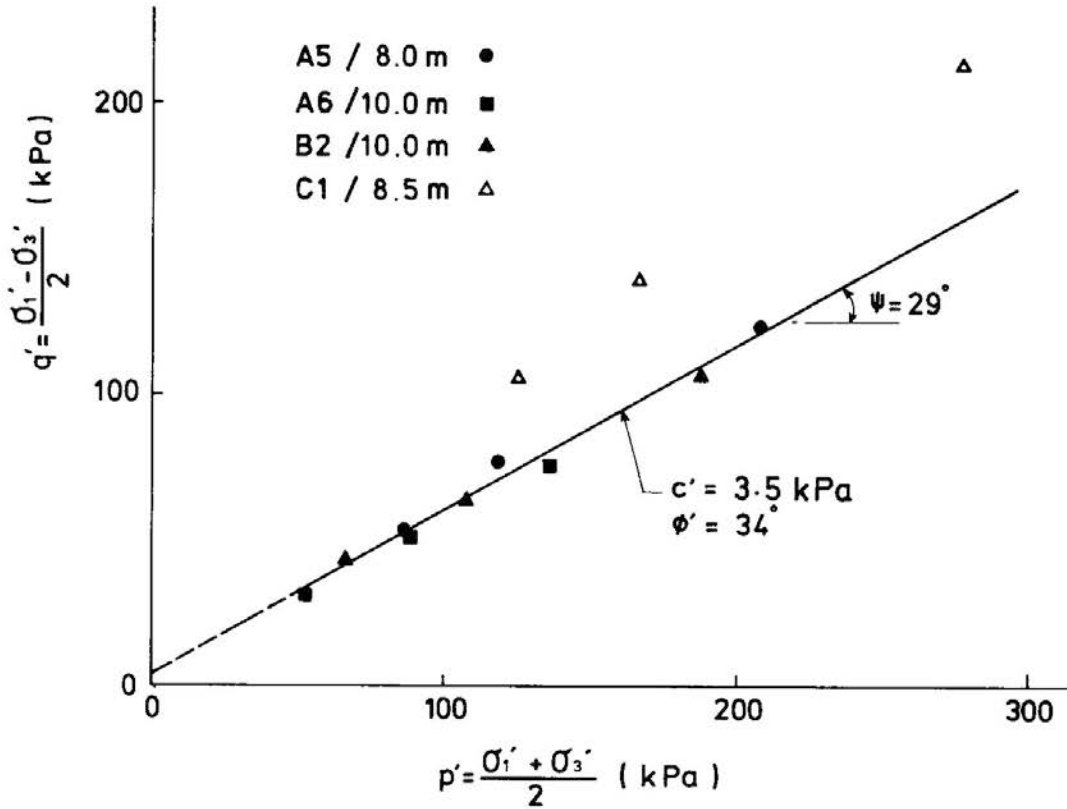
Fig. 8. $p' - q'$ plot for completely weathered rock.

and folding was believed to be present within the site, a conservative value of roughness (i) of $1°$ was adopted, also partly because of concern about long term weathering effects on foliations.

Four soil specimens were tested in consolidated undrained triaxial compression with pore pressure measurement, also using a multistage technique. These specimens were chosen from zones where the metamorphic rock had weathered to a mottled yellow brown sandy clayey silt having a dry density of about 1.4 Mg/m^3. The p'-q' plot for these tests is shown in Figure 8, along with the interpreted shear strength parameters of $c' = 3.5$ kPa and $\phi' = 34°$.

Cut Slope Design

The presence of a number of sets of discontinuities (bedding, cleavage, schistosity, joints) meant that various types of structurally controlled

155

failures were possible, both in the "rock" zones of fresh to moderately weathered metasedimentary rocks and the highly and completely weathered "soil" zones where these discontinuities manifested themselves as relict structures, wherever these discontinuities were unfavourably oriented to the slope. The stability conditions were made more complicated by the intense folding and faulting which had resulted in the structure being variable within short distances even along the same alignment.

The possibility of sliding was also enhanced by the differential weathering in areas of interbedded metasandstones and phyllites where the latter rocks were weathered to clayey silty soil-like materials with reduced shear strengths. Inclined bedding would also allow high pore water pressures to be developed in some weaker more permeable layers.

As reported by many authors (e.g. DE FRIES, 1971; TINOCO & SALCEDO, 1981; DEERE & PATTON, 1971) foliation is one of the most dominant variables affecting the stability of slopes in both fresh and weathered metamorphic rocks. These foliation planes by virtue of their mode of formation contain alignment of micaceous minerals along them, which generally have low frictional properties. The decomposition of such foliation planes results in low strength micaceous clayey silty coatings or infilling early in the weathering process.

Another feature of residual (saprolitic) soils derived from phyllites and schists noted by DE FRIES (1971), TINOCO & SALCEDO (1981) and, AYETEV (1985) is the strain softening properties along foliation planes. Many years after a cut is made, the first symptoms of instability may appear, and then slow movements accelerate until a major slide occurs. The movements then continue until the sliding mass attains a very flat surface. Such strain softening may be explained by further weathering of irregularities so as to decrease their strength or by displacements along an irregular discontinuity surface (DEERE & PATTON, 1971).

Discontinuity controlled failures were expected to govern stability to near the ground surface. Consequently design was based on kinematic analysis for all excavated slopes. The slopes were checked for soil type failures where the rock was completely weathered and where the foliation was favourably oriented (for example the south western slope, Figure 10).

For the 25m high main reservoir cutting (Figure 10, eastern slope) the orientation of the slope is shown in Figure 2 together with the available structural data. Selection of a 28° design angle was based on the available

156
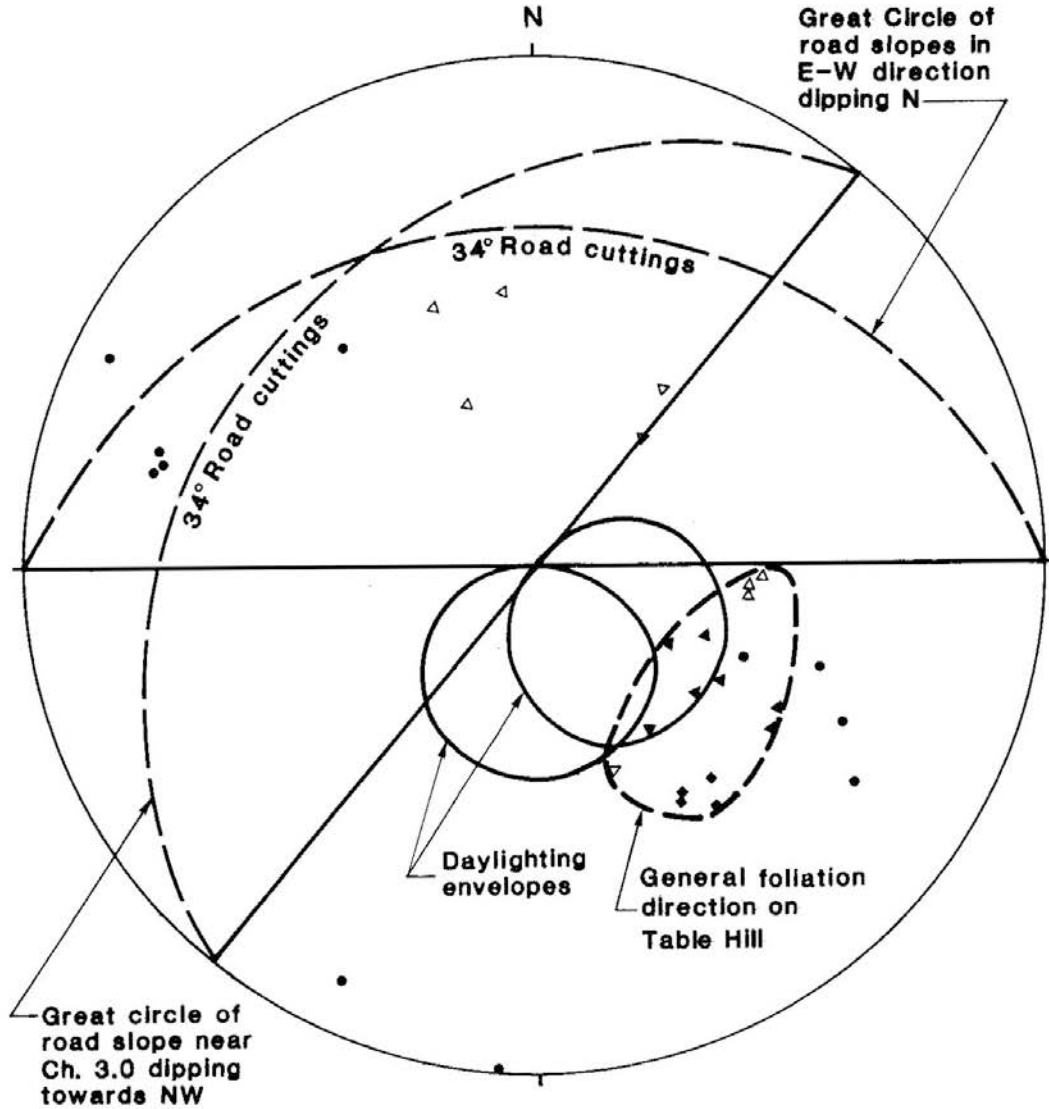
Fig. 9. Stereoplot for design of the main road slopes.

laboratory direct shear data, estimates of roughness, waviness, the persistence of foliations, and anticipated groundwater conditions. For the main road slopes, the stereoplot is given in Figure 9.
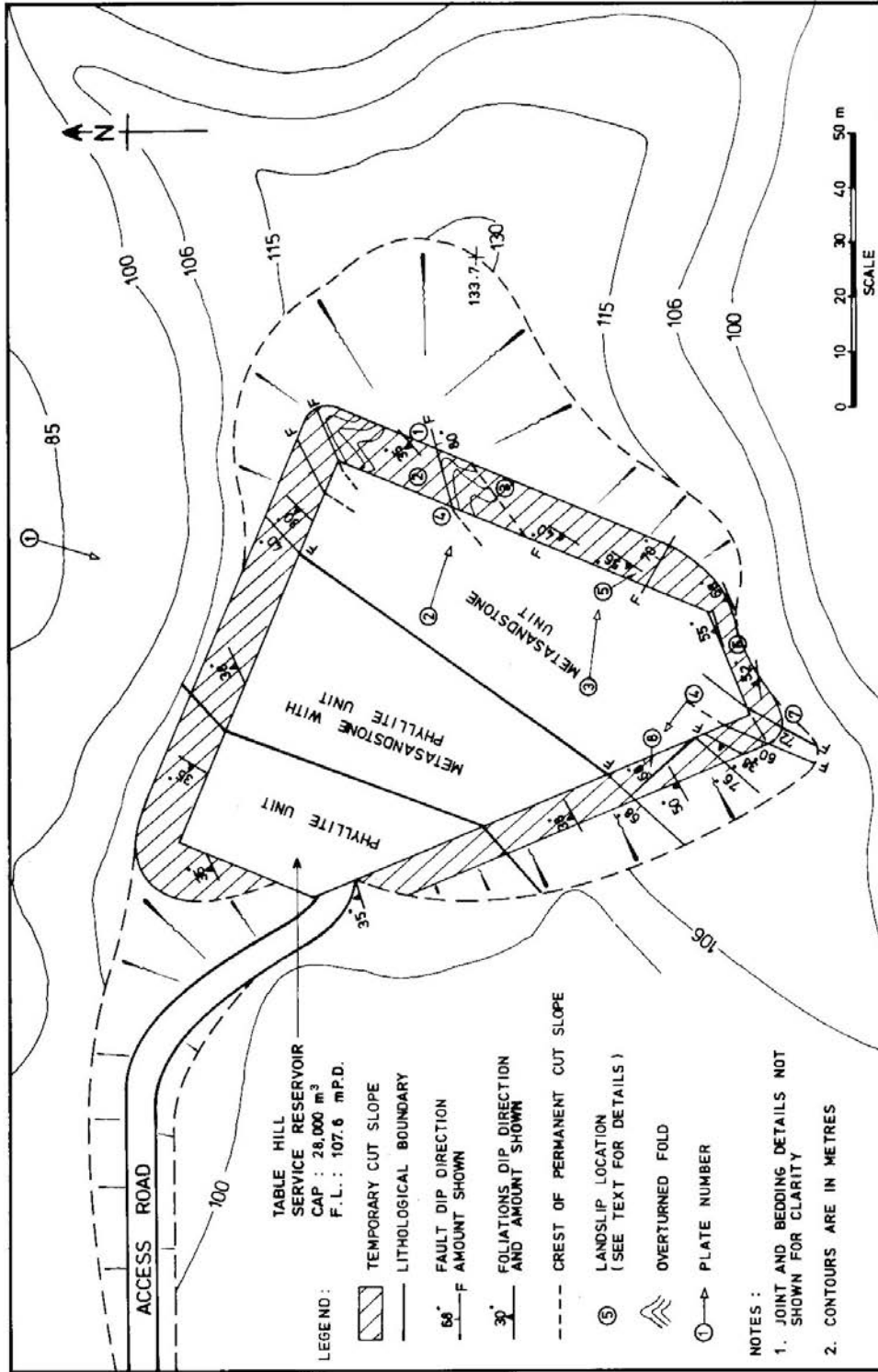
Fig. 10. Geological map of the reservoir site.

Geological observations were continued during the construction phase to continually assess the stability of the temporary and permanent cut slopes, since the original design was based on very limited field data.

CONDITIONS EXPOSED DURING CONSTRUCTION

Solid geology

The excavations for the slopes and foundation of the reservoir revealed that the geological structure and the weathering profile were complex as predicted from the limited field investigations. The main rock types were low grade metamorphosed siltstones and sandstones with some shaly horizons. The lithology is varied over the site and is complicated by extremely intense folding and numerous faults. The mapping of the excavation was carried out in terms of three broad engineering geological units and the weathering grade of the rock mass (Figure 10). The three geological units based on the dominant lithology, from east to west are:

> *Metasandstone unit* - fine to medium-grained, dark grey coloured metamorphosed sandstones, very strong when fresh, with a pronounced undulating schistosity. Occasional bands or beds of folded and sheared shaly rocks.

> *Metasandstone and Phyllitic Siltstone Unit*-interbedded strongly schistose metamorphosed sandstones and finely cleaved phyllitic siltstones and silty shales.

> *Phyllite Unit*-dominantly phyllitic siltstones with a strong cleavage and schistosity. Occasional sandstones and shaly bands.

Discontinuities

Intense folding was observed on one face of the excavation (Plate 2). In the larger exposure bedding could be observed with a similar dip to the schistosity, generally 35° to 40° to the northwest. The area had been subjected to significant faulting with the majority of the faults having a similar trend to the foliation, i.e. NE-SW. Some cross faults (E-W and SE-NW) were also present (Figure 10).

The discontinuities measured during excavation (Figure 11) showed a wider scatter in foliation dip and direction than those measured during the preliminary investigations (Figure 3). The surfaces were highly undulating with dips ranging between 27° and 55° but generally 30° to 35°. The majority
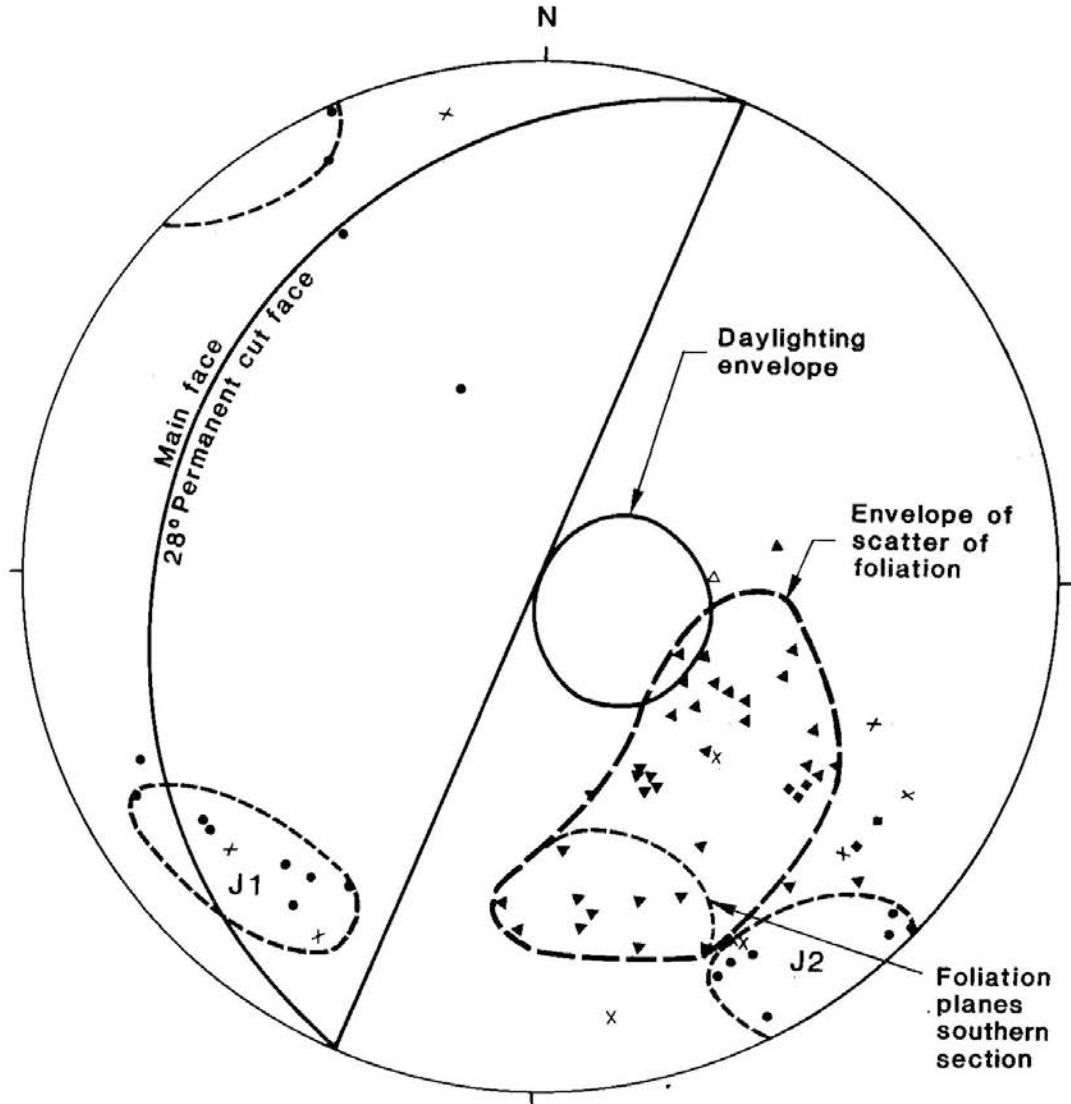
159

Fig. 11. Stereoplot for main cut slope, showing data measured on exposed slope.

of the foliation planes, particularly in the more intensely weathered zones, contained clayey and silty micaceous coatings/ infills/ bands resulting from weathering of mica-rich, aligned layers in the original rock.

Weathering

The weathering grades were observed in the excavation to roughly coincide with the general shape of the hill, with completely and highly weathered rock gradually passing into moderately and slightly weathered rock. Slightly to moderately weathered rock, grades II to III, was exposed on the eastern temporary cutting close to the foundation level of the reservoir, approximately 20 m below the original ground level. The weathering profile was complicated by folding, faulting and lithological variations with phyllitic rocks differentially deeper weathered when compared to the schistose sandstones and quartzites.

A gradual deterioration was observed in highly and completely weathered metamorphic rocks where weakly cemented, highly weathered phyllitic siltstones turned into friable, easily erodible soils as the rocks were exposed to atmosphere and rainwater.

FAILURES IN WEATHERED ROCKS

One major aspect of foliation which was favourable to stability at this site was that the surfaces were often not very persistent and were wavy, with waviness angles up to 20°. Failures in temporary cuts were thus localised. Sliding types of failures were rare on foliation planes gentler than 50° to 55°, particularly in fresh to slightly weathered rocks because of this waviness. The majority of the failures occurred on dry days.

A number of small failures, all less than 100 m³, occurred on the very steep temporary slopes of the reservoir cutting during excavation, and some minor ones on the much gentler permanent slopes. All were discontinuity controlled failures, even in the saprolitic soil.

Many of the failures controlled by the extremely variable structural features could not have been predicted from the preliminary investigations and borehole joint measurements. The failures are described briefly below, following the numbers shown in Figure 10.

Failure 1. A small wedge failure of less than 2 m³ along a 35° foliation plane and a steeply dipping joint plane occurred in slightly weathered

161

metasandstone. The slip surface appeared clean but may have contained a thin coating of clayey infill (Plate 2).

Failure 2. A small sliding failure, less than 2 m³, occurred along a clean foliation plane dipping at about 35° towards the cutting with a vertical J2 joint acting as back release plane. The joints of set J1 acted as side release surfaces (Figure 11 and Plate 3).

Failure 3. A small steep wedge of weathered rock slid mainly along a weathered minor low angle shear surface with an almost vertical J1 joint acting as the other sliding surface. Both the shear zone and the joint contained silty clayey infill. The back release surface was a steeply dipping J 2 joint (Plate 2).

Failure 4. About 1 m³ of soil and rock mixture flowed from a weathered cross fault zone (Plate 2).
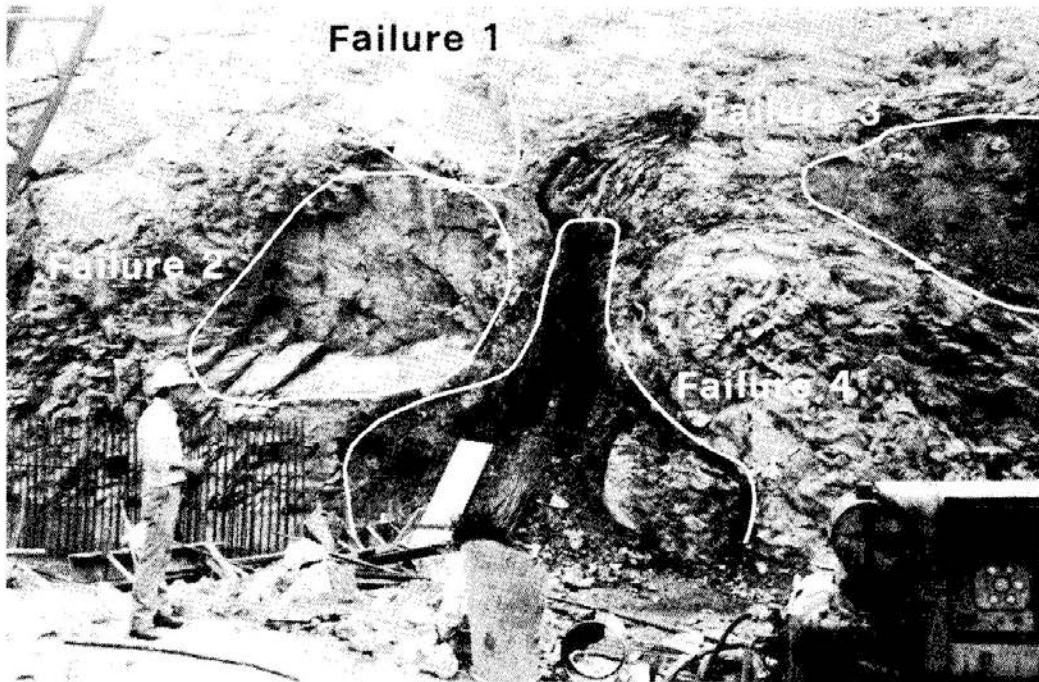
Plate 2 Eastern side of reservoir excavation showing overturned fold in metasandstone and four failures.

Failure 5. Approximately 6 m³ of an almost fresh, closely folded metasandstone block slid along a relatively steeply dipping, very pronounced foliation plane daylighting near the toe of the slope. The foliation plane had a very undulating, shiny micaceous surface with dip varying between 50° and 65°. The northern side release surface was irregular (Plate 3).

162

Failures 6 and 7. The orientation of the foliation planes in the southern cutting assumed a more northerly direction (Figure 10) as a result of intense faulting generally with NE-SW, but also some with NW-SE, trends. The rocks in this area were more deeply weathered so that the small permanent upper cutting and the majority of the lower temporary cutting were in completely to highly weathered metasandstones.

A failure involving some 100 m³ of material occurred during moderate rainfall. This was followed by another planar sliding failure along a steep and undulating foliation plane with average dip 60°, daylighting about 2 m
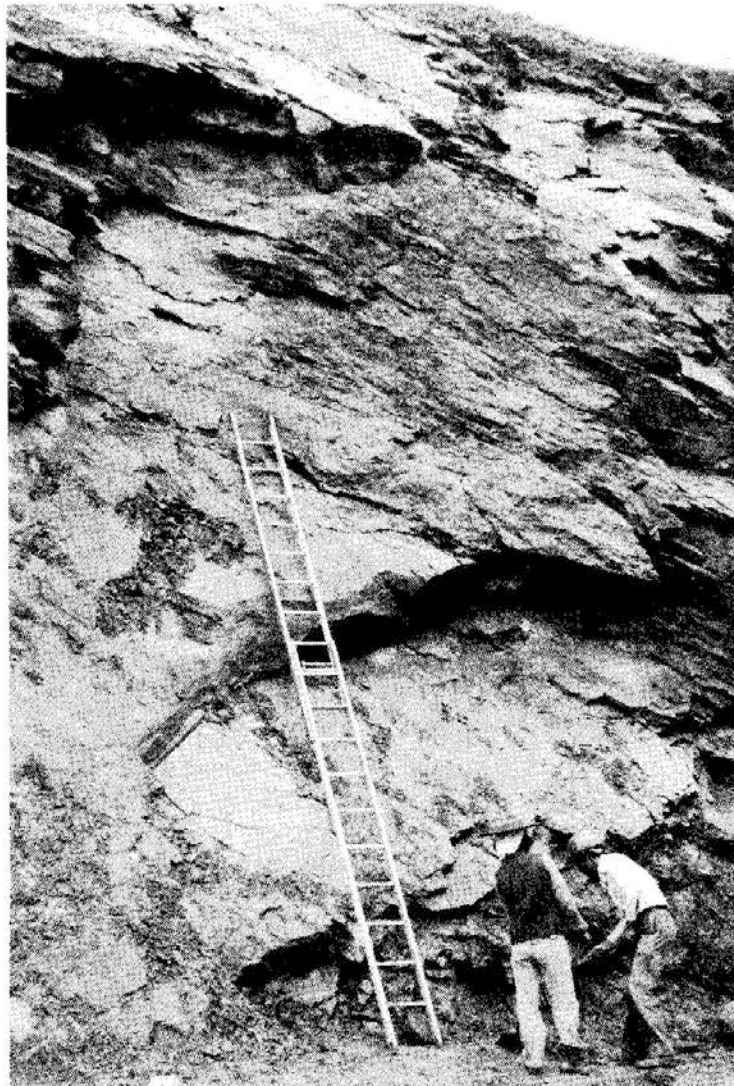
Plate 3 Failure along foliation (failure no. 5).

163

above the slope toe. The slope was cut at 73°. The side release surfaces were the weathered joints of J1 set. A number of open, vertical joints of set J2 parallel to the slope surface were present in the failure area indicating that the failure, which occurred sometime after the excavation, might have been initiated by the opening up of these joints due to stress release. The latter failure was also of similar mode and the slip surface was largely controlled by the undulating foliation plane. The fault zone, which contained 50 to 500 mm thick weathered, clayey fault gouge, acted as the western side release

Plate 4 Failure along fault (failure no. 8).

surface. Two small wedge failures conditioned by foliation planes and moderately dipping joints of J1 set were also apparent towards the head of the latter slip in less weathered metasandstones (Failure 7).

Failure 8. Both the 8 m high and 100 m long temporary slope (at 85°) and the overlying gentler (34°) 6 m high permanent slopes of the western reservoir cutting performed satisfactorily due to favourable jointing, bedding and foliation orientations in this area except for a rather unexpected failure in the temporary slope. Orientation of both the foliation and bedding planes were more consistent, less steep (35° to 40°) and generally perpendicular to the cutting face. The rocks were variable from metasandstones at the southern end to phyllites at the northern end. They were all highly to completely weathered. The failure occurred along a 68° dipping fault which contained 50 to 150 mm of crushed rock and clay mixture striking rather obliquely, by about 20°, to the cut face. The slip occurred on a dry day towards the end of the dry season.

Road Slopes

The cuttings along the access road generally performed satisfactorily, particularly the road sections with faces dipping north. The majority of the road cuttings followed an E-W trend with faces dipping north at 34°, i.e. at the average gradient of foliation planes dipping very obliquely to cut face. Along one section of the road the slope face was parallel to the northwest dipping dominant foliation direction (Figures 4 and 9) in highly to completely weathered, mainly phyllitic rocks. Minor slides developed locally where foliation planes were steeper than the slope face with the joints of set J2 (Figure 11) acting as back release planes.

CONCLUSIONS

A case history of slope formation and performance in low grade metamorphic rocks in Hong Kong has been presented. Permanent slopes, were designed on the basis of direct shear test results on weathered foliations. Steep adversely oriented temporary cuts suffered a number of failures during construction. The extent of these was limited by the waviness and complex folding of the sediments. Many of these failures could not have been predicted from the preliminary investigations and borehole joint measurements.

REFERENCES

ALLEN, P.M. & STEPHENS, E.A. (1971). *Report on the Geological Survey of Hong Kong.* Hong Kong Government Press, 116p.

AYETEV, J.K. (1985). Slope stability investigations and design parameter studies in phyllites in Ghana. *Bulletin of the International Association of Engineering Geology,* no. 31, pp. 19 - 23.

DEER, D.U. & PATTON, F.D. (1971). Slope stability in residual soils. *Proceedings of the 4th Panamerican Conference on Soil Mechanics & Foundation Engineering.* Puerto Rico, vol. 1, pp. 87 - 170.

DE FRIES, C.K. (1971). Personal communication in Deere, D.U. & Patton, F.D. (1971). Slope stability in residual soils. *Proceedings of the 4th Panamerican Conference on Soil Mechanics and Foundation Engineering.* Puerto Rico, vol. 1, pp. 87 - 170.

HENCHER, S.R. (1987). The implications of joints and structures for slope stability. In *Geotechnics and Geomorphology of Mass Movement* edited by M.G. Anderson & K.S. Richards, pp. 145 - 186, John Wiley and Sons, Chichester, England.

HOWAT, M.D. (1985). Empirical slope design for metamorphic saprolites. *Proceedings of the First International Conference on Geomechanics in Tropical Lateritic and Saprolitic Soils,* Brasilia, vol. 4, pp. 353 - 356.

TINOCO, F.H. & SALCEDO, D.A. (1981). Analysis of slope failures in weathered phyllite. *Proceedings of the International Symposium on Weak Rock;* Tokyo, vol. 1, pp. 55 - 62.

DRIVEABILITY OF PILES AND THE EFFECTS OF FOLLOWERS

K.Y. WONG[1], Y.K. CHOW[2], G.P. KARUNARATNE[2], and S.L. LEE[3]

SYNOPSIS

This paper presents a wave equation study on the effects of using pile followers on driveability and driving stresses, as well as driveability analyses of large diameter offshore piles at three sites. The analyses were carried out using a new wave equation model. These show that the use of followers which are impedence matched can result in minimal loss of driveability. The analyses also included followers for land piles driven below ground as may be required for piles supporting basements. For the driveability analyses, driveability of large diameter piles at three offshore sites were investigated. These cases were for piles driven in chalk, clay and sand.

INTRODUCTION

In pile driving operations, a follower or chaser is frequently used as an intermittent element to transmit the hammer energy to the pile. Followers are extensively used for example, in offshore piling and in situations where the top of the pile is out of reach of the working level of the hammer. These situations are common for piles slotted into jacket legs. For these followers used offshore, gravity connectors are used. An advantage of pile followers is that the followers may be removed after driving and reused.

Whereas followers for offshore piles are usually the same size and material as the piles, followers for land piles may be of different dimensions and materials. There can be doubts on the efficiency of followers in transmitting the hammer impact energy to the pile, moreso, if the followers are of a different material from the pile. The non-rigid joints and the change in material properties at the pile-follower interface can result in changes in the stress wave propagation characteristics. It is, therefore, of interest to study the effects of using pile followers on driveability and driving stresses.

In most driveability analysis, the wave equation model used is that due to SMITH (1960). The input parameters required in the SMITH (1960) model are generally obtained by correlation with load test results and driving records. Some experience is required in selecting these parameters to enable a reasonable driveability prediction.

1. Research Scholar, 2. Senior Lecturer and 3. Professor and Head, Department of Civil Engineering, National University of Singapore, Kent Ridge, Singapore.

A new one dimensional wave equation model was presented by LEE et al (1987). The soil model is derived using visco-elasto dynamic theory. Unlike the SMITH (1960) model, the input parameters consist of conventional soil mechanics parameters. These soil parameters are determinable from laboratory tests or correlated to conventional soil properties. A major improvement of this new model over the SMITH (1960) model is the proper modelling of energy losses through the propagation of shear waves to the soil mass. This mode of energy dissipation is commonly known as radiation damping. In addition, the failure load in this new model includes the rate effects (for example, see LITKOUHI & POSKITT, 1980) that enhance the failure load to above that for the static failure load when soil is rapidly loaded. Recommendations for the selection of these rate effects parameters are presented in LEE et al (1987) to facilitate their selection in the absence of experimental data.

The effects of residual stresses on pile driveability were investigated using the new wave equation model presented by LEE et al (1987). These residual stresses were accounted for by carrying out multiple hammer blow analysis. The studies showed that in general, for piles with small tip resistances, for example piles in cohesive soils, the blowcounts determined from a single blow and that from a multiple blow analysis are similar. Predicted driving stresses are, however, found to have increased for multiple blow analysis. For piles with a large tip and/or shaft resistance, for example a pile driven in sand, the blowcounts determined from a single blow analysis are lower than that determined from multiple blow analysis. Predicted driving stresses are also increased for multiple blow analysis. Therefore, although driveability of piles in cohesive soils may be determined by a single blow analysis, peak driving stresses should be determined by multiple blow analysis. Driveability and driving stresses predictions for piles driven in sand or tip bearing in sand should be carried out by multiple blow analysis. It was found that five blows applied consecutively is usually sufficient to build up the residual stresses to a relatively 'stabilised' value.

PILE FOLLOWER STUDY

This section presents a study of the effects of the geometric and material properties of a pile follower on driveability and driving stresses. The gravity connector is assumed to transmit only compressive stress waves. Furthermore, the connector is assumed to be in contact with the pile prior to the impact of the hammer.

Wave equation simulations using the SMITH (1960) model on the effect of followers on the driveability of offshore piles were reported by HEEREMA (1979). These simulations showed minimal loss of driveability for a follower having the same material and geometric property as the pile. However, during pile installation, some driveability loss was observed. HEEREMA (1979(a)) attributed this driveability loss to the 'shakiness' of the joint and the concentrated mass due to the gravity connector at the joint which changes the stress wave characteristics. There can be other possible reasons for the increased blowcounts, for example, the delivered hammer energy may be less than that assumed in the wave equation simulations or variations in the soil profile.

The implications of a follower that can result in minimal loss of driveability are significant, both from economic and construction viewpoints. The improper selection of offshore followers and connectors may result in driveability losses that may result in the need for costly remedail solutions. For land piles supporting basements, the use of a properly selected follower could result in significant cost savings. A possible manner of installation of these piles is to drive full length piles to the desired depth, excavate to the intended level and cut off the excess lengths. This procedure, however, results in difficult excavation works for closely spaced piles. Higher construction cost is inevitable due to the longer excavation time and pile wastage due to cut-offs. However, if a follower is driven to the intended excavation depth, excavation can be carried out in an unhindered manner upon completion of driving.

Impedance Matching

The finite stiffness of a pile implies that the dynamic spatial responses will not occur simultaneously at every location in the pile when subjected to dynamic loading, i.e., a wave action is present. Five parameters may be identified that can result in a change in the wave propagation characteristics in the pile. These are;

   (i)   the geometrical and material properties of the pile,
  (ii)   the location of the cushion (for concrete pile driven by steel followers),
 (iii)   the effect of the no tension joint,
 (iv)   the soil resistance distribution,
  (v)   material damping of the pile.

The geometrical and material properties affecting the characteristics of the propagation of a longitudinal wave in the pile element may be defined by the

169

impedance of the element. The impedance, Z, is defined as $E_p A_p / c$ where c is the speed of wave propagation in the element. This wave speed, c, is defined as $\sqrt{E_p / \rho_p}$. It may be shown (FISCHER, 1984), that the force pulse transmitted from one pile element to another, in the absence of external soil resistance, depends on the ratio of the impedances of these two pile elements. Appendix II illustrates the effects of impedance difference of two elements on the propagated stress waves. It is evident from Appendix II that by impedance matching the two elements, the efficiency of transmission of the stress-wave is maximum.

For land piles, the common pile materials are steel, concrete and timber. For steel piles, steel followers are used. To ensure minimal loss of driveability, one needs to select the same cross sectional area for the follower as the pile. However, for concrete piles, steel followers are commonly used. The typical Young's modulus is $210 \times 10^6 \, kN/m^2$ and $31 \times 10^6 \, kN/m^2$ and the typical density is 7.8 tonnes/m^3 and 2.5 tonnes/m^3 for steel and concrete respectively. Therefore, the cross-sectional area ratio of the steel follower to the concrete pile for impedance matching is approximately 0.225.

Wave Equation Simulations

Wave equation simulations were carried out for followers of various material and geometric properties to study the effect of the change in impedance of the follower on the driveability and driving stresses in the piles. For followers below ground surface, the shaft resistance from the soil per unit length of the follower is assumed to be the same as that acting per unit length on the pile. Fig. 1 shows the representation of a pile driven with and without a follower used in the analyses. Four cases are presented to illustrate the effects of pile followers on drivability and driving stresses in the pile. These cases are:

(1) The effect of a steel follower of the same geometric property on the driveability of a large diameter steel pipe pile. This follower is above ground level. The pile has an outer diameter of 914 mm and a cross sectional area of 0.088 m^2. The pile is driven to a depth of 35m by a Menck 3000 hammer. The soil has an average undrained shear strength of 200 kN/m^2. The remoulded shear strength during driving was assumed to be a third of the undrained shear strength. For this high undrained shear strength, the rate effects coefficients were assumed to be $0.3 \, (s/m)^{0.2}$ and $0.2 \, (s/m)^{0.2}$ for the soil at pile shaft and tip respectively. The soil plug is assumed to be 50 percent of the pile penetration.
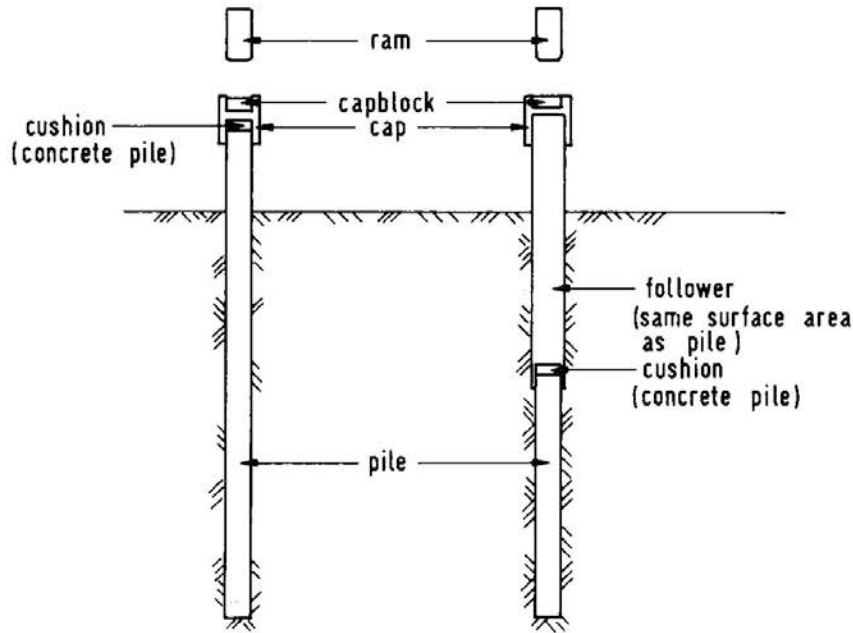
Fig. 1. Representations of a full pile and a pile driven using a follower.

(2) The effect of a steel follower driving a concrete pile in a homogeneous cohesive soil. The pile is 280 × 280 mm square driven to a depth of 32 m by a Kobe 25 hammer. The soil has an average undrained shear strength of 60 kN/m². The remoulded shear strength during driving was assumed to be a third of the undrained shear strength. The rate effects coefficient were assumed to be $1.0 \ (s/m)^{0.2}$ and $0.4 \ (s/m)^{0.2}$ for the soil at pile shaft and tip respectively. This follower is driven to 12 m below ground level.

(3) The effect of a steel follower driving a concrete pile in a twolayer cohesive soil. The pile has a diameter of 0.4 m and is driven to a depth of 30 m with a Kobe 35 hammer. The upper soil layer has an undrained shear strength shear of 100 kN/m² while the lower soil layer has an undrained shear strength of 50 kN/m². The remoulded shear strength during driving was assumed to be 0.4 times the undrained shear strength. The rate effects coefficients were $1.0 \ (s/m)^{0.2}$ and $0.3 \ (s/m)^{0.2}$ for the soil at pile shaft and tip respectively. This follower is driven to 10 m below ground level.

(4) The effect of the same driving system, follower and pile as in Case (3) above, but the soil profile is reversed.

Driveability curves of penetration depth versus blowcounts for various impedance ratios of follower to pile and for the full driven length of the pile are presented in Fig. 2. In addition, the variation of maximum compressive
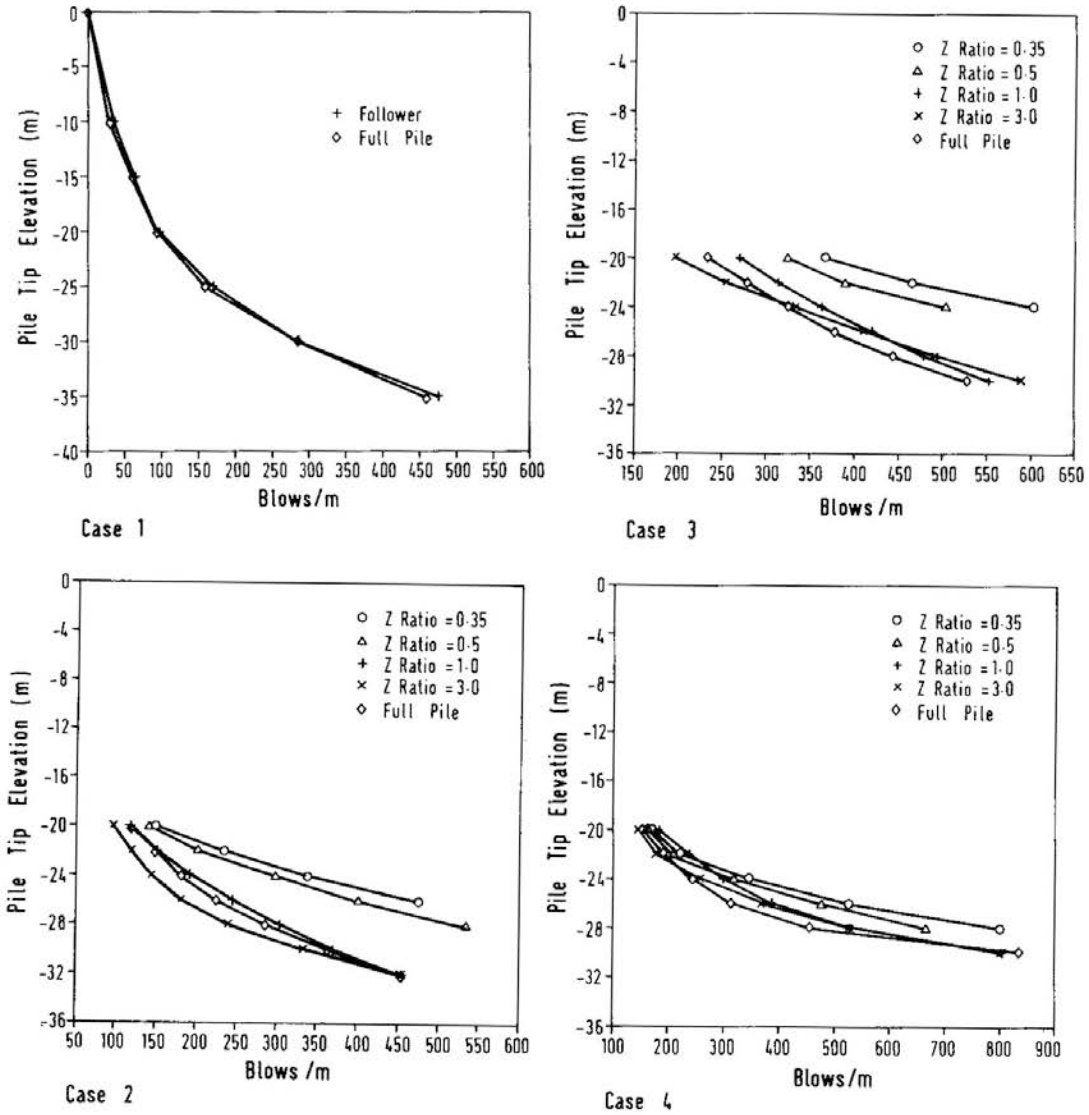
Fig. 2. Blowcounts versus penetration curves for the cases studied for various impedance ratios of follower to pile.

and tensile stresses along the pile for the case of matched impedance and the case of driving the full length of pile at final penetration, are presented for Cases 2, 3 and 4 in Fig 3.

From Fig. 2, it is evident that the smaller impedance followers result in substantial driveability loss when compared to that for the full pile. The impedance matched follower consistently shows minimal driveability loss.

172

The primary differences between the impedance matched follower and the full pile are the location of the cushion and the "no-tension" joint between the follower and the pile. From the analyses carried out, it appears that the location of the cushion and the "no-tension" joint for the impedance matched follower results in minimal driveability loss. It therefore appears that followers may be used to drive piles below ground with acceptable driveability losses if the followers are impedance matched with the piles.

The larger impedance follower shows slightly easier driveability when the depth of embedment of the follower is small. However, the rate of increase in blow counts with penetration suggests that at deeper penetrations the larger impedance follower may result in harder driveability as illustrated by Case 3. One possible reason for the driving behaviour of the larger impedance follower may be due to the change in stress wave characteristics by the increased soil resistance at deeper penetration. Note that the impedance of the pile cap is usually larger than that of the cushion and pile. For the cases presented, the smaller β ratio of the pile cap to follower for the case of the larger impedance follower (compared to that for the full pile or impedance matched follower) results in a slightly larger transmitted energy from the larger impedance follower across the cushion to the pile at shallow penetration. Thus, at shallow penetration, the driveability of the larger impedance follower is slightly easier than the full pile. However, at larger penetration, the increased soil resistance and the cushion can result in significant changes in the stress wave characteristics propagated to the pile. The increased soil resistance results in a smaller particle velocity in the larger impedance follower, and the larger β ratio of the follower to cushion for the larger impedance follower, results in larger reflected waves from the follower-cushion interface compared to that for the impedance matched follower. The full pile will only experience a reduction in particle velocity. The consequence of these changes in the stress wave characteristics in the larger impedance follower results in a smaller transmitted energy to the pile than that for the full pile or the impedance matched follower. Thus, at larger penetration, the rate of increase of blowcounts with depth increases for the larger impedance follower at a rate that is greater than the full pile or the impedance matched follower.

An interesting feature of the use of followers on pile stresses is the reduction of peak compressive driving stresses in the pile as shown in Fig. 3. The maximum compressive stresses during driving generally occur around the ground level as shown in Fig. 3. Therefore, the compressive stresses may exceed the compressive strength of the concrete if higher energy is delivered

173
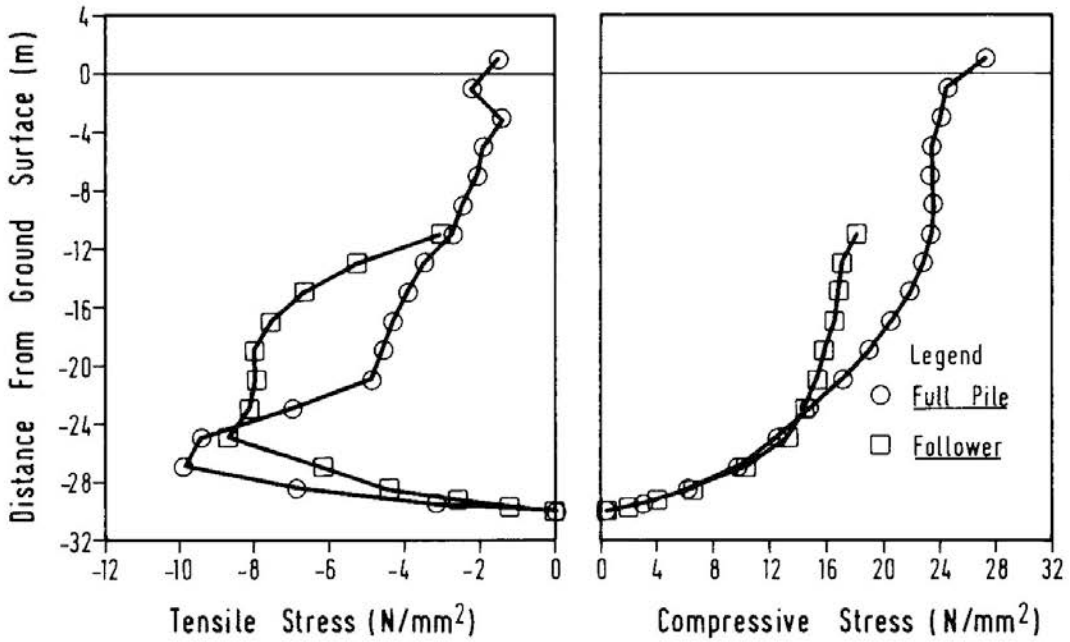
Penetration = 30 m

Case 2 - Homogeneous Cohesive Soil
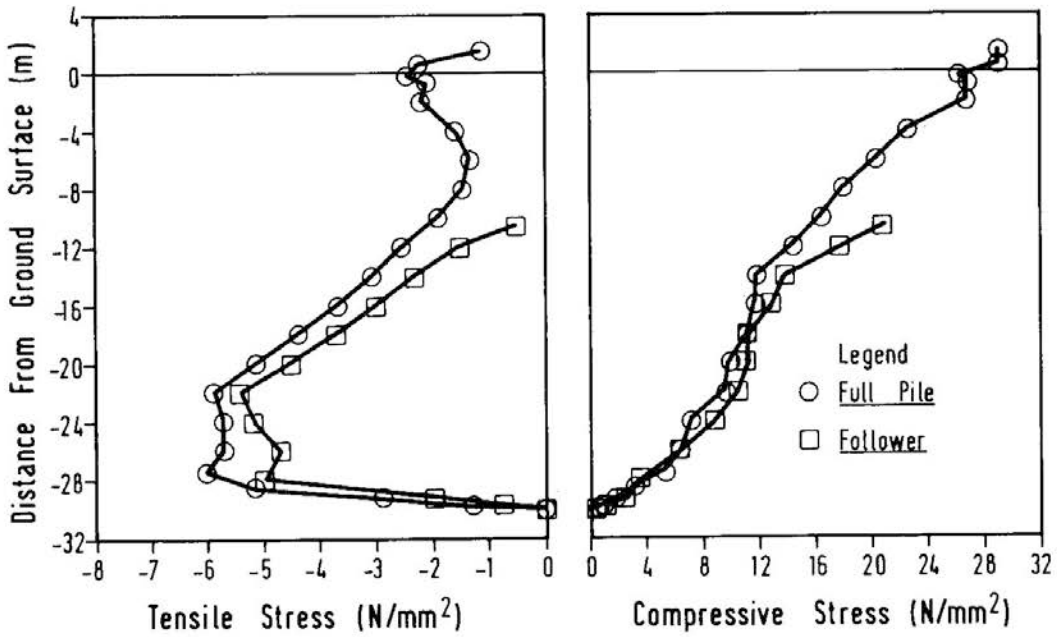
Penetration = 30 m

Case 3 - Stiff Clay to Soft Clay Profile

Fig. 3. Maximum driving stresses along pile for Cases 2, 3 and 4 for the full pile and for an impedance matched follower at final penetration.

174

Penetration = 30 m
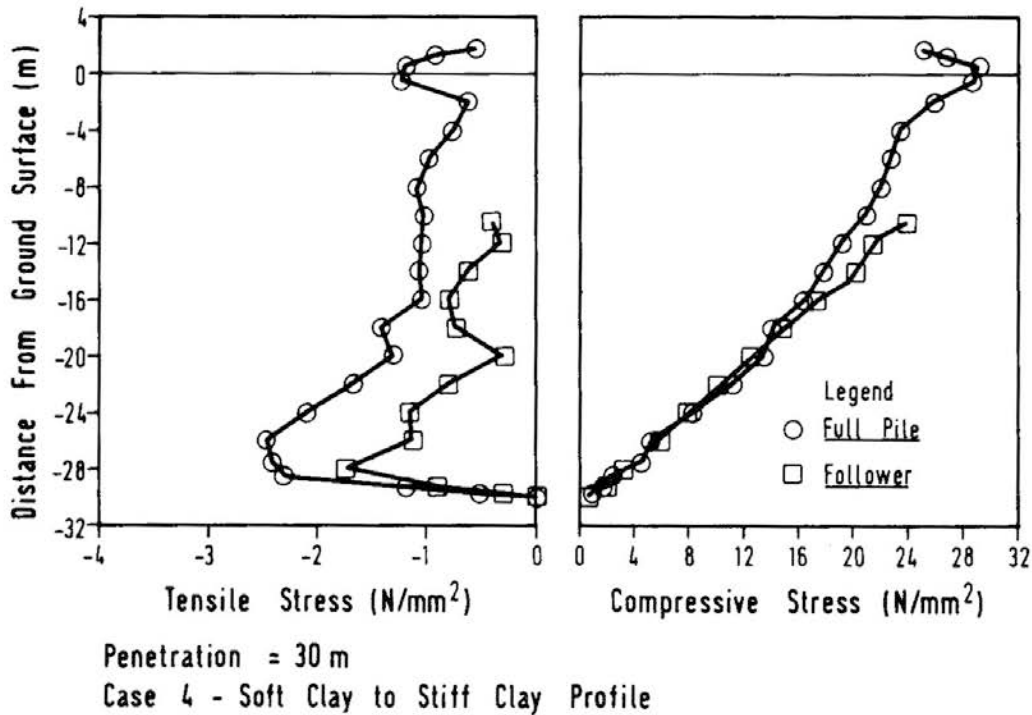Case 4 - Soft Clay to Stiff Clay Profile

Fig 3. (Continued) Maximum driving stresses along pile for Cases 2, 3 and 4 for the full pile and for an impedance matched follower at final penetration.

under hard driving conditions. With a follower, the maximum compressive stresses occur in the follower resulting in acceptable compressive stress in the pile. It is interesting to note that the use of a follower does not result in significant differences in the peak tensile driving stress, even for the case where large tensile stresses developed in the full pile. Case 4, with the large tensile stresses illustrates this point. The general trend of tensile stresses distribution in the pile for the follower case is also similar to the trend of the tensile stresses in the full pile.

Practical Considerations

The four cases presented indicated that it is possible to use followers to drive piles with acceptable loss of driveability if the followers are impedance matched with the piles. In the analysis it was assumed that the follower and pile are in contact prior to the hammer impact. For a follower above ground, this is easily achieved since, the weight of the follower would ensure contact with the pile. For followers driven below ground, a mechanical device may be required to realise this assumption. This is because a slack may develop due to the 'no tension' criteria for the follower-pile connection at the end

175

of the hammer blow. The weight of the follower may not be adequate to overcome the side soil resistance acting on the follower to ensure contact with the pile. The type of device must be designed with considerations based on the follower and pile geometry. A clamp type device may be one possibility. The detailed design of this device is beyond the scope of this paper. A method of extracting the pile follower may also be required for followers driven some distance below ground. Finally, a method to perform and evaluate the load carrying capacity of the pile has to be determined.

DRIVEABILITY ANALYSIS

This section demonstrates the capability of the new wave equation model to predict the driveability of large diameter offshore piles. In the preceding section, it was shown that the effect of an impedance matched follower on driveability loss is negligible. Therefore, in the driveability analysis if a follower of the same dimension as the pile is used, the follower may be treated as a segment of the pile. Three driveability cases are presented. In these examples followers were not used. In the three case studies presented, one case is for piles installed in the North Sea while the other two cases are for piles installed in the Arabian Gulf. The North Sea installation was first described by VIJAYVERGIYA & CHENG (1978) for piles driven in chalk. The Arabian Gulf installations were described by STEVENS et al (1982).

The static soil resistance during driving for cohesive soil was estimated from the remoulded shear strength of the soil. For cohesionless soils, the static soil resistance was estimated using the effective stress method recommended in API RP 2A (1981). The soil shear modulus, G_s, was estimated using the correlation with the undrained shear strength and the vertical effective stress for cohesive and cohesionless soils respectively. A G_s/c_u and G_s/σ_v' ratio of 150 and 200 was used for the cohesive and cohesionless soils respectively. The ratio of G_s/c_u of 150 is commonly assumed in the analysis of axially loaded piles in cohesive soils while the G_s/σ_v' ratio of 200 was determined by the authors, from back analysis of driving records and load tests of driven piles in sand (CHOW et al, 1987). The rate effects coefficient for the shaft, J_s^* was taken to be zero for the North sea installation. This is because of the low liquidity index (approximately zero) of the cohesive soil at that site the high undrained shear strength of the clay stratum and the brittle nature of the chalk. For Case 2, for sand, J_s^* was also taken to be zero (DAYAL & ALLEN, 1975 and HEEREMA, 1979b). For Case 3, for clay, J_s^* was assumed to be 0.3 $(s/m)^{0.2}$. This value of J_s^* was assumed

176

due to the high undrained strength at the site. The rate coefficient for the tip, was assumed for the three cases to be 0.1 $(s/m)^{0.2}$. The exponent N was assumed to be 0.2 (LITKOUHI & POSKITT, 1980).

A major uncertainty in the analysis of open-ended pipe piles is the soil plug behaviour. CHOW & SMITH (1984) and SMITH et al (1986) showed, using three-dimensional (axisymmetry) finite element analyses, that during driving the full internal soil resistance may be mobilised even though the pile may behave plugged during a static load test. Therefore, in the driveability analyses presented here, the soil plug resistance is assumed to be mobilised for the soil plug length assumed. A reduction of 50 percent of the internal shaft resistance was assumed with the use of a driving shoe.

North Sea Installation

Case A - This site is located in the Rough field. The site consists of a thick layer of very stiff clay overlying chalk. The average undrained shear strength for the clay, c_u, was 316 kN/m^2 (3 tons/sq ft). The average undrained shear strength of the chalk was 211 kN/m^2 (2 tons/sq ft). The shear strength of remoulded samples of the clay and chalk is about a third of the average undrained shear strength. 914 mm diameter steel pipe piles, with wall thickness of 31.75 mm, were driven to about 46 m below mudline. The piles were installed for an eight legged drilling platform and an eight legged production platform. The range of driving records for the production platform using the Menck 2500 hammer is shown in Fig. 4.

VIJAYVERGIYA & CHENG (1978) estimated the soil resistance to driving by considering only the outer shaft friction and end bearing due to the pile cross sectional area. Internal shaft resistance was neglected. The unit end bearing for the chalk was estimated to be 4.8 N/mm^2.

The driveability predictions using the new wave equation model are also shown in Fig. 4. The lower bound driveability curve was obtained using the same assumption of VIJAYVERGIYA & CHENG (1978), that is the neglection of the internal shaft friction. The upper bound curve was obtained assuming a mobilised internal shaft resistance contributed by a plug length of 50 percent of the pile penetration. This curve bounds the upper field driving limit closely.
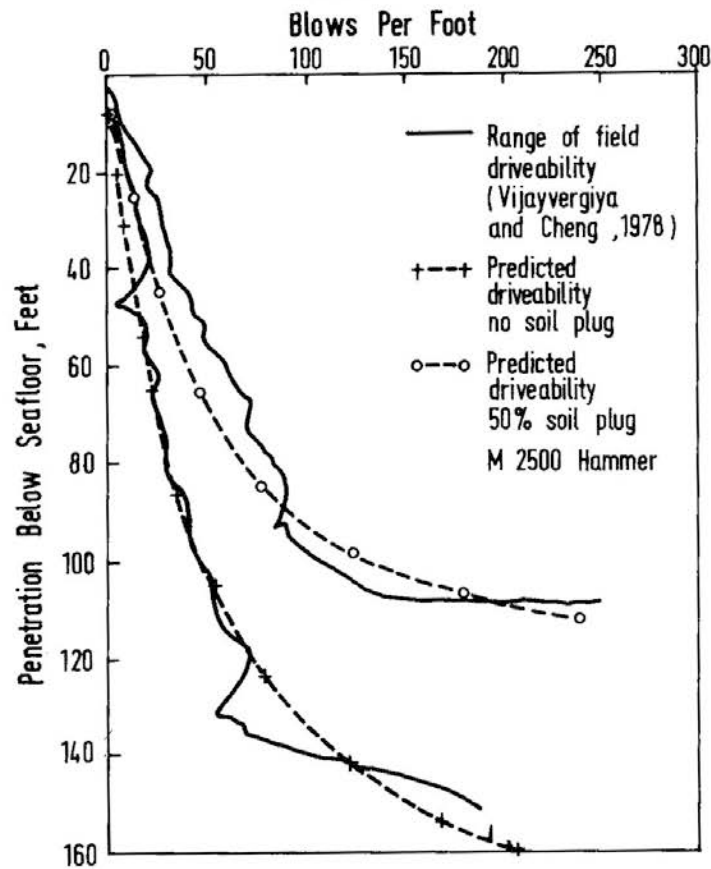
Blows Per Foot

Fig. 4. Driveability curves for Case A (North Sea Installation - Rough Field).

Arabian Gulf Installations

Case B- This site is located in the Safaniya field. The soil at this site consists of a layer of loose to dense calcareous clayey sand underlain by a layer of very dense fine sand and a layer of very dense clayey fine sand. Cemented sand seams were also present. Steel pipe piles 1.07m in diameter with a wall thickness of 38.1 mm were used. These piles were driven by a Menck 1800 hammer. The hammer performance, cushion stiffness and coefficient of restitution and their variations with penetration depths were monitored by instrumentation of one pile and are shown in Fig. 5 (a).

Using the measured hammer and cushion data, the predicted driveability curves for the instrumented pile, for the two soil plug lengths of 50 and 75 percent pile penetration are shown in Fig. 5 (b). The predicted driveability is in close agreement with the observed driveability for the pile. The two predicted driveability curves are also shown in Fig. 5 (c), for comparison with the observed range of driveability for all the piles installed for the platform. The predicted driveability curves are representative of the field driveability.

178

(a)

(b)

(c)

Fig. 5. Driveability curves for Case B (Arabian Gulf Installation - Safaniya Field).

Case C - This site is located in the Zuluf field. The soil at this site consists of a loose to very dense clayey fine to medium sand underlain by a layer of hard calcareous clay with gypsum fragments. A weak layer of gypsum was present between the calcareous clay layer. Steel pipe piles of the same dimensions as in Case B were used. These piles were driven using the Vulcan 560 hammer.

179
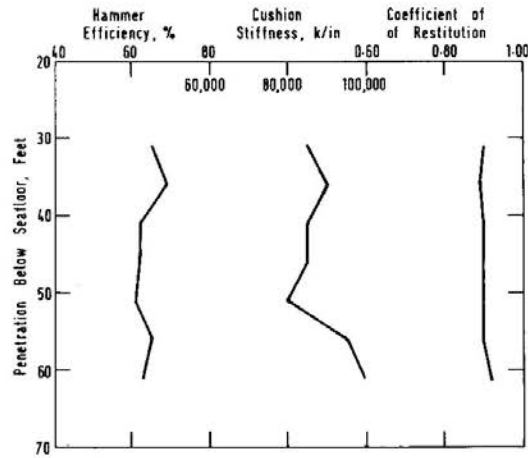
(a)
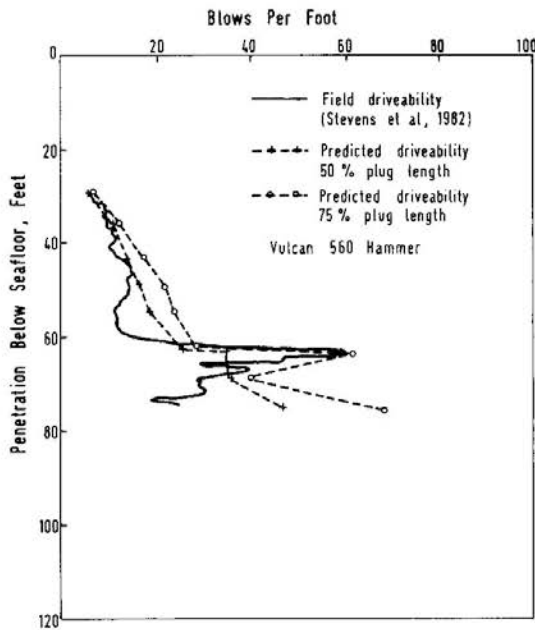
(b)
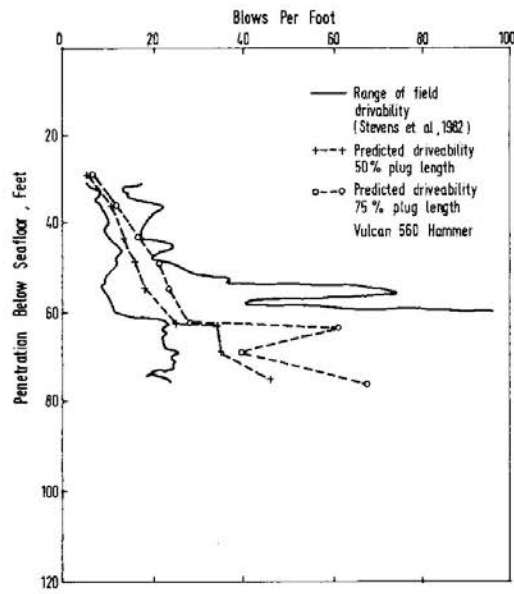
(c)

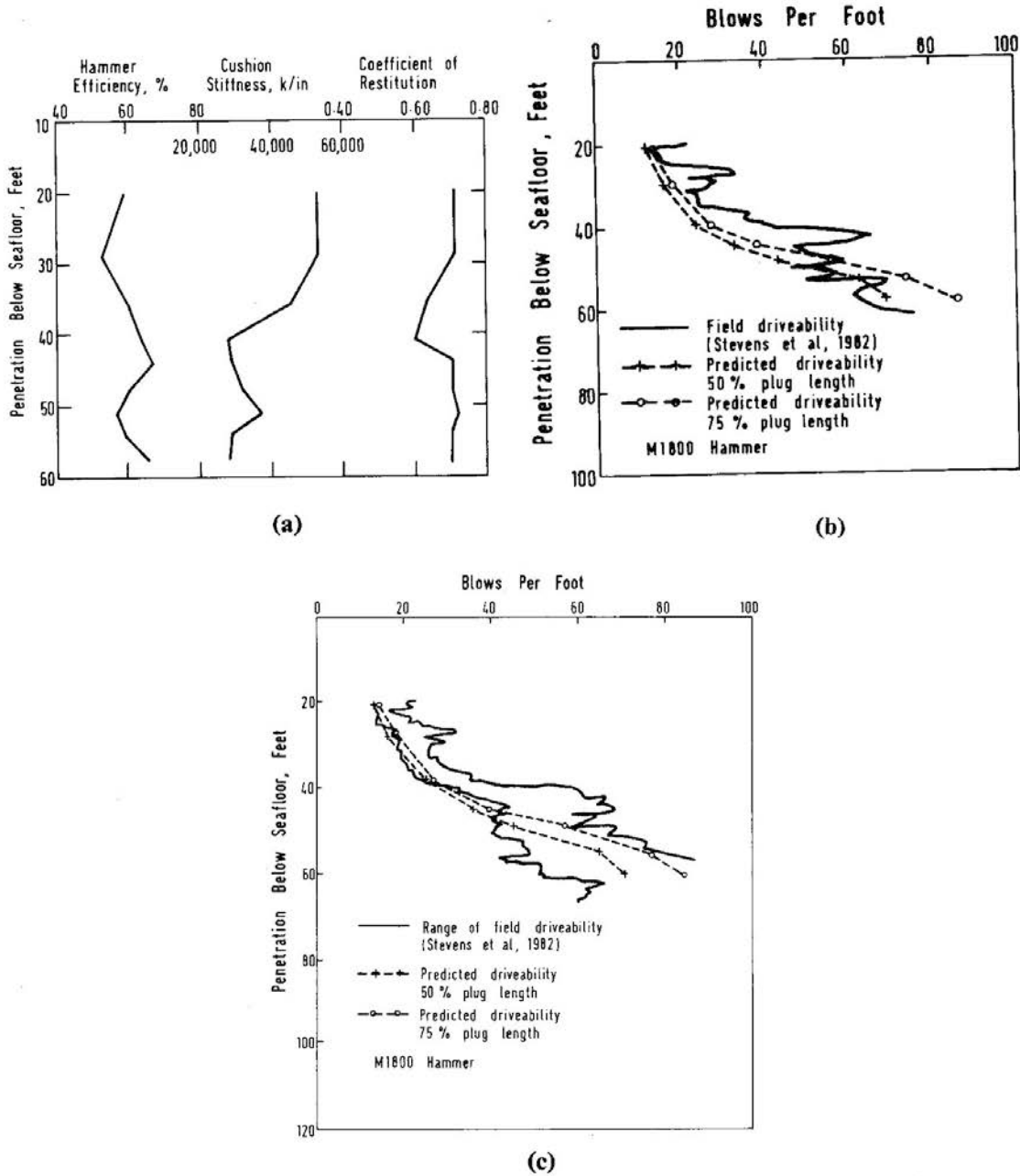**Fig. 6. Driveability curves for Case C (Arabian Gulf Installation-Zuluf Field).**

From the estimated soil resistance to driving versus penetration curve presented by STEVENS et al (1982), the average undrained shear strength of the calcareous clay was about 250 kN/m². The remoulded shear strength of the calcareous clay is assumed to be one third of the undrained shear strength. The resistance by the gypsum layer was estimated by assuming the layer to be

180

cohesionless.   This assumption is reasonable since fragmentation of this weak layer is likely due to the driving action.

One of the piles was instrumented to monitor the hammer and cushion performance. The measured values for the hammer and cushion performance are shown in Fig. 6 (a).   These measured values were used in the wave equation analysis.

The predicted driveability curves, assuming 50 and 75 percent soil plug lengths, are shown in Fig. 6 (b) for the instrumented pile. Beyond the 60 feet penetration, the hammer and cushion performance were assumed to be those at 60 feet penetration. The predicted curves are in close agreement with the field driveability curve. These predicted driveability curves are also compared with the range of field driveability in Fig. 6 (c).

General Comments

From the driveability analyses presented for open-ended pipe piles, apart from treating the internal soil column as unplugged during driving, an additional uncertainty in the analyses is the contribution by this soil column to the resistance during driving.   The effectiveness of the driving shoe in reducing internal shaft friction and the soil plug length assumed in the analysis will, undoubtedly, affect the driveability perdiction. The analyses presented herein indicated that a 50 percent reduction assumed for the internal shaft friction due to the use of the driving shoe and a soil plug length of 50 to 75 percent resulted in reasonable driveability predictions.   Until better understanding of the internal soil column behaviour during driving is available, apriori assumptions of the contribution of resistance of this soil column during driving is required.

CONCLUSIONS

The studies using the new wave equation model proposed by LEE et al (1987), showed that a pile may be driven with a follower with minimal loss of driveability if the follower and pile are impedance matched. For followers driven below ground level, the compressive driving stresses in the pile may be substaintially reduced when compared to that of a full pile. The tensile stresses for the full pile and a pile driven with an impedance matched follower appear to be similar. The driveability analyses for piles driven into chalk, clay and sand at three offshore sites demonstrated the ability of the new model to reasonably predict driveability of large diameter offshore piles.

REFERENCES

API RP2A (1981). *"Recommended practice for planning, designing and constructing fixed offshore platforms"*, American Petroleum Institute, 12th Edition, Dallas.

CHOW, Y.K., KARUNARATNE, G.P., WONG, K.Y. & LEE S.L. (1987). "Load carrying capacity predictions of driven piles", Paper submitted to the Canadian Geotechnical Journal for publication.

CHOW, Y.K. & SMITH, I.M. (1984). "A numerical model for the analysis of pile driveability", *Proc. Second Int. Conf. on the Application of Stress Wave Theory on Piles.* Stockholm, Sweden, 319-325.

DAYAL, U. & ALLEN, J.H. (1975). "The effect of penetration rate on the strength of remoulded clay and sand samples". *Canadian Geotechnical Journal*, 12, 336-348.

FISCHER, H.C. (1984). "Stress wave theory for pile driving application", *Lecture presented at The Second Int. Conf. on the Application of Stress Wave Theory on Piles*, Stockholm, Sweden.

HEEREMA, E.P. (1979 (a)). "Pile driving and static load tests on piles in stiff clay", *11th Annual Offshore Technology Conference Houston* 1135-1145.

HEEREMA, E.P. (1979(b)). "Relationships between wall friction, displacement velocity and horizontal stress in clay and in sand for pile driveability analysis", *Ground Engineering*, 4 (6), 30-46.

LEE, S.L., CHOW, Y.K., KARUNARATNE, G.P. & WONG, K.Y. (1987). "A rational wave equation model for pile driving analysis", *Journal of Geotechnical Engineering, ASCE*. (In Press).

LITKOUHI, S. & POSKITT, T.J. (1980). "Damping constants for pile driveability calculations", *Géotechnique*, 30 (1), 77-86.

SMITH, E.A.L. (1960). "Pile driving analysis by the wave equation", *Journal of Soil Mechanics and Foundation Division ASCE* 86 (4), 35-61.

SMITH, I.M, TO,P. & WILLSON, S.M. (1986). "Plugging of pipe piles", *Paper presented at the 3rd Int Conf on Numerical Methods in Offshore Piling*, Nantes, France, 53-73.

STEVENS, R.S., WILTSIE, E.A. & TURTON, T.H.(1982). "Evaluating pile driveability for hard clay, very dense sand and rock", *Paper presented at the 14th Annual Offshore Technology Conference* Houston, 465-482.

VIJAYVERGIYA, V.N. & CHENG, A.P. (1978). "Offshore pile foundations in chalk", *GEOCON- Conf on Geotechnical Engineering*, New Delhi, India, 484-491.

182

APPENDIX I — NOTATION

The following notations are used in this paper.

A_p — cross sectional area of pile,

c — speed of longitudinal wave propagation in pile,

c_u — undrained shear strength of cohesive soil,

E_p — Young's modulus of pile,

F_i — incident force pulse,

F_r — reflected force pulse,

F_t — transmitted force pulse,

G_s — shear modulus of soil,

J_p^* — rate effects coefficient for soil at pile tip,

J_s^* — rate effects coefficient for soil at pile shaft,

N — exponent for rate effects,

v_i — incident particle velocity,

v_r — reflected particle velocity,

v_t — transmitted particle velocity,

Z — impedance of pile $(E_p A_p/c)$

β — ratio of impedance of follower to pile

σ_v' — effective vertical stress.

APPENDIX II — EFFECT OF IMPEDANCE CHANGE ON STRESS WAVE PROPAGATION

Consider two elements in series and let Z_1 and Z_2 denote the impedances of elements 1 and 2 respectively.

The boundary conditions at the interface 'b' require that,

$$v_b = v_i + v_r \text{ and,}$$
$$F_b = F_i + F_r \qquad \dots\dots\dots\dots (1)$$

where
$$F_i = Z_1 v_i \text{ and}$$
$$F_r = -Z_1 v_r \qquad \dots\dots\dots\dots (2)$$

and v and F represent the particle velocity and force pulse respectively. The subscripts i and r denote incident and reflected respectively.

$$\text{Let } \beta = Z_1/Z_2 \qquad \dots\dots\dots\dots (3)$$

Consider an incident force pulse F_i. At the interface 'b', the transmitted force and particle velocity waves are,

$$F_t = F_i + F_r \text{ and}$$
$$v_t = v_i + v_r \qquad \dots\dots\dots\dots \text{(4)}$$

but $\quad v_t = F_t/Z_2$ and therefore

$$F_t/Z_2 = v_i + v_r \qquad \dots\dots\dots\dots \text{(5)}$$

Substituting Eqn. 3 in Eqn. 5 we have,

$$F_t \beta/Z_i = v_i + v_r \qquad \dots\dots\dots\dots \text{(6)}$$

or $\quad F_t\beta = F_i - F_r \qquad \dots\dots\dots\dots \text{(7)}$

Using Eqns. 1 and 7 we have,

$$F_t/F_i = 2/(1 + \beta)$$
$$F_r/F_i = (1/\beta - 1)/(1/\beta + 1)$$
$$= -v_r/v_i \text{ and}$$
$$v_t/v_i = 2\beta/(1 + \beta) \qquad \dots\dots\dots\dots \text{(8)}$$

Note that for β equals one, elements 1 and 2 are impedance matched. Under this condition F_t equals F_i and v_t equals v_i. Other values of β result in a loss of transmission efficiency of the incident waves due to the presence of reflected waves.

EFFECT OF VERTICAL LOAD ON FLEXURAL BEHAVIOUR OF PILES

NIRMAL KUMAR JAIN[1], GOPAL RANJAN[2] and GOVINDACHETTIAR RAMASAMY[3]

SYNOPSIS

The state of the art is discussed in some detail and it is brought out with adequate evidence that whereas the analytical investigations suggest an increase in lateral deflection when a vertical pile is axially loaded some published experimental investigations, both field tests and laboratory model tests, suggest a reduction in lateral deflection due to the presence of vertical load. The possible reasons for this contradiction are hypothesised. One reason is the reduction in tensile stress for axially loaded concrete sections. The restraint to the pile head imposed by the loading device used for the application of a vertical load is suspected to be another cause and this is investigated in detail. For this purpose, a loading device was designed and fabricated which facilitated application of a vertical load without causing restraint to the pile head. Using the device, tests on fully and partially embedded model piles subjected to vertical and lateral loads were carried out. The results show that the presence of vertical load causes an increase in lateral deflection which is in agreement with this trend predieted by analytical methods. This confirms that the restraint offered by the loading device used for the application of vertical load, was in fact, one of the causes of the reduced lateral deflection observed by many past investigators.

INTRODUCTION

The lateral deflection of piles is generally determined without taking into account the effect of vertical load as it is considered to have a marginal effect on the flexural behaviour of piles (DAVISSON, 1960). However, the results of a number of field and laboratory investigations reported in the literature show that the presence of vertical load can reduce lateral deflection significantly. On the contrary, the results of almost all analytical studies have shown that the effect of vertical load is to increase deflection and moment. The existence of this contradiction is brought out by describing briefly some of the investigations and results reported in the literature on the subject matter. Based on the results of these investigations, the possible reasons for this contradiction are hypothesized. One of the possible reasons is that the loading arrangement used for the application of vertical load could cause restraint to the pile head, thus reducing deflection under an applied lateral load. In order

---

[1]Assistant Professor, Civil Engineering Department, Madhav Institute of Technology, Qwalior, India.
[2]Professor of Civil Engineering, [3]Reader, Civil Engineering Dept., University of Roorkee, Roorkee, India.

to examine this aspect a special loading device was designed and fabricated which facilitates the application of vertical load without causing any restraint to the pile head. Using the device, model tests on fully and partially embedded piles were carried out. The results are presented and discussed to bring out the influence of vertical load on the flexural behaviour of piles.

STATE OF THE ART

The effect of vertical load on the flexural behaviour of piles has been examined through analytical and experimental investigations by many investigators in the past. The details and the results of some of these investigators are presented briefly and discussed.

Analytical Investigations

DAVISSON (1960) presented an analysis for a fully embedded vertical pile subjected to moment, shear and axial load. The analysis is based on the modulus of subgrade reaction approach. The axial load is assumed to be invariant with depth. The solution for the governing differential equation was obtained using an analog computer and the results were presented in non-dimensional form. The results show that for a given lateral load, the axial load magnifies the pile head deflection and maximum moment of the pile. It was concluded that when the axial load is within 10 percent of buckling load the increase in deflection and maximum moment is only marginal.

RAMASAMY (1974) presented an analysis for fully embedded piles assuming the behaviour of the soils to be elasto-plastic. Piles of uniform cross section and also tapered section embedded in cohesive and cohesionless soils were considered. The transfer of axial load due to skin frictional resistance was also taken into account. The results show that the axial load magnifies the top deflection and maximum moment in the pile considerably. It was found that the effect of vertical load becomes increasingly felt as the magnitude of lateral load and thus the lateral deflection increases.

GORYUNOV (1975) presented an approach based on elastic theory and analysed a 24 m long flexible steel tubular pile of 50 cm diameter, subjected to vertical and lateral loads. The values of deflection and bending moment at the pile head obtained for a fixed headed pile are given in Table 1.

The results show that for a given lateral load the presence of vertical load increases the lateral deflection and moment significantly.

186

to examine this aspect a special loading device was designed and fabricated which facilitates the application of vertical load without causing any restraint to the pile head. Using the device, model tests on fully and partially embedded piles were carried out. The results are presented and discussed to bring out the influence of vertical load on the flexural behaviour of piles.

STATE OF THE ART

The effect of vertical load on the flexural behaviour of piles has been examined through analytical and experimental investigations by many investigators in the past. The details and the results of some of these investigators are presented briefly and discussed.

Analytical Investigations

DAVISSON (1960) presented an analysis for a fully embedded vertical pile subjected to moment, shear and axial load. The analysis is based on the modulus of subgrade reaction approach. The axial load is assumed to be invariant with depth. The solution for the governing differential equation was obtained using an analog computer and the results were presented in non-dimensional form. The results show that for a given lateral load, the axial load magnifies the pile head deflection and maximum moment of the pile. It was concluded that when the axial load is within 10 percent of buckling load the increase in deflection and maximum moment is only marginal.

RAMASAMY (1974) presented an analysis for fully embedded piles assuming the behaviour of the soils to be elasto-plastic. Piles of uniform cross section and also tapered section embedded in cohesive and cohesionless soils were considered. The transfer of axial load due to skin frictional resistance was also taken into account. The results show that the axial load magnifies the top deflection and maximum moment in the pile considerably. It was found that the effect of vertical load becomes increasingly felt as the magnitude of lateral load and thus the lateral deflection increases.

GORYUNOV (1975) presented an approach based on elastic theory and analysed a 24 m long flexible steel tubular pile of 50 cm diameter, subjected to vertical and lateral loads. The values of deflection and bending moment at the pile head obtained for a fixed headed pile are given in Table 1.

The results show that for a given lateral load the presence of vertical load increases the lateral deflection and moment significantly.

186

Table 1 : Results obtained by Goryunov (1975)

Load in Tonnes		Deflection at pile head		Moment at the pile head	
Lateral	Vertical	Deflection mm	Percentage increase due to vertical load	moment t-m	Percentage increase due to vertical load
10	0	72.0	-	60.0	-
10	100	82.0	13.9	68.2	13.7
10	200	96.0	33.3	79.2	32.0
10	300	114.0	58.3	94.2	75.0

KLEIN & KARAVAEV (1979) presented a finite element analysis for the design of a reinforced concrete pile, subjected to the action of vertical and lateral loads. The analysis takes into account the non-linear stress-strain behaviour of concrete and cracking in the concrete. The results were presented for a reinforced concrete pile 30 × 30 cm in section, with 2.5 m unsupported length and 2 m of embedded length. Based on the results it was concluded that the vertical load can increase the lateral load capacity of the pile embedded in dense soil.

Experimental Investigations

Field Tests

EVANS (1953) carried out lateral load test with and without vertical load on different types of piles (Raymond, Union Monotube, H-Section and precast). The piles were 10.5 m to 15.0 m in length. At the ground surface the soil was a brown clay loam which graded to a sandy loam at 3.0 m depth. The results of the lateral load tests are presented in Fig. 1. These results show that both vertical and batter (out batter) piles with vertical load exhibit greater resistance to lateral load than those without vertical load.

McNULTY (1959) performed two series of lateral load tests, one on Raymond Standard piles and the other on timber piles. Three unreinforced concrete piles (Raymond) were embedded 4.3 m, 6.7 m and 7.9 m in a deposit consisting of sandy clay followed by fine silty sand. The 7.9 m deep pile broke at a lateral load of 5.4 tonnes. The other two piles were loaded vertically to 20 tonnes before the lateral load was applied. These piles could be loaded laterally upto 10.8 tonnes per pile without causing failure of piles. The first pile had virtually no resistance to the flexure caused by the lateral load. The other two

Table 1 : Results obtained by Goryunov (1975)

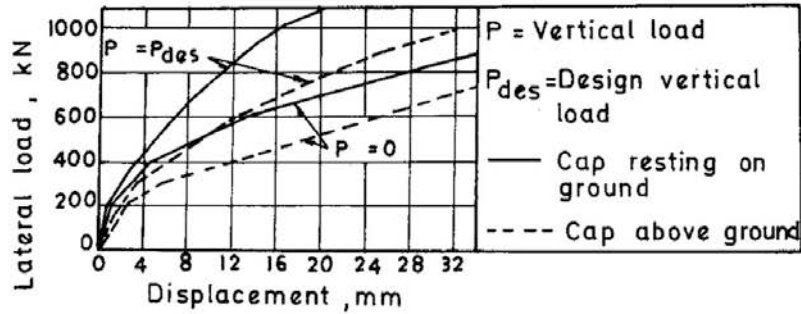| Load in Tonnes		Deflection at pile head		Moment at the pile head	
Lateral	Vertical	Deflection mm	Percentage increase due to vertical load	moment t-m	Percentage increase due to vertical load
10	0	72.0	-	60.0	-
10	100	82.0	13.9	68.2	13.7
10	200	96.0	33.3	79.2	32.0
10	300	114.0	58.3	94.2	75.0

KLEIN & KARAVAEV (1979) presented a finite element analysis for the design of a reinforced concrete pile, subjected to the action of vertical and lateral loads. The analysis takes into account the non-linear stress-strain behaviour of concrete and cracking in the concrete. The results were presented for a reinforced concrete pile 30 × 30 cm in section, with 2.5 m unsupported length and 2 m of embedded length. Based on the results it was concluded that the vertical load can increase the lateral load capacity of the pile embedded in dense soil.

Experimental Investigations

Field Tests

EVANS (1953) carried out lateral load test with and without vertical load on different types of piles (Raymond, Union Monotube, H-Section and precast). The piles were 10.5 m to 15.0 m in length. At the ground surface the soil was a brown clay loam which graded to a sandy loam at 3.0 m depth. The results of the lateral load tests are presented in Fig. 1. These results show that both vertical and batter (out batter) piles with vertical load exhibit greater resistance to lateral load than those without vertical load.

McNULTY (1959) performed two series of lateral load tests, one on Raymond Standard piles and the other on timber piles. Three unreinforced concrete piles (Raymond) were embedded 4.3 m, 6.7 m and 7.9 m in a deposit consisting of sandy clay followed by fine silty sand. The 7.9 m deep pile broke at a lateral load of 5.4 tonnes. The other two piles were loaded vertically to 20 tonnes before the lateral load was applied. These piles could be loaded laterally upto 10.8 tonnes per pile without causing failure of piles. The first pile had virtually no resistance to the flexure caused by the lateral load. The other two
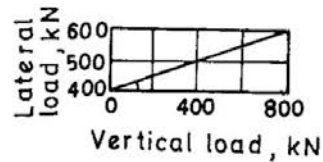
(a) Load vs horizontal displacement

(i) Subjected to lateral load only

(ii) Subjected to vertical and lateral loads
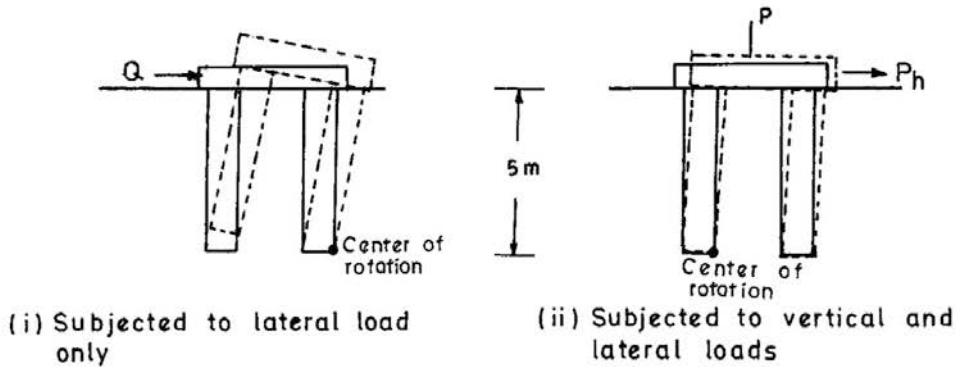
(b) Displacement of pile group
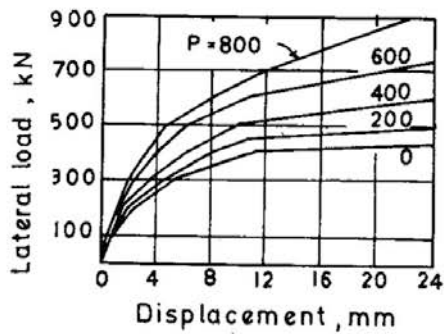
(c) Load vs horizontal displacement under different vertical load

(d) Effect of vertical load on lateral load capacity

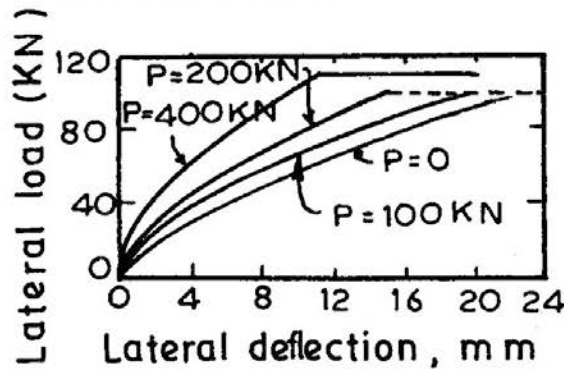Fig. 2. Results of load tests by Sarochan et. al. (1976).

Fig. 3. Results of load tests by Karasev et. al. (1977).

KARASEV et al. (1977) carried out experimental investigations on full-size cast-insitu short concrete piles. The tests were carried out at a site consisting of sandy loam. The piles were 60 cm in diameter and 3 m long and reinforced over the entire length. A pile cap 50-60 cm high was concreted on top. In all the tests the pile cap was above the ground level. The loading arrangement was such that vertical load could be applied centrally and it provided free movement of the pile cap under the effect of horizontal load. The results are presented in Fig. 3. It can be seen that the vertical load has a favourable effect on the lateral capacity of piles. It was also reported that with the increasing value of vertical load the centre of rotation shifts downwards indicating reduction in displacement of the base of the pile. This may
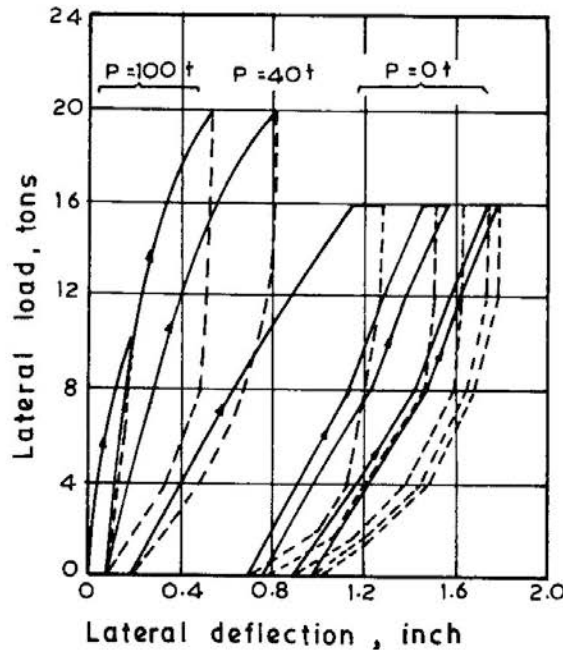

Fig. 4. Results of load tests on Raymond Step taper piles.

191

be due to the fact that the frictional forces at the base of the pile (piles being short) increases due to the vertical load.

A step taper pile with a 37.5 cm butt diameter was tested for its lateral load capacity under axial compressive loads of 100, 40 and 0 tonnes (RAYMOND INTERNATIONAL INC., 1977). The length of the pile was 12.0 m. The upper 3.7 m length of the pile was reinforced. The results are presented in Fig. 4 which show that the vertical load has a favourable effect on the lateral capacity of piles.

ZHUKOV & BALOV. (1978) carried out load tests on full size concrete piles embedded in saturated clay deposits. The tests were carried out on 43 piles in all, at two different sites. The piles were driven by 2 to 4 m into the ground and the height above the ground surface was about 2.5 m. Table. 3 gives the results for some of the tests which show that the piles with vertical load have exhibited increased lateral capacity for the same magnitude of horizontal pile head deflection. Further, it was noted that the cracks in piles with no vertical load have developed at much lower lateral load than the pile with vertical load.

Table 3 : Results of the load tests reported by Zhukov et al., 1978.

Case	Vertical load, p Tonnes	Lateral load at a deflection of 10 mm, Tonnes	Lateral load causing	
			Appearance of crack, Tonnes	Complete fracture of pile, Tonnes
I	0	1.32	0.88	1.33
	0	1.29	1.00	1.42
	32	1.97	1.04	2.40
	32	2.15	1.38	2.16
II	0	1.80	0.78	1.80
	0	1.55	0.90	1.62
	32	Fractured	2.58	3.18
	28	3.25	2.67	3.35
III	0	1.45	1.30	2.00
	0	1.50	0.60	2.00
	7.1	1.87	1.50	2.30

Model Tests

Model studies on single pile and pile groups have been carried out by PISE (1975), MAJUMDAR (1980) and SAXENA (1982). The piles were aluminium
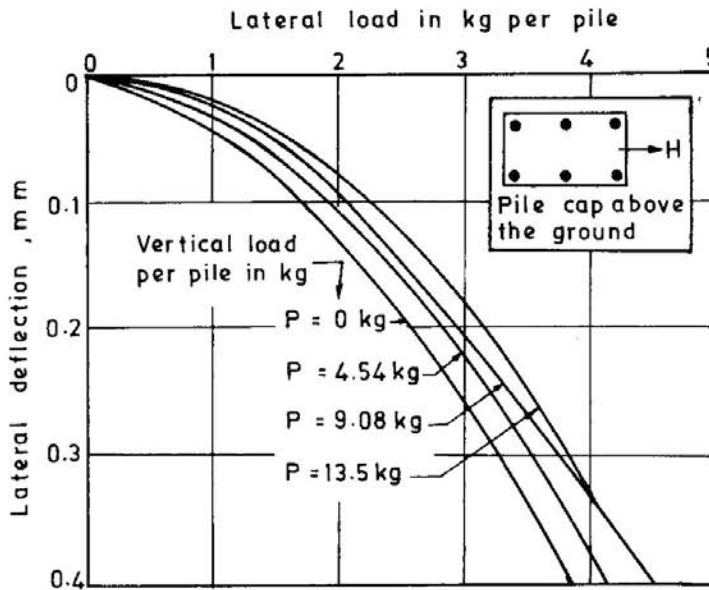
192

Fig. 5. Results of tests on model pile group (After Pise, 1975).

alloy tubes, the outer diameter varying from 1.9 cm to 3.2 cm. The piles chosen were long enough to be considered as long flexible piles. The piles were embedded in prepared sand beds. The results of all these investigations show that the presence of vertical load reduces lateral deflection. A typical result for a 2 × 3 group (PISE, 1975) is presented in Fig. 5.

A careful examination of the results of the above reported investigations suggests the following :-

1. Analytical studies (DAVISSON 1960; GORYUNOV 1975; RAMA-SAMY 1974) have shown that for a given lateral load, the presence of vertical load increases the lateral deflection. The increase in deflection is because of the fact that the vertical load causes additional moment at the deflected position of the pile.

2. In the case of short rigid piles, the vertical load increases the friction at the tip of the pile and this results in reduction in rotation and deflection (SAROCHAN & BYKOV, 1976 and KARASEV et al. 1977).

3. In the case of long flexible piles, the reduction in lateral deflection due to vertical load may be due to the following reasons.

(i) In cases of concrete piles, the tensile stresses due to bending and there-fore the cracking in concrete are reduced by the presence of vertical load. The reduction in cracking results in an increased effective section

193

(i.e. effective moment of inertia is large), thus reducing lateral deflection under combined vertical and lateral loading. This is amply substantiated by the results of field tests reported by McNULTY, 1956; BEATY, 1970; BARTOLOMEY, 1977 and ZHUKOV & BALOV 1978 and the analytical studies reported by KLEIN & KARAVAEV (1979).

(ii) The device for the application of vertical load may provide lateral restraint to the pile head.

EXPERIMENTAL INVESTIGATIONS

One of the reasons for the reduction in lateral deflection due to vertical load is suspected to be the restraint imposed by the loading mechanism to pile head. In order to investigate this, an experiment was planned on fully and partially embedded long flexible piles subjected to lateral load with and without vertical load. The aims of the experimental investigation were to design and fabricate a loading system for the application of vertical load which does not offer any restraint to the pile head at the time of lateral loading and to use the loading system so designed to carry out load tests on model piles to study the effect of vertical load on fully and partially embedded piles.
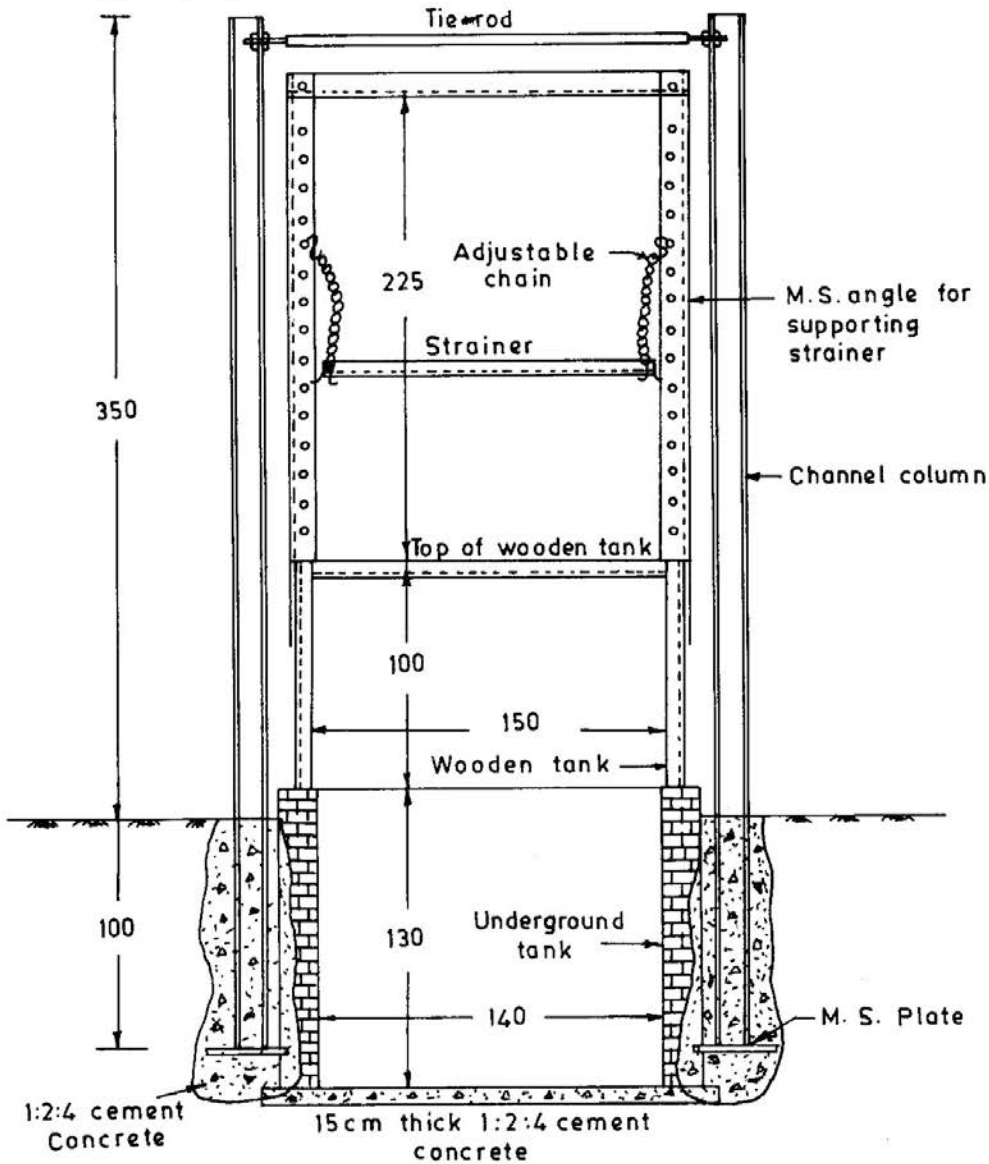
Loading System

For satisfactory performance of the loading device, the following requirements should be satisfied :

(i) The reaction loading frame should be independent of the tank so that loading does not cause any disturbance to the test bed.

(ii) The loading device for the application of vertical load should be such that the vertical load is applied centrally on the pile cap and remains central and vertical throughout the lateral load test. Such a condition can be satisfied only when the loading device moves in the direction of lateral loading by the same amount as that of the pile cap.

(iii) The vertical load assembly should not offer any restraint to the pile cap i.e. the pile cap should remain perfectly free to deflect under lateral load.

(iv) It should be possible to position the vertical load assembly at any location over the plan area of the tank such that the load may be applied on a pile/pile group which is placed anywhere in the tank.

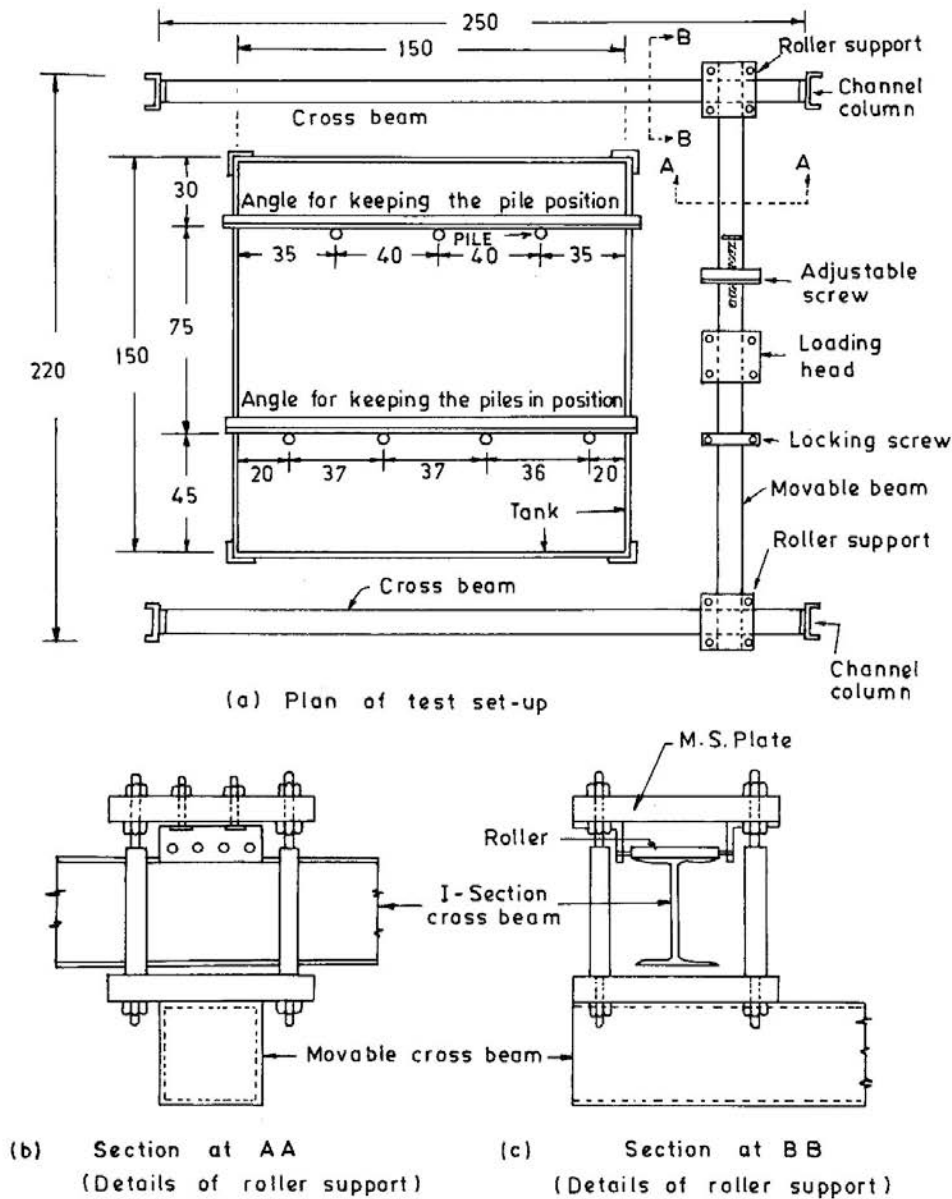(v) It should be possible to apply a vertical load of about 1.0 tonne.

194

(vi) It should be possible to position the loading assembly at any convenient height above the top of the tank so that the tests can be conducted on partially embedded piles.

(vii) The loading assembly should not obstruct the sand filling operations.

A loading assembly satisfying the above requirements was designed, fabricated and installed, the details of which are briefly discussed in the following paragraphs :

Fig. 6. Elevation details of the test set-up.

195

(a) Plan of test set-up

(b) Section at AA
(Details of roller support)

(c) Section at BB
(Details of roller support)

All dimensions are in cm

Fig. 7. Plan details of the test set-up.

Vertical Loading Assembly

The details of the loading assembly are shown in Figs. 6 to 8. The loading assembly consisted of a steel frame made up of 4 vertical columns of single channel section. The columns were braced to provide rigidity with mild steel rods. Two cross beams made up of single I-sections (125 × 75 × 6mm) were fixed to the columns as shown in Fig. 7. These cross beams can be fixed at any
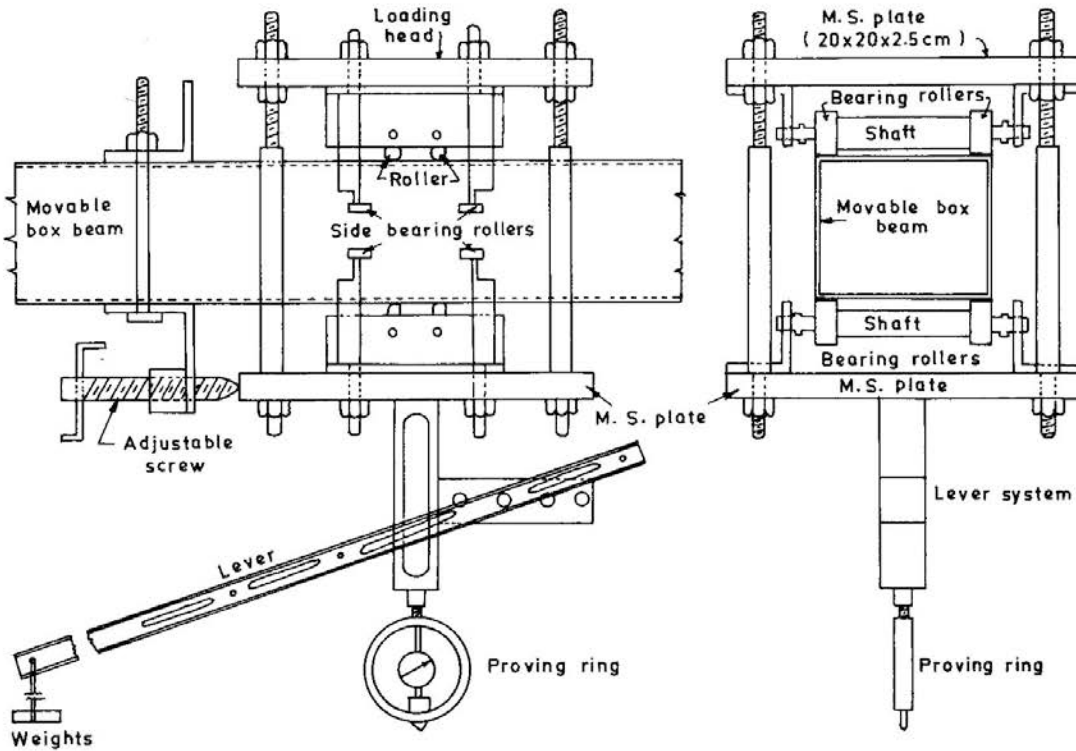
196

Fig. 8. Details of movable head used for applying vertical load.

elevation with the help of nuts and bolts. A movable beam with rollers moves on these cross beams. A loading head (Fig. 7 and 8) is attached to this movable beam. The vertical load is applied through the loading head using a lever arrangement. The loading head can be moved over this movable beam. Thus, by adjusting the position of the movable beam and the loading head, the loading can be done anywhere on the tank.

The four vertical columns of the loading frame were made from single channel section of size $150 \times 75 \times 6$mm. The columns were 4.50 m in length out of which 1.0 was embedded into the ground and bolted to a cement concrete block foundation. Holes were made at 15 cm vertical intervals along the length of the column so that the cross beams can be fixed at any desired elevation.

The movable beam is made up of two M.S. channel section of size $100 \times 50 \times 5$mm welded front to front. This movable beam is provided with the rollers at both ends such that it moves freely over the cross beams (Fig. 7). All the surfaces of this cross beam were finished very smoothly so as to make it
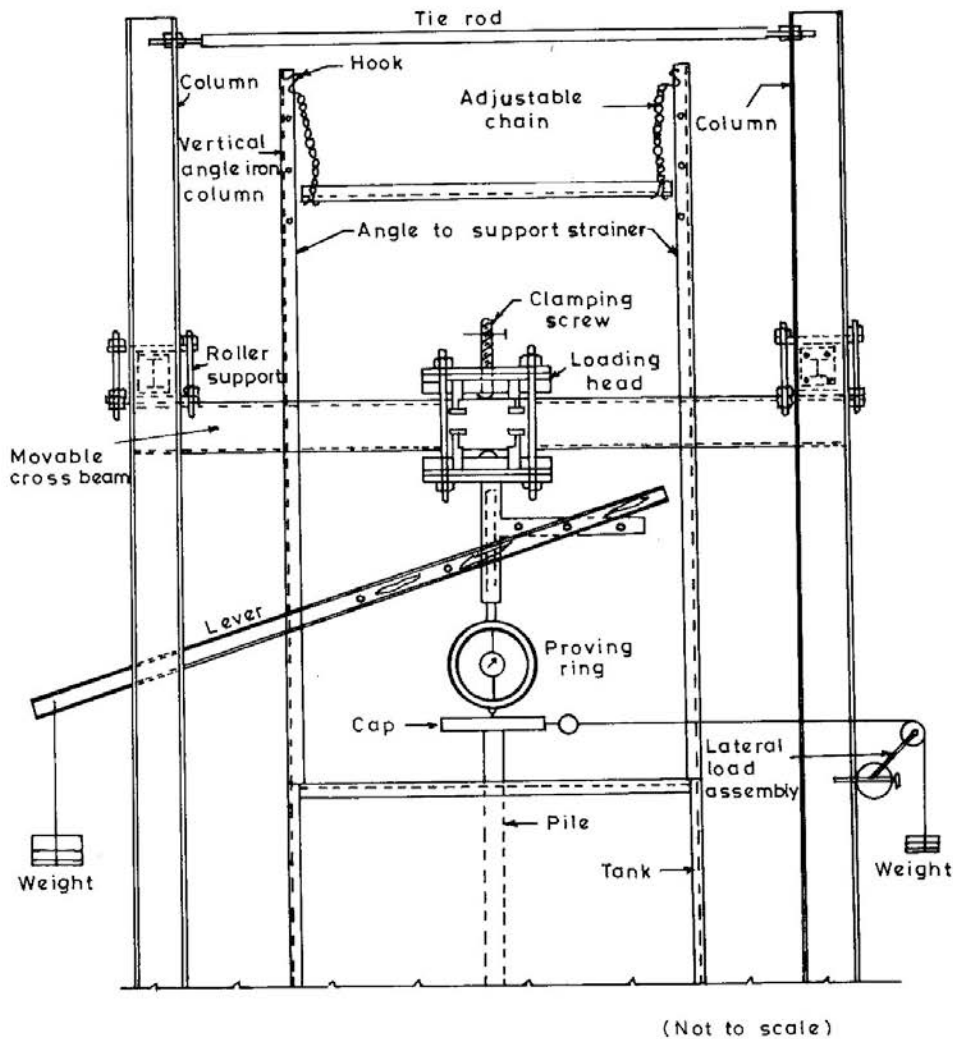
197

Fig. 9. Line diagram showing the details of the test set-up.

frictionless. During sand filling operations this beam can rest on the portion of the cross girder which is outside the tank as shown in Fig. 7.

The loading head consisted of two square plates of size $20 \times 20 \times 2.5$ cm connected by 4 vertical rods (Fig. 8). This loading head is provided with rollers as shown in Fig. 8, so that it can move over the movable beam. A lever system is attached to the bottom plate of the loading head. The vertical load is transferred to the pile cap through a plunger and proving ring. The magnitude of the vertical load is measured by the proving ring. Inspite of providing rollers, made up of ball bearings, to the loading head some of the preliminary tests indicated that the loading head does not move by exactly the same

198

amount as the pile cap moves under the application of lateral load. Therefore an adjustable screw system (Fig. 8) was incorporated so that the loading head can be moved such that the load remains vertical and at the centre of the pile cap.

A line diagram of the complete set up is shown in Fig. 9.

Lateral Loading Assembly

The lateral loads on pile/pile groups were applied by means of a cable connected to the pile and passing over a frictionless pulley with a hanger attached at the other end for placing dead weights.

Details of the Tests

Tests were carried out on model aluminium tube piles embedded in a prepared sand bed. The sand bed was prepared in a test tank of size 1.5 m × 1.5 m in plan and 2.3 m deep. The tank was filled by adopting a rainfall technique, wherein the sand was allowed to fall freely over a height of 180 cm through a strainer of size 150 cm × 150 cm. The tank was filled initially upto a certain depth and the piles were placed in position and clamped to angle irons fixed to the top of the tank. The sand filling was then continued keeping the height of fall of sand as 180 cm by raising the level of the strainer as the level of the sand bed increased. The unit weight of the sand achieved by this fall of sand was 1.60 gm/cc and the corressponding relative density was 78%. The piles were aluminium tubes of 32 mm outer diameter and 28.8 mm inner diameter. Some trial lateral load tests with embedments ranging from 50 cm to 180 cm showed that piles with an embedment of 100 cm or more showed the same load-deflection behaviour. Therefore, all the tests were conducted with a pile embedment of 100 cm. Aluminum alloy plates 2.5 cm thick were used for making the pile caps.

The vertical displacement of the pile cap was measured by means of two dial gauges mounted vertically on the top of the pile cap. The dial gauges were kept at equal distance from the centre of the pile cap. The line joining the dial gauge positions was kept parallel to the direction of lateral load. The measurement of vertical displacement at the ends of the cap was also used to compute the rotation of the pile cap. The horizontal displacement of the pile cap was measured by means of two dial gauges with their stem in contact with the face of the cap at the level of applied lateral load.
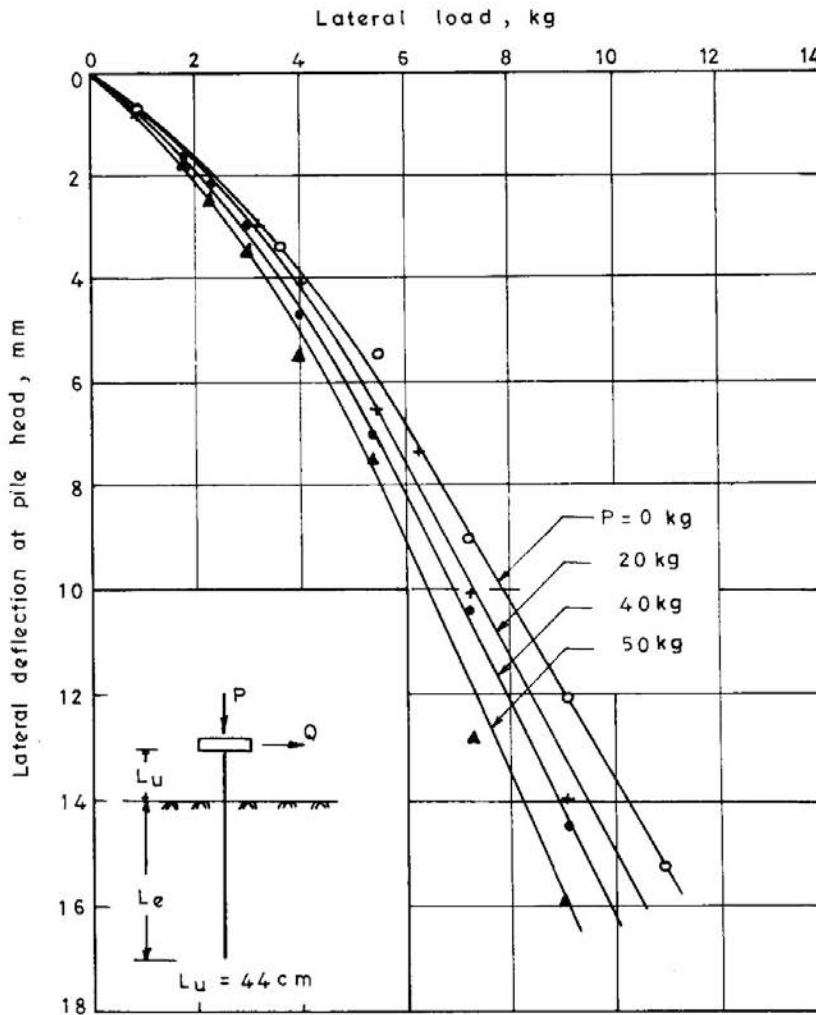
199

Fig. 10. Lateral load vs deflection for a partially embedded single pile.

RESULTS AND DISCUSSION

Tests were conducted on fully and partially embedded long flexible single piles, pile bents and groups of 4 piles. In the case of the single pile and pile bent the tests were conducted with unsupported length, $L_u = 0, 22$ cm and 44 cm. For a group of 4 piles the tests were conducted with $L_u = 0$ and 44 cm only.

Lateral load tests were conducted with and without vertical loads. To determine the magnitude of vertical load that may be applied on the pile/pile group, vertical load tests were conducted on a single pile, pile bent and group of 4 piles. The results of the vertical load tests indicate that the ultimate
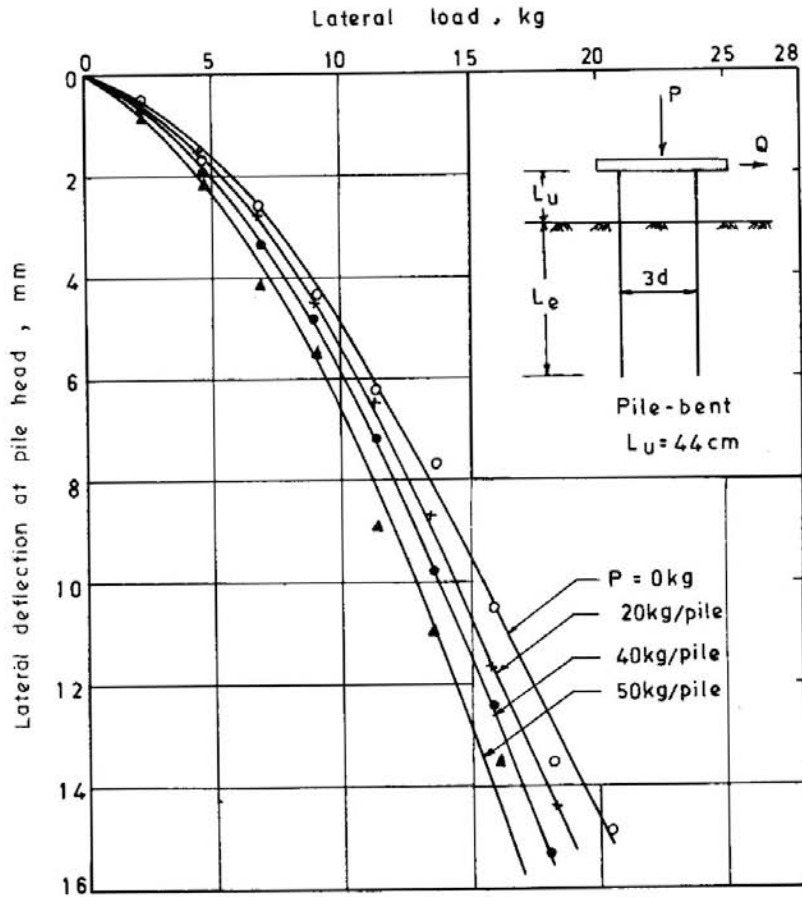
Fig. 11. Lateral load vs deflection for a partially embedded pile bent.

load, P_{ult} is 100 kg in the case of single pile, 204 kg in the case pile bent and 416 kg for the group of 4 piles. For the combined lateral and vertical load tests, the ultimate vertical load per pile was therefore taken as 100 kg. The lateral load tests have been conducted with a vertical load equal to 20 kg, (20% P_{ult}) 40 kg, (40% P_{ult}) and 50 kg, (50% P_{ult}) per pile.

Some typical results in the form of lateral load vs deflection plots for single pile, pile bent and group of four piles are presented respectively in Figs. 10 to 12. These results clearly suggest that the presence of vertical load increases the lateral deflection. A typical set of plots for lateral deflection under a constant lateral load with different vertical load and unsupported length of the pile is presented in Fig. 13. These plots suggest that the increase in lateral deflection due to the vertical load is significant in the case of partially embedded piles. The rotation of the pile cap was also measured during the
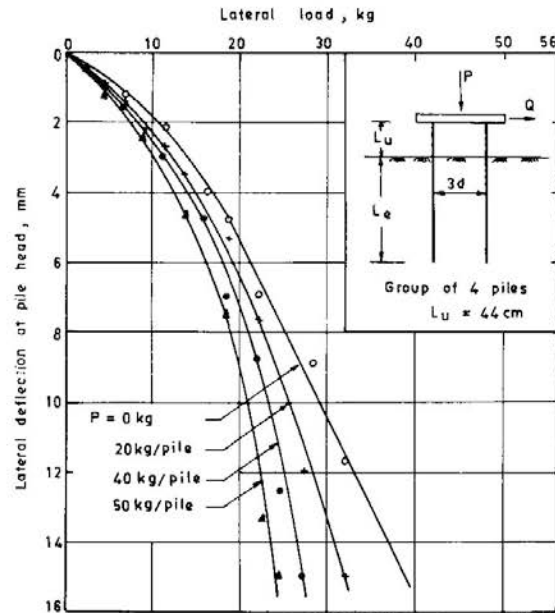
201

Fig. 12. Lateral load vs deflection for a partially embedded pile group.

tests. These results show that the rotation of the pile cap also increased due to the presence of vertical load. These observations are in agreement with those predicted by the analytical methods of DAVISSON (1960), RAMASAMY (1974), GORYUNOV (1975) and JAIN (1983). It may be pointed out here that the loading device used in the present investigation eliminates the possibility of external restraint to the pile head. The contradictory behaviour observed in the field and model investigations on metal piles reported by other investigators could therefore be due to the possible restraint to the pile head imposed by the loading device. In the case of concrete piles, however, the reduction in tensile stresses and therefore a reduction in cracking, could have been another reason for the observed contradictory behaviour. It can therefore be concluded from the results of the present investigation that the vertical load does increase the lateral deflection and therefore reduce lateral capacity in the case of metal piles such as steel piles as analytical methods suggest.

CONCLUSIONS

A careful analysis of the results of investigations reported in the literature shows that whereas analytical studies predict increase in lateral deflection, the experimental studies indicate a decrease in lateral deflection due to the vertical
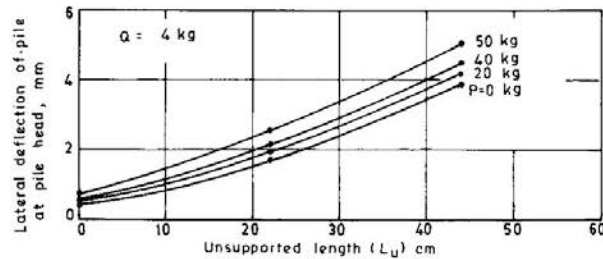
202

Fig. 13. Effect of vertical load on partially embedded piles.

load in a vertically and laterally loaded pile. The reduction in lateral deflection due to vertical load observed in experimental studies on long flexible piles may be due to the following reasons :

(a) In the case of concrete piles, the vertical load reduces the tensile stresses produced by the lateral loading. This reduces cracking in concrete resulting in an increased effective section and therefore an increase in flexural rigidity.

(b) The device used for the application of vertical load may introduce lateral restraint to the pile head.

A loading device which eliminates restraint to the pile head has been designed and fabricated. An experimental investigation on model piles has been carried out using the above loading assembly. The results of the experimental investigation, unlike the results of similar investigations reported by other investigators, show that the vertical load magnifies the lateral deflection. This confirms that the restraint offered by the loading device used for the application of vertical load is in fact a cause of the reduction in deflection due to vertical load observed in the case of metal piles by many earlier investigators.

REFERENCES

BARTOLOMEY, A.A. (1977). Experimental Analysis of Pile Groups under Lateral Loads, *Proceedings of the Special Session 10 of the Ninth International Conference on Soil Mechanics and Foundation Engineering*, Tokyo, pp. 187-188.

BEATY, I.C. (1970). Lateral Load Test on Pile Groups, *Foundation Facts*, Vol.VI, No. 1, pp. 18-21.

DAVISSON, M.T. (1960). *Behaviour of Flexible Vertical Piles Subjected to Moment, Shear and Axial Load,* Thesis Submitted to University of Illinois, Urbana, Illinois, in Partial fulfilment of the requirements for the degree of Doctor of Philosophy.

DAVISSON, M.T. & ROBINSON, K.E. (1965). Bending and Buckling of Partially Embedded Piles, *Sixth International Conference on Soil Mechanics and Foundation Engineering*, Montreal, Vol. 2, pp. 243-246.

EVANS, L.T. (1953). Bearing Piles Subjected to Horizontal Loads, Symposium on Lateral Load Tests on Piles, *ASTM Special Technical Publication* No. 154, pp. 30-35.

GORYUNOV, B.F. (1975). Discussion on "Analysis of Piles Subjected to the Combined Action of Vertical and Horizontal Loads", *Soil Mechanics and Foundation Engineering*, (Translated from Russian), Vol. 10, No. 1, page 10.

JAIN, N.K. (1983). *Flexural Behaviour of Partially Embedded Pile Foundations*, Ph.D. thesis, Civil Engineering Department, University of Roorkee, Roorkee, India.

KARASEV, O.V. et. al. (1977). Investigation of the Work of Single Cast Piles under Different Load Combinations, *Soil Mechanics and Foundation Engineering* (Translated from Russian) Vol. 14, No. 3, pp. 173-177.

KLEIN, G.K. & KARAVAEV, V.N. (1979). Design of Reinforced Concrete Piles for Vertical and Horizontal Loading, *Soil Mechanics and Foundation Engineering*, (Translated from Russian) No. 6, pp. 321-324.

MAJUMDAR. J.P. (1980). *Fixity Effect of Axial Load on Laterally Loaded Piles*, M.E. Thesis, Submitted to University of Roorkee, Roorkee, India.

McNULTY, J.F. (1956). Thrust Loading on Piles, *Journal of the Soil Mechanics and Foundations Divison, ASCE*, Vol. 82, No. SM 2, Proc. Paper 940, pp. 1-25.

PISE, P.J. (1975). Investigation on Laterally Loaded Pile Groups, *Symposium on Recent Developments in the Analysis of Soil Behaviour and its Application to Geotechnical Structures*, University of New South Wales, Australia, pp. 129-144.

RAMASAMY, G. (1974). Flexural Behaviour of Axially and Laterally Loaded Individual Piles and Groups of Piles, Thesis Submitted to Indian Institute of Science, Bangalore for the degree of Doctor of Philosophy.

RAYMOND INTERNATIONAL INC. (1977). *Raymond Step Taper Piles Construction Manual*, Concrete Pile Division of Raymond International Inc., New York N.Y.

SAROCHAN, E.A. & BYKOV V.I. (1976). Performance of Groups of Cast in Place Ples Subjected to Horizontal Loading, *Soil Mechanics and Foundation Engineering*, (Translated from Russian) Vol. 13, No. 3, pp. 157-161.

SAXENA, P.K. (1982). *Prediction and Performance of Lateral Load-Deflection Behaviour of Piles*, M.E. Thesis Submitted to University of Roorkee, Roorkee, India.

ZHUKOV, N.V. & BALOV, I.L. (1978). Investigation of the Effect of a Vertical Surcharge of Horizontal Displacements and Resistance of Pile Columns to Horizontal Loads, *Soil Mechanics and Foundation Engineering* (Translated from Russian), Vol. 15, No. 1, pp. 16-21.

CAVERNOUS GROUND IN YUEN LONG, HONG KONG

D. PASCALL*

SYNOPSIS

A site investigation in Yuen Long, Hong Kong, has revealed the presence of substantial caves within the marble bedrock. Rockhead across the site is very irregular and it is overlain by a residual detrital soil and by alluvium. The caves, which are up to 20m high, are filled with water or are paritally filled with soft mud derived from the overlying sediments.

The caves have formed by solution of limestone along steeply dipping joints. The full extent of the cave system only became apparent after a close grid (5 m x 5 m) of boreholes was drilled.

INTRODUCTION

The site is located to the east of Yuen Long (Figure 1) in an area that was formerly occupied by vegetable gardens and a fish pond. Fill has recently been placed over the area as part of a site formation. The proposed development
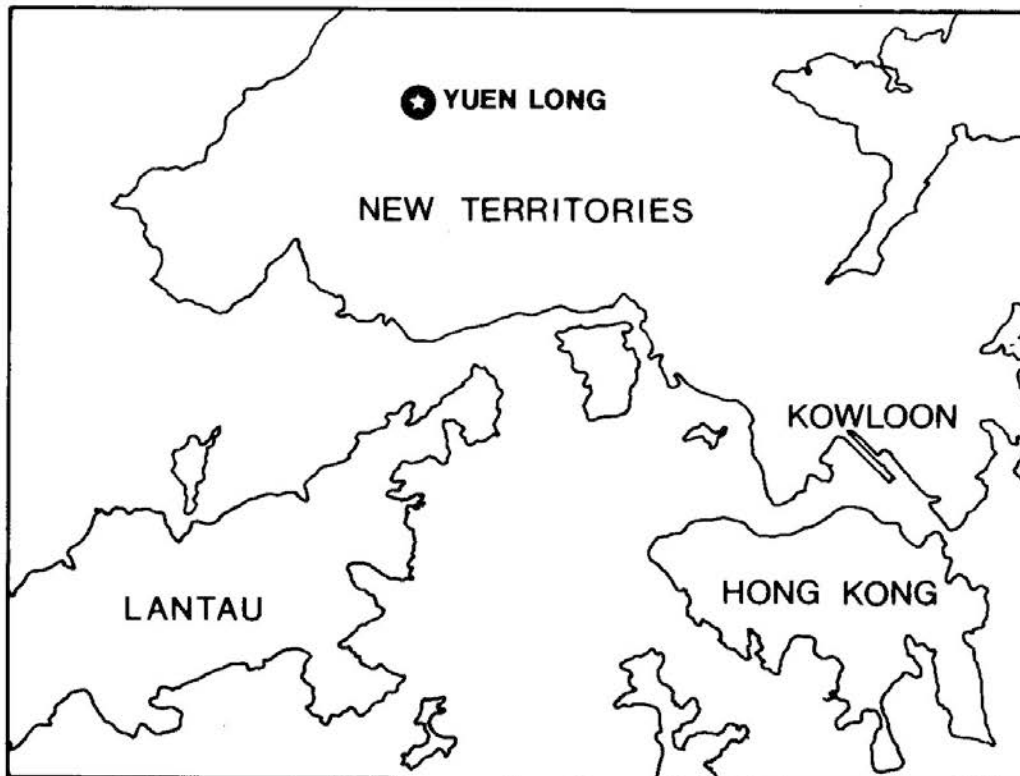

Fig. 1. Location Plan.

*Ove Arup & Partners (HK) Ltd, Hong Kong

consisted of several tower blocks above a commercial podium covering the whole site. The area was originally mapped as being underlain by Lok Ma Chau metasediments (ALLEN & STEPHENS, 1971) of a granular nature but they were subsequently found to contain metamorphosed limestone (marble) (SIU & WONG, 1985).

SITE INVESTIGATION

An initial investigation of this site, prior to the involvement of the author, had consisted of eight boreholes (prefixed D in Figure 2) of which six reached rock and were terminated after penetrating 5m into the rock. Two boreholes to the west of the site indicated that the rock level dropped in this direction with one borehole stopping at 70m depth within highly to completely decomposed rock (Grade IV/V (GEOLOGICAL SOCIETY, 1971)). Only one of the six boreholes within the site encountered a cave within the marble bedrock, but, as it was known that caves had been encountered within the marble on a site several hundred metres to the south (SIU & WONG, 1985), additional investigation work was carried out on this site.

Initially this work consisted of 23 boreholes drilled at a spacing of approximately 25-30m across the whole site. Standard Penetration Test (SPT) samples within the soil and either HX or NX size core in the rock were obtained from these boreholes. In addition, Mazier samples were obtained from five of the boreholes to provide material for a visual examination of the soils. To begin with, it was intended that these boreholes should penetrate 15m into rock, but, as sizeable caves were encountered in some of the early drillholes, later holes were required to penetrate 60m into rock.

Two additional boreholes were drilled close to Borehole 14 (Figure 2) which had encountered the largest cave of all the boreholes. These extra boreholes 14A and 14B, were 3m from Borehole 14 and confirmed the presence of substantial caves, though these did not occur at the same levels as those in Borehole 14. Because of the size of these caves, it was decided to examine the ground conditions beneath one of the proposed tower blocks in greater detail. Despite their usefulness under other circumstances (McCANN et al 1987), geophysical methods were rejected due to uncertainties as to their accuracy in predicting the presence of caves beneath what would be large concentrated foundation loads. It was therefore decided that the detailed investigation should consist of a grid of closely spaced probe-holes.

The probe-holes, which were on a 5m grid, were rotary drilled to depths of 30 and 45m below rockhead. To begin with, this detailed investigation was
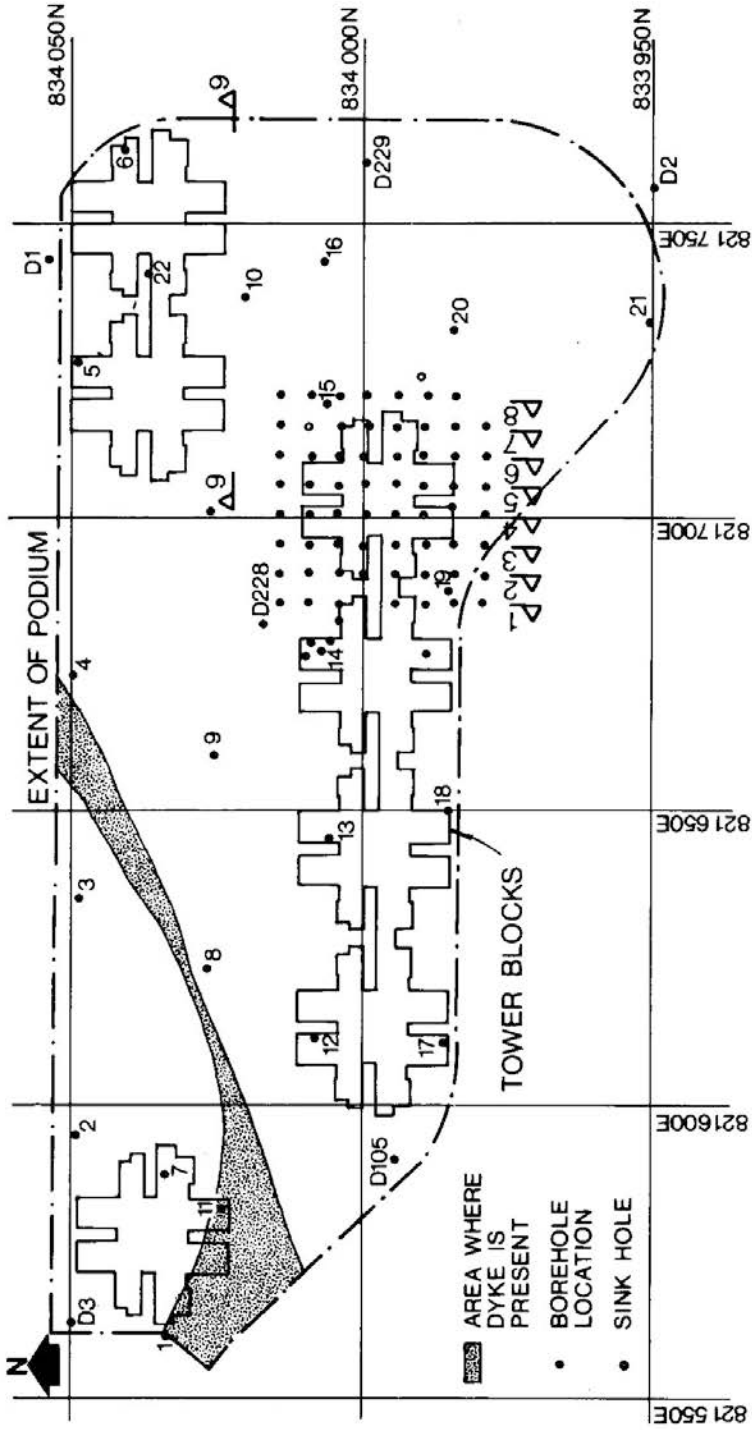
206

Fig. 2. Site Plan.

207

carried out with the water flush rotary coring rigs that were already on site. In an attempt to expedite the drilling programme and to make some economies, an air-flush rotary percussive rig was brougth on to the site. However, problems of jamming were experienced once the bit had passed through a cave. The jamming may have resulted from the loss of air flush once a cavity was encountered, but is more likely to have been due to the deflection of the drill string once the bit had encountered a steeply dipping rock surface. Hence its use was abandoned, and the investigation continued using only coring rigs, though even these could not progress the borehole after passing through the larger caves. The proposed tower block site selected for this detailed investigation was immediately to the east of Borehole 14 (Figure 2), and the investigation was set out on a 5m square grid. Drilling was continued to depths of 30 and 45m below rockhead. Four inclined holes were drilled to intersect at two of the caves identified by the vertical drilling.

Once the boreholes within this grid had been completed it was decided to cover the remainder of the site with boreholes on an eight metre triangular grid with the boreholes penetrating to 30m below rockhead. This triangular grid extended over the full area beneath the proposed podium irrespective of whether or not there were tower blocks above.

GROUNDWATER INVESTIGATION

A pumping test was also carried out as part of the site investigation. This was to establish whether the site could be effectively dewatered if a hand dug caisson solution were to be adopted for the foundations. SIU & WONG (1985) report a pumping test in which an extraction rate of 11,000 litres/hour only achieved a drawdown of 1m in the pumped well with no detectable drawdown in piezometers a short distance away. For the test at this site four wells were pumped simultaneously with a virtually constant total yield of 32,000 litres/hour.

The wells were created by enlarging Boreholes 14, 14A and 14B and drilling a fourth borehole, 14C. The wells were provided with a slotted screen. Pumping continued for 18 days, and a maximum drawdown of 16m was achieved in a pumped well, with a drawdown of half this value being measured in piezometers 20-30m away. The most interesting aspect of the pumping test was that the drawdown increased throughout the duration of the test, creeping down from a maximum of 10m at the beginning to 16m at the end.

Towards the end of the pumping test, a sinkhole appeared close to Borehole 15 (Figure 2). At the surface this was about 4m in diameter and 4.5m deep.
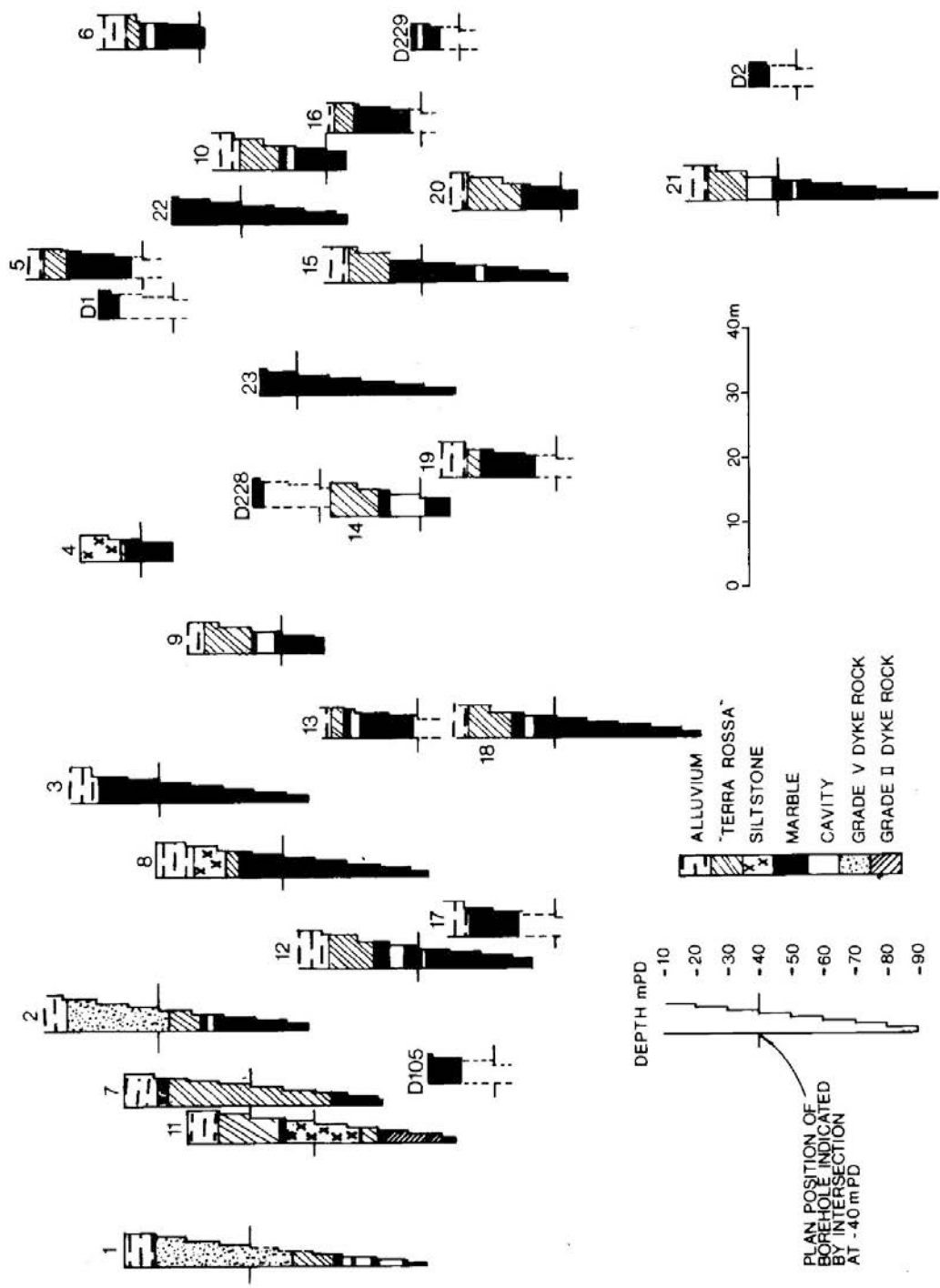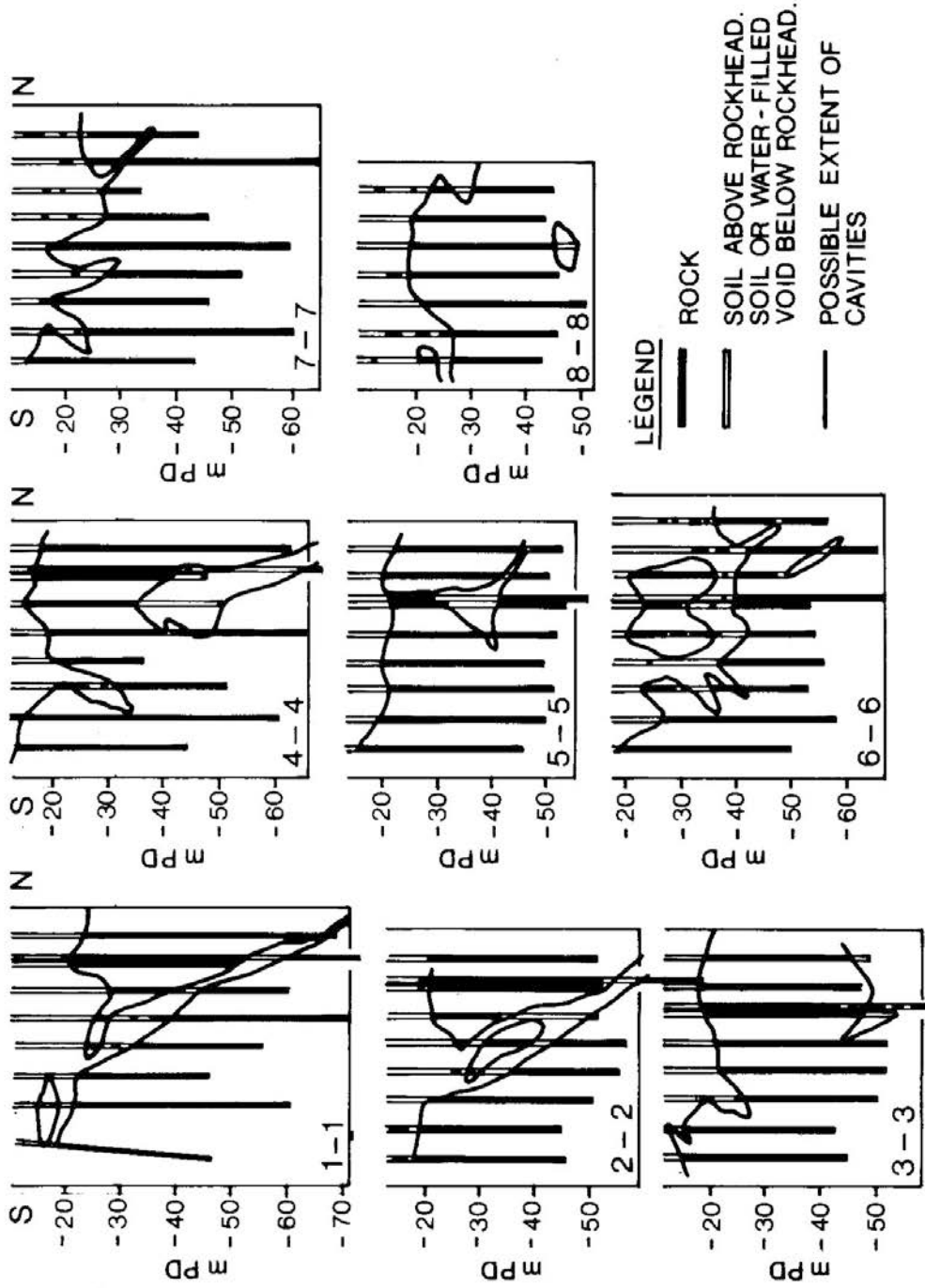
Fig. 3. Borehole Sections.

Fig. 4. Cross-sections 1-1 to 8-8 in the Area of the 5m Close-Centre Drilling.

Previously a smaller sinkhole had appeared when, at the start of the investigation, six holes were being drilled on the north-east to south-west diagonal of the grid. Whilst this work was underway a sinkhole 1.8m deep and 3-4m wide appeared to the east of the 5m grid close to Borehole 20 (Figure 2).

These various sinkholes were thought to be caused by the soil collapsing into the caves with the resulting void migrating upwards to the ground surface. During the pumping test the increase in drawdown is attributed to the blocking of the caves by the collapsing soil. The sinkholes that appeared originally had an arched roof, and had only appeared at the surface once the migrating cavity, leaving collapsed materials in a cone on the floor, had daylighted.

SITE GEOLOGY

Although most of the site is underlain by marble, igneous dykes and weathered sedimentary rocks are present within the marble at the western end of the site. The dykes are in part weathered in situ to Grade V (completely weathered) material. Elsewhere there is residual detrital soil (Terra Rossa) above the marble with alluvial deposits above. The synoptic logs for the first 23 boreholes are presented in Figure 3. In this Figure, the plan positions of these boreholes are indicated by the line marking the-40mPD level, and they are also shown in Figure 2. The approximate site ground level is 4mPD. Sections through the boreholes on the 5 metre grid are shown in Figure 4.

Alluvium

The alluvium consists of mottled red and grey well graded sandy clays and sands that are only weakly structured, i.e. showing horizontal depositional banding.

There are, however, changes in the composition with the quantity of sand increasing over short distances. Occasionally there are bands of cleaner silty medium to coarse sand. The gradings (Figure 5) show the material to vary from slightly clayey sand to silty clay and the Atterberg Limits indicate a clay of medium plasticity.

Residual Soil

Three types of residual soil are present within the site. Two are in situ weathered igneous and sedimentary rocks, and the third is a detrital soil above the marble.
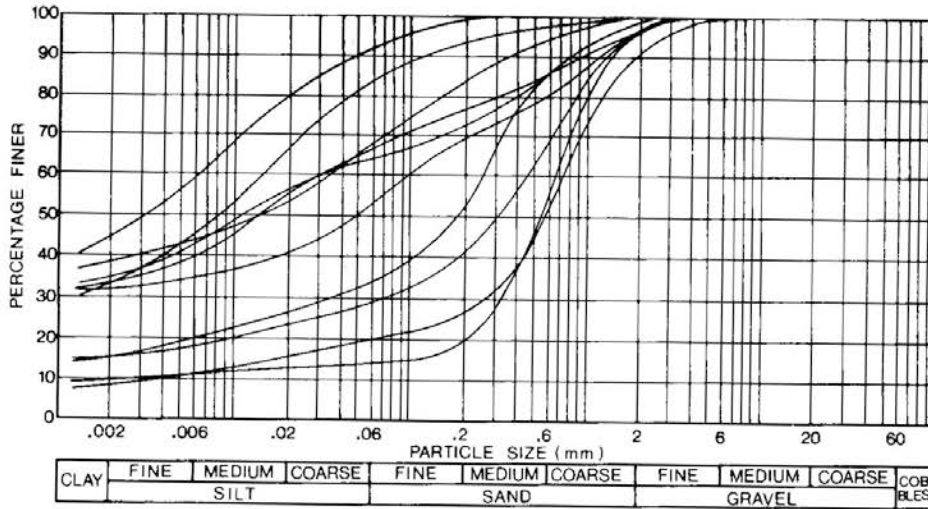
211

Fig. 5. Particle Size Distribution - Alluvium.

The in situ weathered igneous rock is a mottled white and brown silty sand with black manganese dioxide (MnO_2) stained joints. The gradings (Figure 6) show the material to be sandy silt, slightly gap-graded and deficient in coarse silt and fine sand. SPT "N" values within the weathered igneous rock are high (Figure 7). The in-situ weathered sedimentary rocks are siltstones and silty sandstones of the Lok Ma Chau Formation. They are white and brown in colour and contain relict joints stained with manganese dioxide (MnO_2). These soils are silty sands and silts (Figure 8).
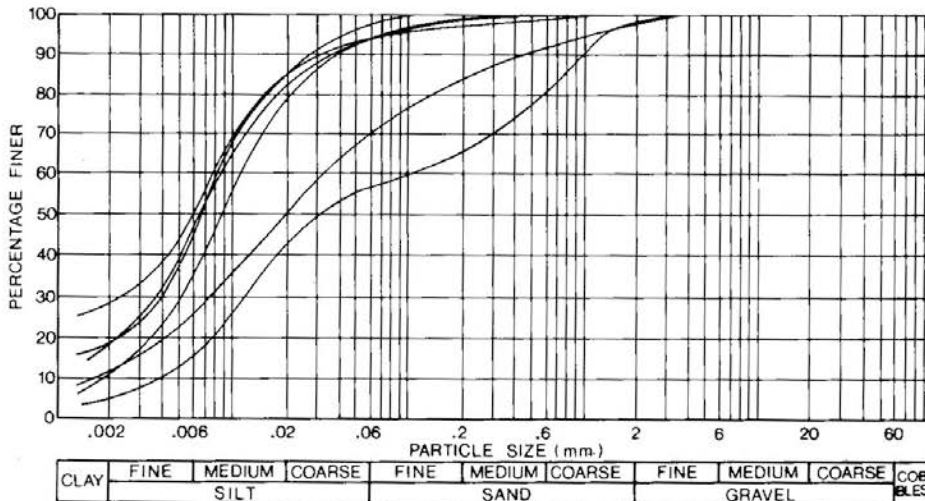
Fig. 6. Particle Size Distribution-Weathered Dyke Rock.

212
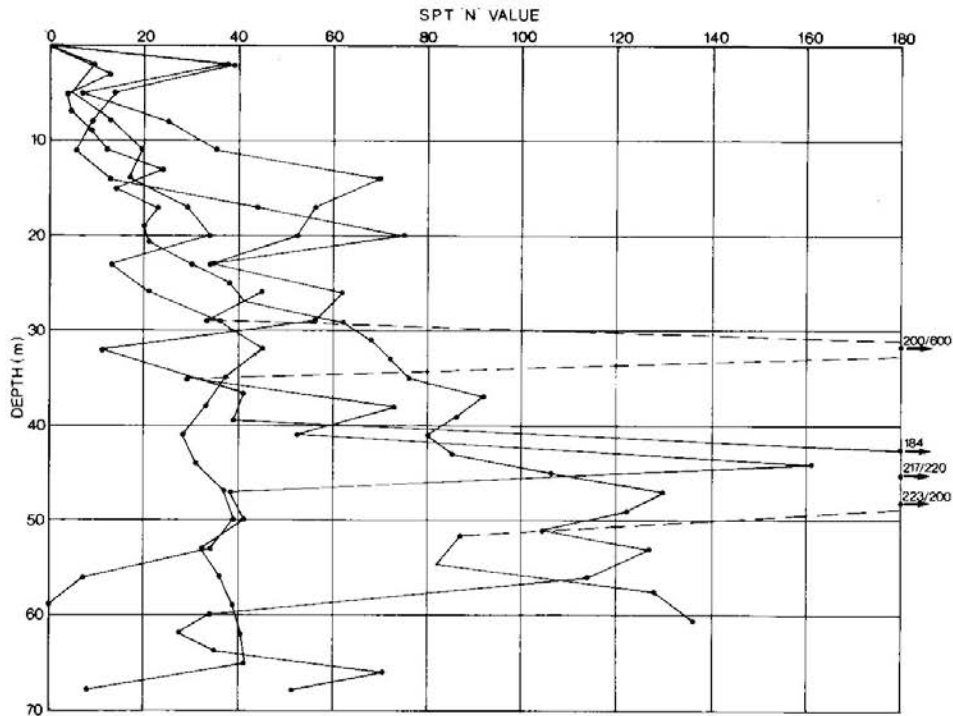
Fig. 7. Standard Penetration Tests Within the Area of the Dykes.

The residual soil above the marble, which has been called "Terra Rossa" for reasons described later, is a reddish brown sandy clay with some gravel of weathered siltstone and vein quartz. The detrital rock fragments are Lok Ma Chau Formation Sediments, and it is believed that the marble also forms part

Fig. 8. Particle Size Distribution-Lok Ma Chau Siltstones and Sandstones.

213

Fig. 9. Standard Penetration Tests above Marble Bedrock.

of the same formation. The soil is structureless and becomes darker in colour close to the marble bedrock. This may be due to the lower part containing fine dark detrital material from the dissolved marble. In Boreholes 1 and 2 the Terra Rossa is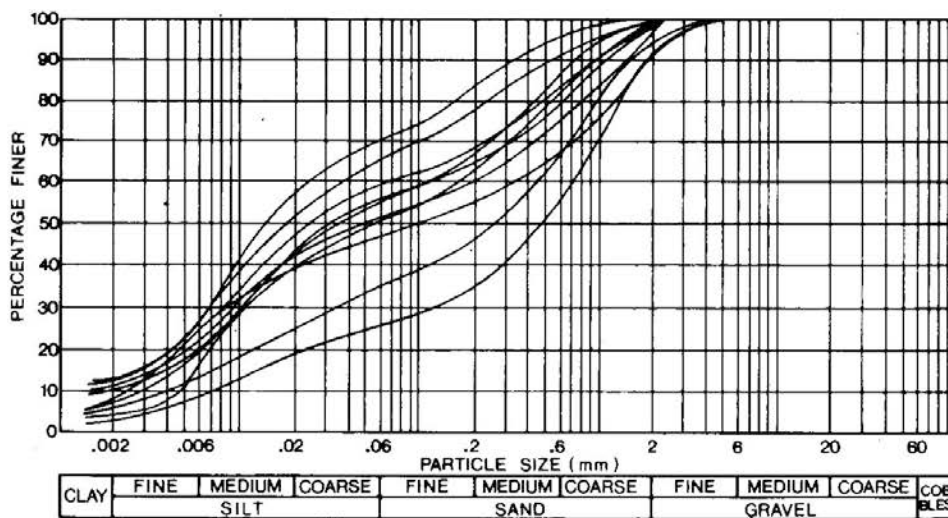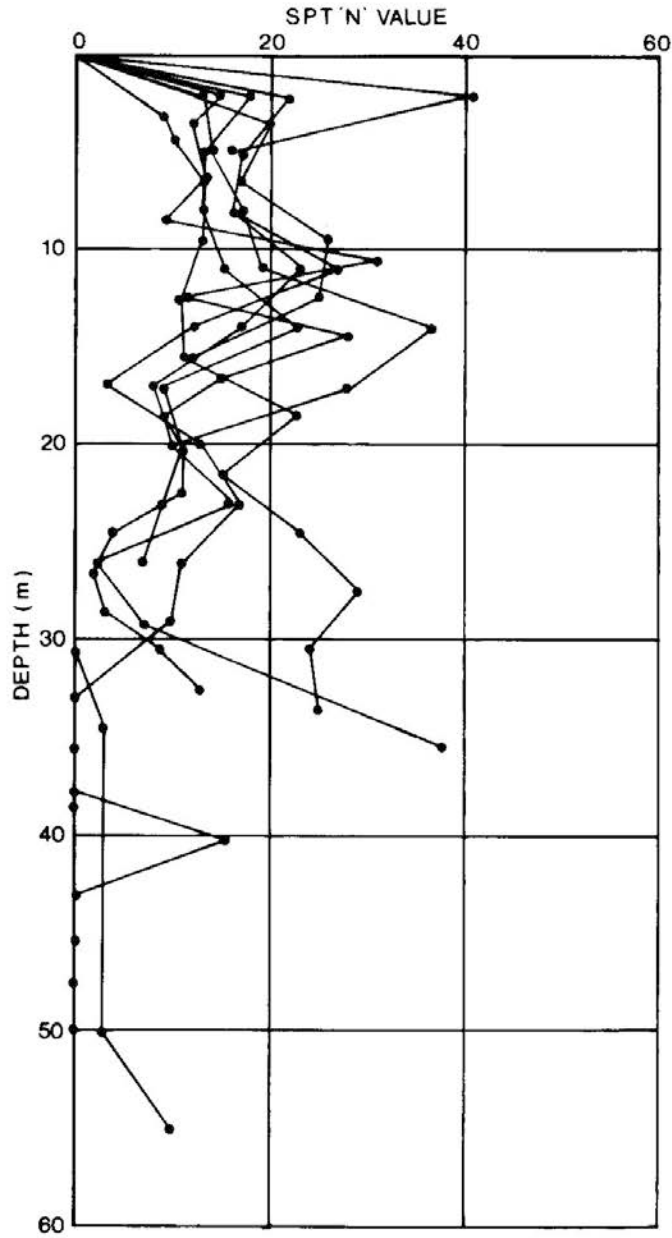 present beneath weathered dyke rock, and it is most likely that it has crept into the cavity formed as the dissolving marble shrank away from the overlying cover of weathered metamorphic and igneous rocks. The structureless nature of the soil and the decreasing SPT "N" values close to rockhead (Figure 9) indicate that the material has been disturbed through softening and collapse. A similar weak zone above rockhead has been reported in Malaysia (TAN, 1987) which similarly is attributed to the collapse of the soil into the caves. The gradings (Figure 10) and the Atterberg Limits show the material to be a sandy clay of medium plasticity.
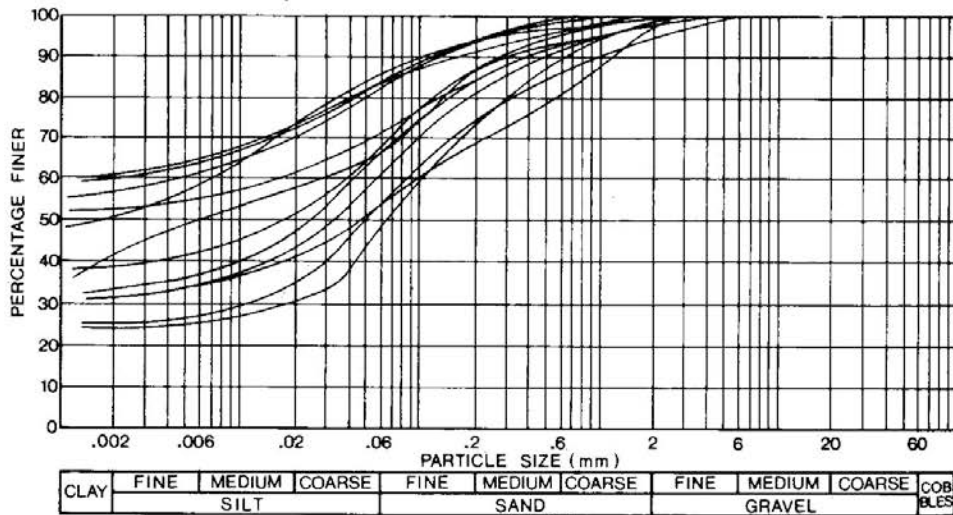
Fig. 10. Particle Size Distribution "Terra Rossa".

Rock

The rocks present on this site are igneous dyke rocks and metamorphosed rocks termed the Lok Ma Chau Formation by ALLEN & STEPHENS, (1971). At the time of the Allen and Stephens survey the presence of marble below the Lok Ma Chau Formation had not been recognised. Only with the high rise development in the area has it been discovered, and is regarded in the current geological remapping programme in Hong Kong to underlie the Lok Ma Chau Formation (ADDISON, 1987). Only the marble is present as an unweathered rock, the siltstones and sandstones being variably weathered. The weathered siltstones and sandstones are present over the western part of the site, where they are associated with the igneous intrusions. The main igneous rock is a

215

quartz feldspar porphyry which has been intruded directly into the marble. The edge of the dykes have a chilled fine grained margin which sometimes contains calcareous inclusions. The other igneous rock was encountered in two boreholes. It is rich in hornblende and has a dyke-like contact with the marble. It appears to be a basic dyke that was in the original limestone before the latter was metamorphosed to marble.

The marble is typically a white or light grey medium grained equigranular metamorphosed limestone. The rock is strong and unconfined compression tests on 10 samples gave an average strength of 43MPa. Microscope thin sections show the rock to be virtually pure calcite but occasionally there are dark grey areas that contain small amounts of impurity, partly pyrite and partly a finely disseminated but unidentified black mineral. These areas have a banded appearance with the darker minerals segregated from the white calcite in between. In addition to these dark impurities there are occasional small vugs of hard clay up to about 50mm in size.

The marble varies from being medium to very widely jointed. In Borehole 17 the joint spacing is extremely wide with only one joint present in a 15m length of marble. The joints are mostly dipping at between 45°, and 60°, but with some close to vertical, and with few low angle or horizontal fractures. Many of the 60° joints are slickensided due to differential movement of the rock on either side of the joint. The slickensides take the form of grooves on the joint surfaces indicating the direction of differential movement. The orientations of these are at low angles and this combined with the presence of conjugate shears, show the displacement to be mostly horizontal. Joints are sometimes covered with a veneer of chlorite and sometimes with a layer of powdered calcite.

Three of the boreholes in the 5m close spaced grid have had orientated core obtained from them, and also impression packer test have been carried out. Joint orientations from these are shown on the stereographic plot given in Figure 11. These confirm the steeply dipping nature of the joints. The main joints dip north to north-east, and to the south and south-west. Sections through the 5m close centre drilling (Figure 4) show the presence of steeply inclined rifts. The major cave system in the northern part of this grid is formed by erosion along a combination of steep northerly and southerly dipping joints.
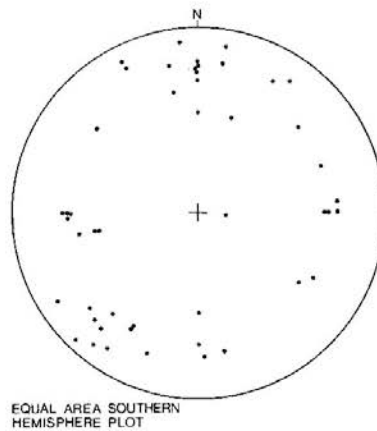
EQUAL AREA SOUTHERN
HEMISPHERE PLOT

**Fig. 11. Equal-area Stereoplot of Joints.**

Buried Karst Features

The karst features in the marble are due to the solution of the calcite by mildy acidic groundwater. The surface of the marble is very uneven and is pinnacled with individual pinnacles up to several metres in height. This is due to the solution of the marble having been concentrated along the discontinuities within the rock mass.

The surface of the marble is uneven on a small scale as well, and these irregularities can be seen in the core samples. The irregularities consist of etching, and more large scale scallops and fluting. The etching is most prominent in the upper parts of the marble and is particularly prominent where the marble is veined. In these parts the etching leaves the calcite veins as an upstanding lattice Plate 1 (a). The marble is stained brown for a few millimetres below the rock surface where solution is already commencing along the boundaries of individual calcite crystals. The surface of the marble is covered with a dusty calcite sand.

Scalloping results in indentations about 50mm across (Plate 1 (b)). When scallops are present along the open joints they are frequently elongate in the direction of ground water flow. The surface of the marble is also stained brown, and is covered by a veneer of brown calcite sand where the individual calcite crystals have separated from the rock mass due to solution.

To assist in the understanding of the cave system, a 1 : 100 scale perspex model was made of the 5m grid boreholes. An examination of this indicated that the cave system had developed along steeply inclined rifts that have orien-

217
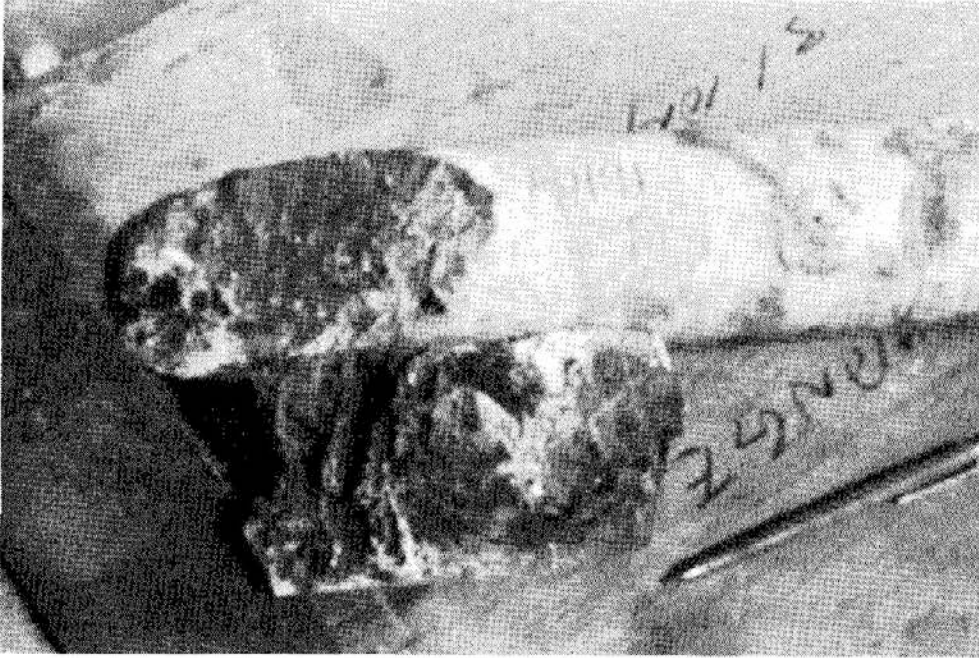
(a) Etching
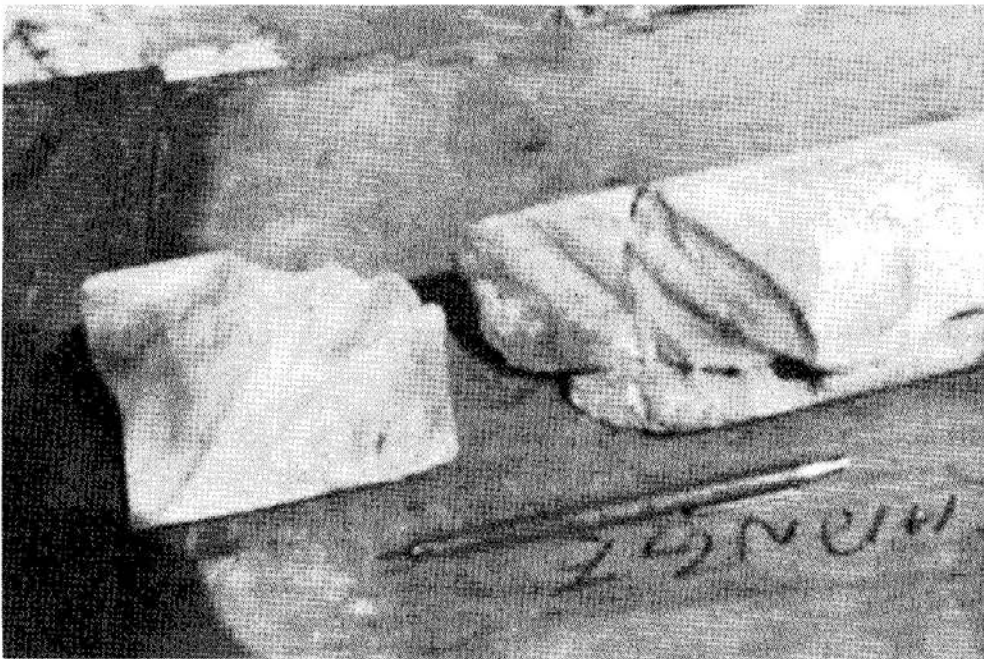
(b) Scalloping
Plate 1. Solutional Features in Marble Drillcore.

tations similar to those of the measured joints. This was particularly the case for Section 1 (Figure 4) where a cavity at the base of the borehole at the northern end appeared to correlate with the inclined rift further south. Additional deeper boreholes (those second from the right in Sections 1, 2 and 4) were drilled and these confirmed the presence of the rift that had not been detected with the boreholes that had only penetrated 30m below rockhead, but was suspected from those that had penetrated 45m into rock. Elsewhere over the site, where the 8m triangular grid has been used, and the boreholes only penetrated 30m it has not been possible to establish the pattern of the cave system even though some of the caves are large (Figure 12). The sections (Figure 4) show that the northerly inclined rift is particularly prominent on the western side of the grid. Moving east, this rift breaks down to a cave system orientated on southerly and northerly dipping discontinuities. Then the rift again opens to the surface of the rock, and it was in this area that the sinkhole appeared at the ground surface during pumping.
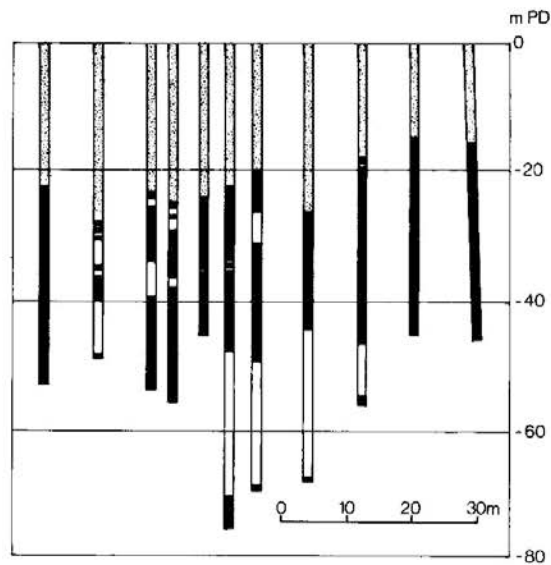

Fig. 12. Cross-section 9-9.

It should be pointed out that even the 5m grid has failed to permit interpretation of the fine detail of the cave system. For example one borehole (third from the right in Section 5-Figure 4) encountered no rock until -40 mPD whereas earlier drilled neighbouring boreholes indicated rockhead at -20mPD.

219

GEOLOGICAL DISCUSSION

The scalloped surfaces on the marble indicate formation within the phreatic zone i.e. above the permanent water table, in the part of the rock mass where the water is running in fast flowing streams. The caves would therefore have to have been formed during a period of lower sea level than at present, such as during the Pleistocene Ice Age when the sea level was at -140mPD (SZE & WANG, 1981), or even earlier during the Tertiary. Since the cave system would have formed by selective solution of the marble along discontinuities within the rock mass, the principal elements of the system can be expected to follow the steeply inclined joints.

Although joint surfaces are slickensided the drilling has not picked up any evidence for faulting in this area. Obviously should a fault be present within the marble it would be a prime site for the development of a cave. A coating of brown sugary calcite sand covers the open joint surfaces especially in the upper part of the marble. This coating could only be preserved if it was formed when the groundwater was static or slow moving, ie. once the cave system had become submerged. The solutional features that are created below the permanent water table differ from those in the part of the rock above this permanent water table (the scallops and fluting) hence the preservation of these features indicates that little additional solution has occurred since the sea rose to its present level 10,000 years ago.

The structureless brown residual clay above the marble is believed to be equivalent to the "Terra Rossa" that is present in the limestone terrain in the Mediterranean Region. The residual clay has been called Terra Rossa to avoid confusion with the term residual soil implying Grade VI in situ weathered soil (GEOLOGICAL SOCIETY 1971).

The Mediterranean Terra Rossa consists of detritus left from within the limestone as it dissolves, and of disturbed remnants of overlying strata. In Yuen Long, remnants of the overlying strata would provide the prinicipal source for the soil as the marble is virtually pure calcite. The residual soil at Yuen Long contains no calcareous material but contains fragments of siltstone and quartzite believed to belong to the Lok Ma Chau Formation of ALLEN & STEPHENS, (1971).

Since the caves have not been filled with the alluvial deposits the Terra Rossa must have provided a seal to the cave system when the area was inundated at the end of the Ice Age, and the alluvial deposits gradually submerged a karst topography similar to a miniature version of the Guilin

Mountains in Southern China. Since burial, gradual stoping of the sediments into the caves has resulted in a softened soil layer immediately above rockhead.

CONCLUSIONS

This study has shown that extensive investigation is necessary if the cave systems within the marble are to be identified, and in this respect it is interesting to note that whilst a reasonable picture of the cave systems was obtained with the 5m grid where some boreholes were extended 45m into rock, this was not the case for the wider 8m triangular grid with 30m penetration into rock.

Although cavernous limestone is well known in many areas of the world, this site appears to be unique, so far, in Hong Kong in having a substantial cave system beneath it. The investigation has shown that very deep close centre drilling is required to satisfactorily identify the nature of the caves, and that even when a pattern has been established additional boreholes can show it to be in error. It has also highlighted the fact that drilling. or the extraction of water from the marble, can cause problems by inducing sinkholes in the superficial materials.

REFERENCES

ADDISON, R, (1987). Personal Communication.

ALLEN, P.M. & STEPHENS, E.A. (1971). *Report on the Geological Survey of Hong Kong 1967-1969*, Hong Kong Government Press, 116p plus 2 maps.

GEOLOGICAL SOCIETY (1971). *Working Party Report on the Logging of Rock Cores for Engineering Purposes*. Geological Society, London.

McCANN D.M., JACKSON D. & CULSHAW M.G. (1987). The use of geophysical surveying methods in the detection of natural cavities and mine shafts. *Quarterly Jourual of Engineering Geology*. Vol. 20 No. 1 pp. 55-74.

SIU, K.L. & WONG, K.M. (1985). Concealed Marble at Yuen Long. Proc Conf. on Geological Aspects of Site Investigation, *Geological Society of Hong Kong. Bulletin* No. 2, pp. 75-88.

SZE Y.C. & WANG C.T., (1981). The fluctuations of climate, glaciation and sea level during the Quaternary in China. *Selection from the Third National Quaternary Academic Meeting* (in Chinese).

TAN B K, (1987). Geology and Urban Development of Kuala Lumpur, Malaysia, in, The Role of Geology in Urban Development, *Geological Society, Hong Kong. Bulletin* No. 3.

CONFERENCE NEWS

CARE'88 – Conference on Applied Rock Engineering, Newcastle England, 6-8 January 1988. All enquiries to : The Conference Office, Institution of Mining & Metallurgy, 44 Portland Place, London WIN 4BR, England.

Inst. Symposium on 'Tunnels for Water Resources and Power Projects', New Delhi India, 19-22 January 1988. All enquiries to : C.V.J. Varma, Member Secretary, Central Board of Irrigation and Powers, Malacha Marg, Chanakyepori New Delhi, 110 021 India.

9th Australian Geological Convention "Achievements in Australia Geoscience", Brisbane Australia, 31 January - 5 February 1988. All enquiries to : Dr. G.W. Hofmann Secretary 9AGC Geological Survey of Queensland G.P.O. Box 194 Brisbane, QLD. 4001 Australia.

1st Hellenic Conference on Geotechnical Engineering, Athens, Greece, 3-5 February 1988. All enquiries to : Technical Chamber of Greece, 4 Karageorgi Servias St. GR-105 62 Athens, Greace Att: D.G. Coumoulos.

2nd Multidisciplinary Conference on Sinkholes and the Environmental Impacts of Karst, Florida U.S.A., 9-11 February 1988. All enquiries to : Dr F. Beck, Director Florida Sinkhole Research Institute College of Engineering University of Central Florida, Orlando, Florida 32810 U.S.A.

'Leaving Nothing Unattempted'. A 2 day Workshop on Engineering Geophysics, Adelaide Australia, 13-14 February 1988. All enquiries to : K. Frankcombe, P.O. Box 171, Stepney, S.A. 5069 Australia.

'Adelaide '88' ASEG/SEG International Geophysical Conference and Exhibition, Adelaide Australia, 14-21 February 1988. All enquiries to : ASEG/SEG Int. Conference, C/-ELLISERVICE, Convention Management, P.O. Box 753, Norwood, S.A. 5067.

2nd Short Course on 'Soil Dynamics and Foundation Engineering', Missouri U.S.A., 22-26 February 1988. All enquiries to : Shamsher Prakash Dept. Civil Engineering, Butler-Carlton Civil Engineering Hall, Rolla, Missouri 65401-2049 U.S.A.

Asian Mining 88. Int. Conference and Exhibition, Kuala Lumpur Malaysia, 8-11 March 1988. All enquiries to : The Conference Office, The Institution of Mining and Metallurgy, 44 Portland Place, London, WIN 4BR, England.

223

International Conference on Calcareous Sediments, Perth, 15-18 March 1988. All enquiries to: Conference Department The Institution of Engineers, Australia, 11 National Circuit, Barton, ACT 2600.

ISOPT – 1 International Symposium on Penetiation Testing, Orlando U.S.A., 20-24 March 1988. All enquiries to : Dr John L. Davidson Department of Civil Engineering 346 Weil Hall University of Florida Gainesville, FL 32611 U.S.A.

6th International Conference on Numerical Methods in Geomechanics ICONMIG '88, Innsbruck Austria, 11-15 April 1988. All enquiries to : Kongreshaus Innsbruck Iconmig Rennweg 3 A-6020 Innsbruck Austria.

Int. Conference on 'Underground Constructions '88', Prague Czechoslovakia, 11-13 April 1988. All enquiries to : House of Technology Ing. Krejcova Marie Gorkeho namesli 23 112 82 Prague 1 Czechoslovakia.

Tunnelling '88 5th International Symposium, London England, 18-21 April 1988. All enquiries to : The Conference Office Institution of Mining & Metall. 44 Portland Place London, WIN 4BR England.

CENTRIFUGE 88 International Conference on Geotechnical Centrifuge Modelling (under Aegis of ISSMFE), Paris France, 25-27 April 1988. All enquiries to : Mr Jean-Francois Corbe Laboratoire Centradles Ponts et Chaussees B.P. 19, 44340 Bouguenais France.

4th International Conference on Tall Buildings, Hong Kong and Singapore, 27-29 April and 2-4 May 1988. All enquiries to : P. Lee, Department of Civil and Structural Engineering, University of Hong Kong. Hong Kong.

I.S.S.M.F.E. Baltic Conference, Tallin USSR, 10-15 May 1988. All enquiries to : 2nd Baltic Conference on SMFE, Organizing Committee, Gosstroy USSR, Pushkinskaya Str, 26, 103828 Moscow, USSR.

3rd Int. Conf. on the Application of Stress-Wave Theory on Piles, Ottawa Canada, 25-27 May 1988. All enquiries to : Dr Bengt H. Fellenius 3rd Stress-Wave Conference University of Ottawa Dept. Civil Engineering 770 King Edward Avenue, Ottawa, Ontario, Canada KIN 6NS.

Second International Conference on Case Histories in Geotechnical Engineering, St Louis Missouri U.S.A., 1-5 June 1988. All enquiries to : Conference Chairman Prof Shamsher Prakash University of Missouri-Rolla Missouri 65401-0249 U.S.A.

1st Int. Geotechnical Seminar Deep Foundations on Bored and Auger Piles, Ghent Belgium, 7-10 June 1988. All enquiries to : The Secretariat of B.A.P.I.

224

Laboratory of Soil Mechanics Prof. W.F. Van Impe Grotesteenweg-Noord 2-9710 Zwingjaarde Ghent Belgium (Europe).

International Congress on "Tunnels and Water", Madrid Spain, 12-15 June 1988. All enquiries to : The Secretary AETOS Congreso International Calle Martinez Izquierdo 28028 Madrid Spain.

Penetration Testing in The UK 1988, Birmingham, UK, 6-8 July 1988. All enquiries to : Mrs. P.J. Ross, Institution of Civil Engineers, 1-7 Great George Street, London SWIP 3AA, U.K.

V. International Symposium on Landslides, Lausanne Switzerland, 10-15 July 1988.

ASCE Specialty Conference on Hydraulic Fill Structures, Fort Collins, Colorado, 7-10 August 1988. All enquiries to : W.D. Carrier III, Bromwell & Carrier, Inc., P.O. Box 5467, Lakeland, Florida, U.S.A.

"Prediction Versus Performance" 5th ANZ Geomechanics Conference, Sydeny, 22-26 August 1988. All enquiries to : The Conference Manager The Institution of Engineers, Australia, 11 National Circuit, Barton, ACT 2600.

International Conference on Engineering Problems on Regional Soils (ICEPRS '88), Beijing China, 11-15 August 1988. All enquiries to : CHINA CIVIL ENGINEERING SOCIETY P.O. Box 2500 Beijing, China.

3rd Int. Underground Space and Earth Sheltered Buildings Conference, Shanghai China, 1-6 September 1988. All enquiries to : Mr Zhov Zhixing, Dept. Geotechnical Engineering, Tongji University Shanghai, China.

International Conference on Rheology and Soil Mechanics, Coventry U.K., 12-17 September 1988. All enquiries to : Christine Brown Coventry Consortium Coventry Lanchester Polytechnic Priory Street Coventry CVI 5FB England.

"Engineering Geology as related to the Study, and Preservation of Ancient Works, Monuments and Historical Sites. International Symposium Sponsored by IAEG., Athens GREECE, 19-23 September 1988. All enquiries to : 1988 Symposium Secretariat P.O. Box 19146 GR117 10, Athens Greece.

I.A.E.G. Int. Symposium on 'Engineering Geology of the Shelf and Continen tal Slope of Seas and Oceans', Tbilisi U.S.S.R., 1-6 October 1988. All enquiries to : Hydrogeology and Engineering Geology, Academy of Sciences of the Georgian SSR 31, Rustaveli av. Tbilisi 380008 U.S.S.R.

International Geotechnical Symposium on Theory and Practice of Earth Reinforcement, Fukuoka City, Japan, 5-7 October 1988. All enquiries to : Prof. N. Miura. Department of Civil Engineering Saga University Saga 840 Japan.

Aus. I.M.M. 1989 Annual Conference, Perth Australia, April 1989. All enquiries to : To be announced

Inst. Conf. on Shaft Engineering, Harrogate England, 5-7 June 1989. All enquiries to : The Conference Officer The Institution of Mining & Metallurgy, 44 Portland Place, London, WIN 4BR, England.

28th International Geological Congress, Washington D.C. U.S.A. July. 1989.

12th International Conference on Soil Mechanics and Foundation Engineering, Rio de Janeiro BRAZIL, August 1989.

ANNOUNCEMENTS

XII International Conference on Soil Mechanics and Foundation Engineering

The Brazilian Society of Soil Mechanics, on behalf of the International Society of Soil Mechanics and Foundation Engineering, takes pleasure in inviting the members of the International Society, their companions, and others who are interested, to attend the XII International Conference on Soil Mechanics and Foundation Engineering to be held in Rio de Janeiro, Brazil in 1989. Bulletins containing information on conference themes, submission of papers, and the conference program will be distributed through the National Societies during the 1986-1989 period. The official languages of the International Society are English and French. At all sessions, simultaneous translation will be provided in English and French. An interesting and exciting social program is being organized. The official travel agent is preparing packages with the purpose of offering to the participants the opportunity to see some of the most interesting attractions of Brazil. In connection with the conference, an exhibition will be arranged to display recent developments in geotechnical engineering equipment and techniques. Brazil is a country of continental dimensions with an area of more than 8.5 million square kilometers. Its population is over 130 million. Rio de Janeiro was founded in 1565 and served as the capital of Brazil from 1763 to 1960 when the seat of government moved to Brasilia. More information can be obtained from:

> Organizing Committee
> XII ICSMFE, Caixa Postal 1559
> 2000 Rio de Janeiro, RJ
> BRAZIL

Golden Jubilee Commemorative Volume of the Southeast Asian Geotechnical Society

Geotechnical Engineering in Southeast Asia, a commemorative volume of the Southeast Asian Geotechnical Society, is now available from Balkema Publishers. This volume contains 11 contributions from Southeast Asia ranging from the behaviour of piles in soft organic clays to landslides and their control. It also includes bibliographies of books, journals, conference publications, theses, etc (c. 2,200 titles) and a directory of consultants and

227

contractors in Southeast Asia. This 352 page document (US$ 40) can be obtained from:

A.A. Balkema Book Distributors
P.O. Box 1675, NL-3000 BR Rotterdam
Netherlands

General Committee Members of SEAGS

The Governing Committee of the Southeast Asian Geotechnical Society for the period 1988-90 is as follows:

Prof. Seng Lip Lee (President)
Prof. A.S. Balasubramaniam (Immediate Past President)
Dr. Ting Wen Hui (Past President)
Dr. E.W. Brand (Past President)
Dr. Za-Chieh Moh (Founder President)
Dr. Tan Swan Beng (Past President)
Prof. Chin Fung Kee (Past President)
Mr. G.W. Lovegrove
Dr. Ooi Teik Aun
Mr. Yu Cheng
Dr. Sirilak Chandrangsu
Mr. Nibon Rananand
Mr. P.G.D. Whiteside (Editor)

SEAGS Newsletter

All correspondence related to the SEAGS Newsletter should be addressed to:

Southeast Asian Geotechnical Society
c/o Division of Geotechnical and Transportation Engineering,
Asian Institute of Technology,
P.O. Box 2754
Bangkok, Thailand 10501.

SI UNITS AND SYMBOLS

The following list of quantities, SI (Système International) units and SI symbols, are recommended for use in Geotechnical Engineering.

Quantities	Units	Symbols
Length	kilometre	km
	metre	m
	millimetre	mm
	micrometre	μm
Area	square kilometre	km^2
	square metre	m^2
	square millimetre	mm^2
Volume	cubic metre	m^3
	cubic millimetre	mm^3
Mass	tonne	t
	kilogramme	kg
	gramme	g
Density ρ (mass density)	tonne per cubic metre	t/m^3
	kilogramme per cubic metre	kg/m^3
Unit weight γ (weight density)	kilonewton per cubic metre	kN/m^3
Force	meganewton	MN
	kilonewton	kN
	newton	N
Pressure	megapascal	MPa
	kilopascal	kPa
Energy	megajoule	MJ
	kilojoule	kJ
	joule	J
Coefficient of volume compressibility or swelling m_v	1/megapascal	MPa^{-1}
	1/kilopascal	kPa^{-1}
Coefficient of consolidation or swelling c_v	square metre per second	m^2/s
	square metre per year	$m^2/year$
Hydraulic conductivity k (formerly coefficient of permeability)	metre per second	m/s

NOTES: The term specific gravity is obsolete and is replaced by relative density. The former term relative density $(e_{max}-e)/(e_{max}-e_{min})$ is replaced by the term density index, I_D.